Appendix 2. Calculation sequence and PSHA sensitivity results in SENSEI for the NPP sites in Finland

L. Fülöp, M. Malm, P. Mäntyniemi, February 2021

The goals of the SENSEI PSHA sensitivity project

The objective of the SENSEI project was to investigate the sensitivity of PSHA output for NPP sites in Finland to different choices of input. It is widely recognised that many PSHA inputs are uncertain and debatable. Such uncertainties, epistemic in nature, are usually incorporated in the PSHA using logic trees, drawn up based on expert judgments. The logic trees comprise different alternatives of the input, such as maximum magnitude, type of faulting, ground-motion prediction equation (GMPE), etc., and each alternative branch is assigned a weight using expert judgment and data testing.

The work in the SENSEI project advanced on the basis of structured discussions between the expert group, the calculation group, and STUK. The work direction was guided by the international expert group. The Finnish technical calculation group was formed from VTT Technical Research Centre of Finland (VTT), former ÅF-Consult Oy (ÅF), current AFRY Finland Oy (AFRY), and Institute of Seismology, University of Helsinki (ISUH).

1. Overview of the proposed calculation sequences for the NPP sites

In this document, we outline the sequence for sensitivity analysis of the PSHA calculations. The sequence comprised the following steps:

- *Establish the baseline*. Baseline PSHA model, its input, and the most representative results were collected from the reports of the utilities. These baselines constituted the basis of comparison with the SENSEI results, in particular the one-branch computations.
- *Condensate the PSHA model*. The PSHA models used by the utilities were complex (e.g., 144 logic-tree branches), and it is not practical to run sensitivity calculations for a given input parameter with such large models. Hence, we first trimmed the logic-tree to its most essential branches.
- *Sensitivity to attenuation (GMPE).* Due to the scarcity of earthquake recordings, GMPE is one of the most difficult issues to handle in PSHA for NPP sites in Finland. Hence, within the sensitivity study, the GMPE was handled as a separate item, before considering other input parameters.
- *Sensitivity to other input parameters.* The last part of the calculation sequence focused on all other PSHA input parameters except GMPE.

2. Description of the PSHA baseline models

The key parameters of the hazard models and the baseline values in PGA hazard curves and hazard spectra for the Loviisa, Olkiluoto, and Hanhikivi PSHA are shown in Figures L1a-d, O1a-d, and H1a-d. They include:

- the median PGA hazard curves (Figures L1a, O1a, and H1a),
- the source area models used (Figures L1b, O1b, and H1b),
- the logic trees used (Figures L1c, O1c, and H1c), and

- the source area contributions to the hazard (Figures L1d, O1d, and H1d).

The input for the PSHA baseline models was collected as follows:

Seismic source area (SSA) models

- Two alternative SSA schemes were presented for the Loviisa and Olkiluoto sites by Korja et al. (2016). They differ in how SSA6 was defined, either as a single large source area or three separate subparts. The scheme of one source area (Model 1 in Korja et al. 2016) was used as the baseline here, because the hazard spectrum has been computed for it only.
- Two alternative SSA schemes were presented for the Hanhikivi site by Korja and Kosonen (2015). Their Model 1 was taken to be the baseline here.

Activity parameters (β, λ)

- Activity parameters β and λ were calculated for each SSA in all the models considering events down to $M_{min\_catalog}$

Depth range

- Two different depth ranges were used for the Loviisa and Olkiluoto source zones (see Chapter 6 in Korja et al. 2016): 0-45 km for the zones in Sweden (SSAs 1-5) and 0-35 km elsewhere (SSAs 6-11).
- The two depth ranges used for the Hanhikivi source zones as a sensitivity study were 0-45 km and 0-30 km (see Tables 6.1.1 and 6.1.2 in Saari et al. 2015). In the present study, we used the depth range 0-45 km as the baseline.

Maximum magnitude (M_{max})

- M_{max} in the previous PSHA models was assumed as M_w5.5, 6.0, 6.5, and 7.0 with the associated weights shown in Figures L1c, O1c, and H1c.

Ground motion prediction equations (GMPEs)

- The GMPEs used in the study for Loviisa and Olkiluoto sites were the versions of the Longitudinal Saguenay (SaguL), Transversal Saguenay (SaguT), Longitudinal Newcastle (NewcL) and Transversal Newcastle (NewcT) GMPEs presented by Leppänen and Varpasuo (2017). Weighting factors of these four GMPEs are shown in Figures L1c and O1c. The GMPE is expressed in hypocentral distance, R_{hypo}.
- The GMPEs used in the Hanhikivi study were Pezeshk et al. (2011) and two versions of the Fennoscandian GMPE (older version presented in Saari et al. 2015, and an updated version in Vuorinen et al. 2018). The GMPE by Pezeshk et al. (2011) and the older version of the Fennoscandian GMPE were used to compute the hazard curves shown in Figure H1a, and the updated version of the Fennoscandian GMPE and GMPE by Pezeshk et al. (2011) to compute the hazard spectra in Figure H2. Weighting factors of the GMPEs are shown in Figure H1c. The Pezeshk et al. (2011) GMPE uses distance metric rupture distance, R_{rup}, and the Fennoscandian GMPE R_{hypo}.

Integration limits and distance

- For each SSA designed in the Loviisa, Olkiluoto, and Hanhikivi studies, the lower integration limit of the hazard integral was $M_{min} = M_{min\_catalog}$ and the upper integration limit was M_{max}.
- The integration distance was R_{hypo} = 0 - 300 km for the Loviisa and Olkiluoto sites and R_{hypo} = 0 - 500 km for the Hanhikivi site.

Structure of the logic tree

- The structure of the logic-tree and the corresponding weighs are shown in Figures L1c, O1c, and H1c.

V_{s30} velocity

- The v_{s30} velocity was not taken into account in the hazard computations, because the NPP sites are situated on bedrock, and therefore soil conditions can be disregarded as long as hard-rock GMPEs are used. This means that many GMPEs, such as NGA-West2, must be disregarded.

The above, complete PSHA models constituted the "Loviisa/Olkiluoto/Hanhikivi baseline model (LBasM/OBasM/HBasM)". The lists of input parameter choices are the "Baseline parameters for the Loviisa/Olkiluoto/Hanhikivi NPP sites (LBasP/OBasP/HBasP)", and the results obtained with the baseline models and the parameters are the "Baseline PSHA results for Loviisa/ Olkiluoto/Hanhikivi NPP sites (LBasR/OBasR/HBasR)" (Figures L2, O2, and H2).

All information about the baseline models and the respective results can be found in the utilities' PSHA reports. E.g., Figures L1a, L1d, O1a, O1d, H1a, and H1d are baseline results for Loviisa, Olkiluoto, and Hanhikivi.

3. Condensation of baseline models

In order to proceed with the sensitivity analysis, we first synthetized the PSHA input model to its core elements. The goal was to reduce the complex PSHA model to those core parameters and logic tree branches which have the largest influence on the baseline results.

This synthetization preserved the core of the baseline model but, however, some information was lost, and the hazard levels were somewhat changed. The hazard results obtained using the synthetized PSHA models were the SENSEI starting-point input for Loviisa/Olkiluoto/Hanhikivi (LSenBR/ OSenBR/HSenBR).

For each PSHA study, individual steps of synthetizing were carried out. They are described in more detail in Tables L1, O1, and H1. The following principles were adhered to:

- When seismic source areas (SSAs) were removed, their contribution was lost.
- When a logic-tree branch was removed, its associated weight was redistributed among the remaining branches.

4. Calculation sequence for Loviisa

The key parameters of the hazard model and the baseline values in PGA hazard, for the Loviisa PSHA are collected in Figures L1a, L1b, L1c, and L1d.

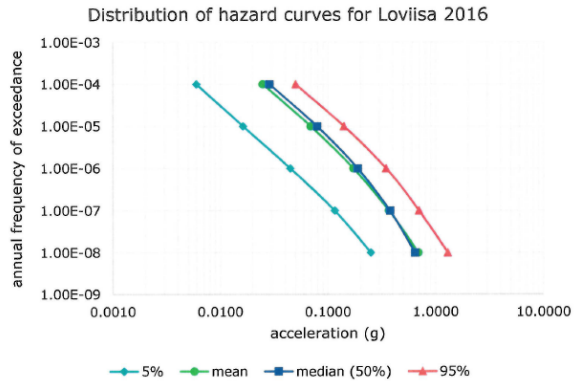

Figure L1a) Median PGA hazard from the "2016" study is the baseline we try to compare to in SENSEI (Figure 3-2 in Saari and Malm 2016).

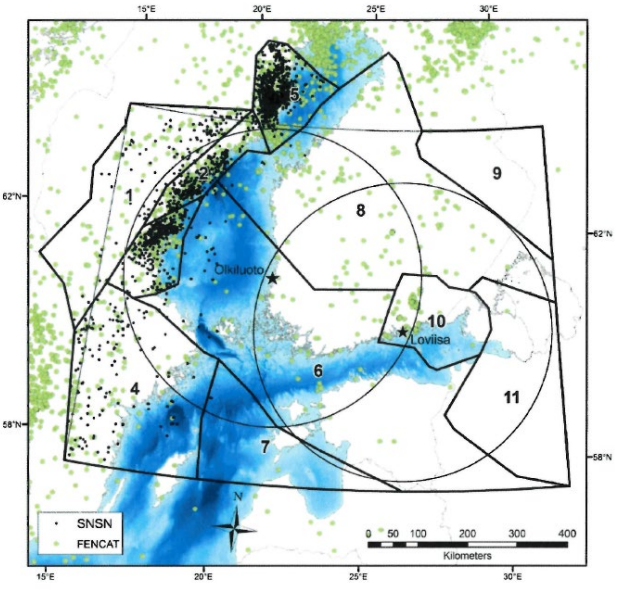

Figure L1b) The result in Figure L1a has been obtained using the source area model shown here (Figure 2-1 in Saari and Malm 2016).

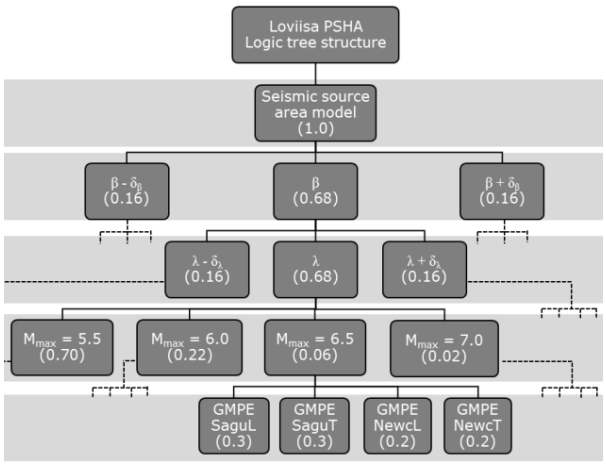

Figure L1c) The logic tree for the results in L1a (Figure 1-2 in Malm and Kaisko 2017a).

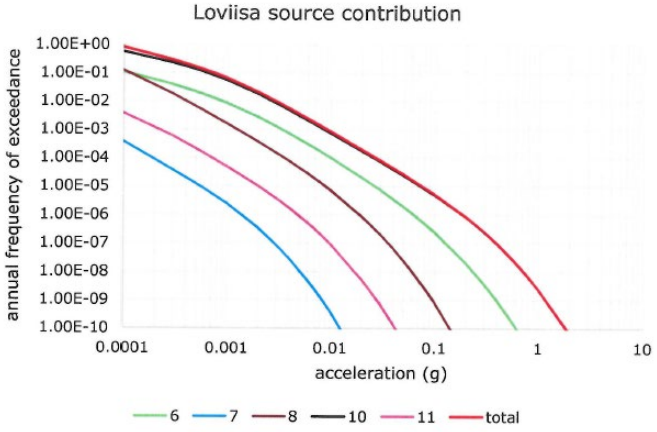

Figure L1d) The contributions of source areas to the hazard in L1a (Figure 3-4 in Saari and Malm 2016)

The Loviisa baseline results (LBasR), namely the PGA median hazard curve and median spectral acceleration (in units of g) for annual frequency of exceedance (AFE) of 10^{-5} are presented in Figure L2.

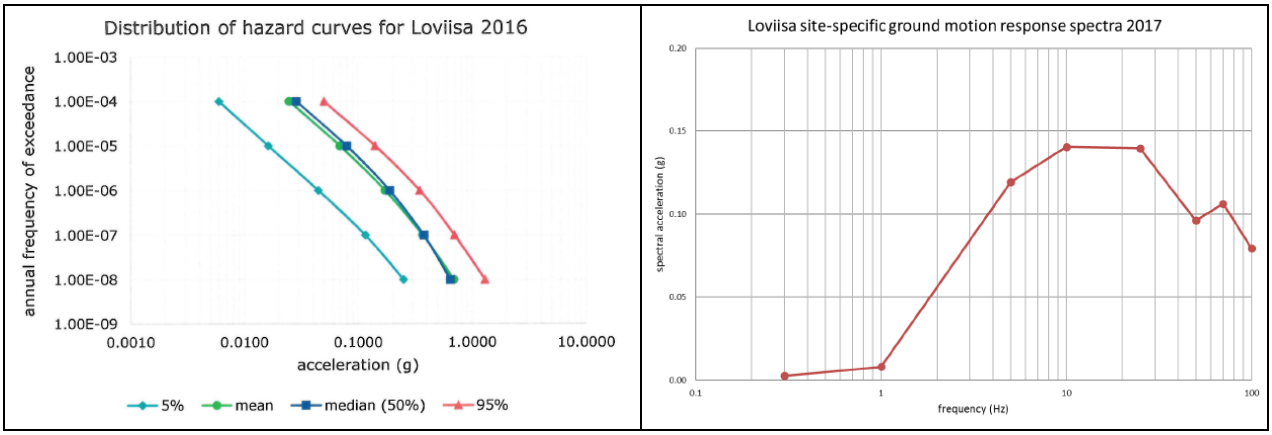

***Figure L2**. The Loviisa baseline results (LBasR): PGA median hazard curve (blue line) and median spectral acceleration (in g) for annual frequency of exceedance of 10^{-5} (Saari and Malm 2016; Malm and Kaisko 2017a).*

The synthetized PSHA model (LSenBM) is described in Table L1. The synthetization was begun with the Loviisa model with 144 branches, developed by Saari and Malm (2016). First, the seismic source zones (SSAs) contributing least to the hazard were removed, retaining only the two most influential SSAs, which are SSA10 (the host zone) and the contiguous SSA6 (Figure L1d). At the same time, the branching levels for β and λ (Figure L1c) were eliminated by collapsing the $\pm\delta_\beta$ and $\pm\delta_\lambda$ branches to the mean β and λ branches. The weight of the mean β and λ branches was set from 68% to 100%. By doing so, the number of logic-tree branches was reduced from 144 to 16 (Table L1).

At the next step of synthetisation, the M_{max} branching was collapsed to $M_w5.5$ with the largest weight (Figure L1c). The other M_{max} branches were removed, and the weight of M_{max}=$M_w5.5$ was set to 100%. The resulting synthesized model had four branches corresponding to the four GMPEs used in the original analysis (Figure L1c).

***Table L1.** Steps to synthetize the Loviisa baseline PSHA model (LBasM) to LSenBM.*

Model name	SSAs	Parameters (β, λ)	Depth distr.	GMPE	SSAs	M_{min}	M_{max}	No. of branches
The reference results in the synthetizing process are the LBasR (e.g., Figure L2)								
LBasM	-	-	—	-	-	-	-	144
*	10 & 6	Mid branches (β, λ) with 100%	-	-	-	-	-	16
**	10 & 6	Mid branches (β, λ) with 100%	-	-	-	-	5.5/ 6/ 6.5/ 7	4 for each M_{max}
LSenBM	10 & 6	Mid branches (β, λ) with 100%	-	-	-	-	5.5	4
The outcome is the LSenBM with LSenBR								

Note: The hyphen stands for the original parameter setting for the LBasM according to Saari and Malm (2016) and Malm and Kaisko (2017a). The two models of intermediate complexity (i.e. * and **) were only used for checking, but not reported in SENSEI.

The results of the LSenBM model are plotted in Figure L3. Comparison of the hazard curves in Figure L2 and Figure L3 demonstrates that the Loviisa synthetized model (LSenBM) captures the main features of the original Loviisa PSHA model with 144 branches quite well.

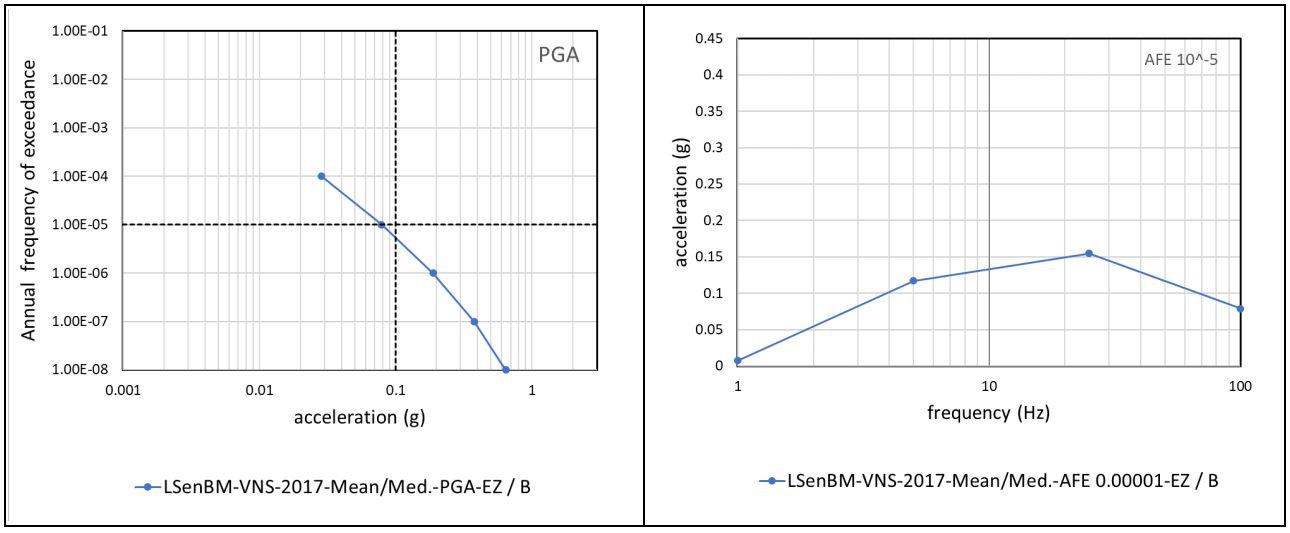

Figure L3. *The Loviisa SENSEI results (LSenBR) used as the basis for comparison in the sensitivity study (Line 4 in Table L1). VNS-2017 = GMPE presented by Leppänen and Varpasuo (2017), EZ = EZ-FRISK software, B = calculation group member "B".*

For the Loviisa sensitivity testing, the results in Figure L3 (LSenBR) were used as the basis for comparison. The first stage of sensitivity testing focused on the influence of GMPEs (Table L2). Since most GMPEs have a limited validity range, these tests were run with a compatible level of M_{min}, and the M_{min} was set to the threshold of M_w4. The primary purpose of the tests was to assess the influence of the earlier and new candidate GMPEs on the hazard results.

Table L2. *Steps for studying the GMPE sensitivity of the hazard at Loviisa NPP site.*

Model name	SSAs	Activity parameters (β, λ)	GMPE	M_{min}	M_{max}	No. of branches
The reference for comparing all the results from these models is LSenBR.						
LG1	10 & 6	Mid branches (β, λ) with 100%	VNS 2017	4	5.5	4
LG2	10 & 6	Mid branches (β, λ) with 100%	VNS 2017	4	6.5	4
LG3	*10 & 6*	*Mid branches (β, λ) with 100%*	*VNS 2018 (removed by comparison)*	*4*	*6.5*	*4*
LG4	*10 & 6*	*Mid branches (β, λ) with 100%*	*SMSIM GMPE*	*4*	*6.5*	*4*
LG5a	10 & 6	Mid branches (β, λ) with 100%	Pezeshk et al. 2011	4	6.5	1
LG5b	10 & 6	Mid branches (β, λ) with 100%	T-97	4	6.5	1
LG6a	10 & 6	Mid branches (β, λ) with 100%	FennoG16, Single-station Sigma	4	6.5	1
LG6b	10 & 6	Mid branches (β, λ) with 100%	FennoG16, Total Sigma	4	6.5	1
LG7	10 & 6	Low branch β- for Zone10, mid branch λ with 100%	NGA-E, weighted average model (WA)	4	6.5	1
LG8	10 & 6	Mid branches (β, λ) with 100%	NGA-E-WA	4	6.5	1
LG9	10 & 6	High branch β+ for Zone 10, mid branch λ with 100%	NGA-E-WA	4	6.5	1
Expected outcome in Figure L4						

Notes: Other parameters were from the original setting of the LBasM model according to Saari and Malm (2016) and Malm and Kaisko (2017a). The underlined models were not completed.

Not every calculation step in Table L2 was completed (Lines LG3 and LG4). In addition to GMPE sensitivity, some models targeted the effect of M_{max} (LG1 vs. LG2), the scale of randomness, σ, in the GMPE (LG6a vs. LG6b) and GR β (LG7 vs. LG8 vs. LG9).

When M_{min} was raised from its original values in the Loviisa baseline model to M_w4, the activity parameters were adjusted accordingly (Table L'). In the baseline model (LBasM), source areas SSA6 and SSA10 were defined with a minimum magnitude of M_w2 and $M_w0.7$, respectively. The corresponding λ values were 0.563 and 1.972 events equal to or larger than M_{min} per year in SSA6 and SSA10, respectively. When increasing M_{min} to M_w4, these values dropped to 0.0033 and 0.0006 events per year in SSA6 and SSA10, respectively. Taking into account that SSA6 is several times larger than SSA10, the activity per unit area of the two zones is quite similar.

***Table L'**. Input parameter adjustment from LBasM to the models for GMPE sensitivity.*

	Baseline model (LBasM)		Models with elevated M_{min} in Table L2			
SSA	Mean β	Mean λ (for M_{min})	a value	b value	β	λ (for M_{min})
6	2.57	0.563 (M_{min}=2)	1.983	1.12	2.57	0.003296649 (M_{min}=4)
10	2.46	1.972 (M_{min}=0.7)	1.044	1.07	2.46	0.00058064 (M_{min}=4)

The results for the GMPE sensitivity models are presented in Figure L4. The panels show the median hazard curve for PGA. Results are given for the models from Table L2. Line LG5 has been split into two, corresponding to T-97 by Vuorinen et al. (2018) and Pezeshk et al. (2011) GMPEs.

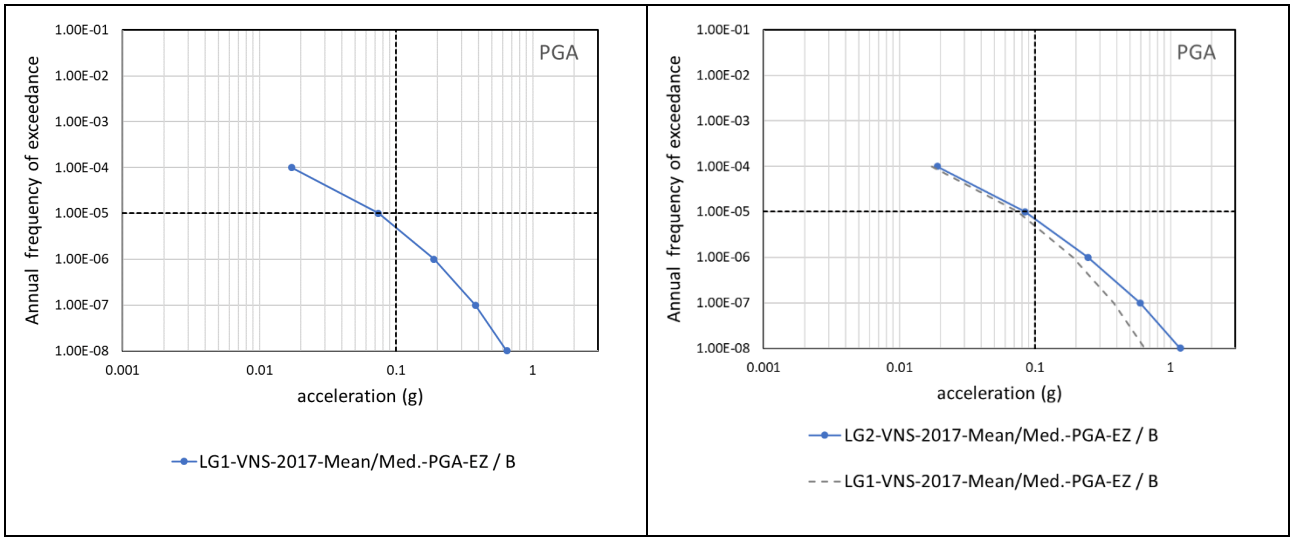

***Figure L4.** The Loviisa SENSEI GMPE sensitivity results for the Table L2 models. The name of the model, from LG1 to LG9, is given in the legend of each graph. Models LG3 and LG4 were not computed. EZ = EZ-FRISK software, B = computation by calculation group member "B".*

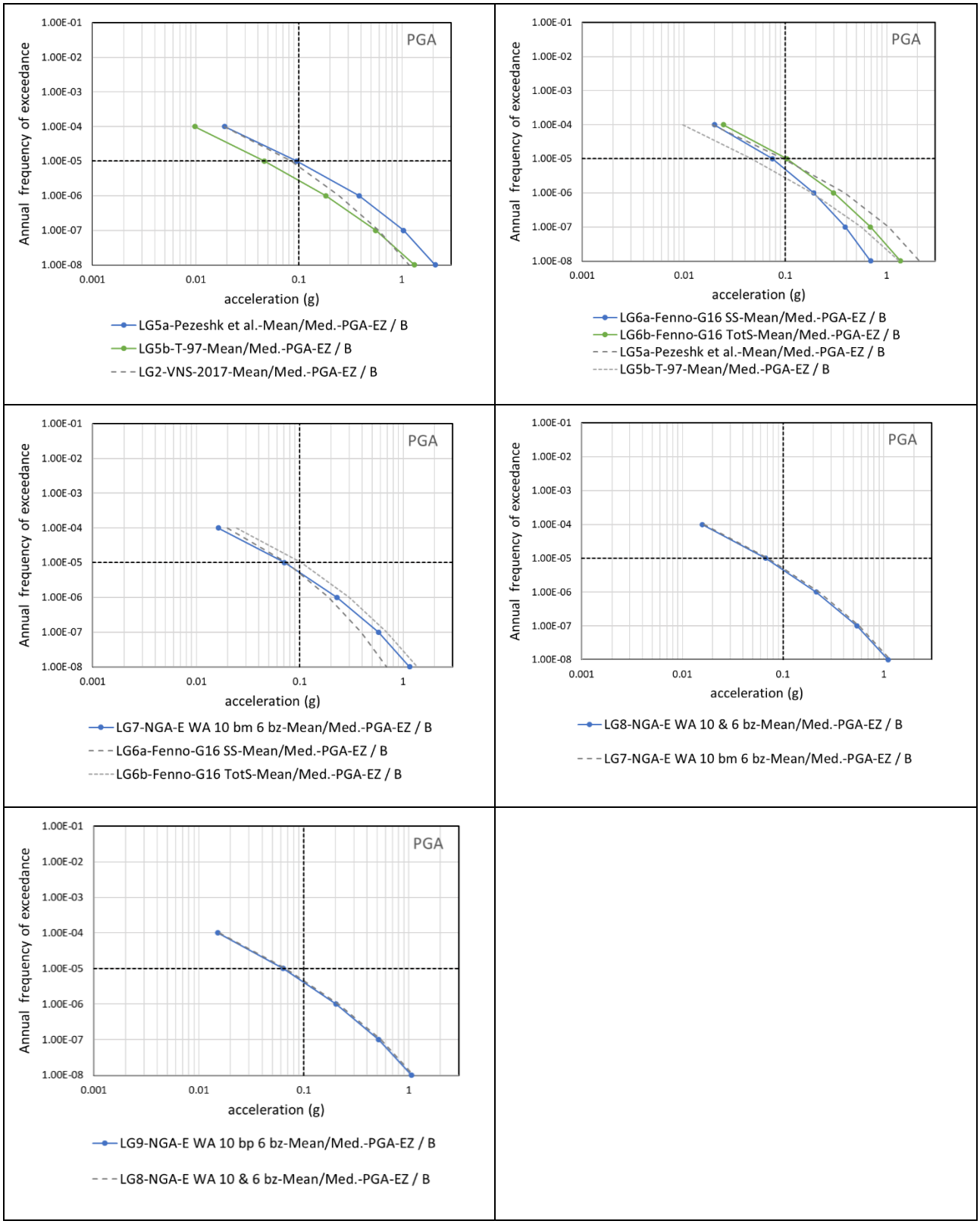

Figure L4 (continued). *The Loviisa SENSEI GMPE sensitivity results for the Table L2 models. The name of the model, from LG1 to LG9, is given in the legend of each graph. Models LG3 and LG4 were not computed. EZ = EZ-FRISK software, B = computation by calculation group member "B".*

The next step provided an idea about GMPEs. We chose a few GMPEs for the rest of this study. The suggested parameter choices are listed in Table L3.

Comparing the LG1 and LG2 models shows that raising the M_{max} had a significant effect on the hazard at low AFE values. This effect is well known from literature. Comparing model LG5 to LG2 shows that both the Pezeshk et al. (2011) and T-97 GMPE used for Hanhikivi imply slower attenuation of the ground motion in terms of PGA than the VNS-2017 GMPE used in the Loviisa-Olkiluoto study. The significant difference between the Pezeshk et al. and T-97 predictions is also striking. The two hazard curves align almost parallel with each other, with the lower prediction from T-97. These two GMPEs were used in combination, for different ranges of magnitudes, in the hazard calculation for Hanhikivi. However, their significantly different prediction would need to be studied before they are merged into a single hazard model.

The FennoG16 GMPE predictions LG6a and LG6b highlight the importance of randomness of the GMPE prediction to hazard at low AFE values. The total σ (TotS) of FennoG16 is in the range of 0.7-0.85 for different spectral frequencies, and the single-station sigma (SS σ) is between 0.47-0.63 (Fülöp et al. 2020). The lower values of SS σ apply to PGA and high spectral frequencies, and the higher values apply to low spectral frequencies. Comparing LG6a to LG6b shows that σ is responsible for the elevated PGA hazard at low AFE and the slope of the hazard curve. A small σ leads to a steeper hazard curve, and a large σ to a more gently dipping hazard curve.

This observation on the effect of σ on the hazard correlates well with the comparison between LG5 and LG2. The VNS-2017 GMPE has a comparatively low σ at several frequencies, for example, the NewcL σ is in the range 0.179-0.451 for all frequencies except for 70Hz, for which σ is 1.218. The Pezeshk et al. (2011) GMPE has σ in the range of 0.23-0.869 at the frequencies of interest (1Hz, 5Hz, 25Hz, and PGA), FennoG16 has its recommended total σ of 0.7-0.85, and NGA-East GMPE ergodic sigma has a central estimate in the range of 0.529-0.792. Hence, the steeper hazard curves correspond to GMPEs with smaller σ values (i.e., FennoG16 with SS σ and VNS-2017).

Since the models use extensively the NGA-East GMPE model, a short summary of the σ definitions of that GMPE is described, based on Goulet et al (2018), in the following paragraphs.

Repeated recordings at a given NPP site are not available, instead GMPE prediction rely on data collected at a broad range of sites and from different earthquake sources. The ground-motion variability over these sites and sources is assumed to be applicable to the hazard prediction at the individual NPP site (the assumption of ergodicity). Such treatment of the randomness in a ground motion dataset leads to the largest value of σ, called total or ergodic standard deviation. The total σ is calculated from the difference, in natural logarithm units, between an observed and the GMPE predicted ground motion parameter (i.e. the residual), which can be writes as:

$$\Delta_{es} = \delta_{be} + (\delta S2S_{ss} + \delta WS_{es})$$

Where: Δ_{es} is the total residual of the prediction, including the δ_{be} the between events part and the within event part, composed of site-to-site residual ($\delta S2S_{ss}$) and the single-station within-event residual (δWS_{es}).

If repeated recording exists at the site of interest, an attempt can be made to only account for the randomness at that specific site of interest. This randomness should comprise the between-event residual (δ_{be}) and the single-station within-event residual (δWS_{es}) for the NPP site. This treatment

of the GM dataset would lead to a decrease of the randomness leading to a σ specifically to the NPP site, called a single-station sigma σSS,

However, the use of SS σ in the PSHA analysis, would require the estimation of the site term (i.e. how much the median site observations deviates from the median perdition of the GMPE) and its epistemic uncertainty and the epistemic uncertainty of the single-station within-event deviations at different sites within the dataset. Hence, the larger variability of the total σ, would be replaced by a smaller variability (σSS) and two elements of epistemic uncertainty. The advantage is that both epistemic uncertainties are reducible, e.g. by acquiring additional data or knowledge.

The NGA East GMPE provide three estimates for the total/ergodic σ and for the SS sigma. The three estimates are termed "low", "medium" and "high" estimates (Goulet et al, 2018). The FennoG16 GMPE provide estimates for the total and SS σ, but due to data limitations it only recommends the use of the total σ (Fülöp et al, 2020).

Comparison of LG6 and LG7 shows a difference between the FennoG16 and the NGA-East weighted average prediction. NGA-East is a suite of 17 GMPEs for mean prediction of the ground motion with 6 options of σ prediction. There is a significant variation in the mean prediction. In addition, σ is given as single-station σ low, mean and high estimate and ergodic σ low, mean and high estimate. The weighted average GMPE model (NGA-East-WA) used here is weighted between the 17 mean predictions, using weights published together with the GMPEs. For randomness the ergodic σ (ES) central prediction was used. The ES-Central σ of NGA-East is somewhat lower than that of FennoG16 total σ, and the FennoG16 mean prediction is higher than that of the NGA-East WA prediction. The two effects result in an elevated hazard from the FennoG16 model (i.e., LG6 result being above LG7).

The GMPE sensitivity calculations reconfirm that any GMPE must have a well-justified variability/randomness (σ), which can only be achieved by calibration on a large set of ground motions. This condition is not fulfilled by the VNS-2017 GMPE. The option of reducing σ could be interesting to nuclear-related site-specific PSHAs. It could be feasible by separation of the different constituents of the total randomness. Separation would be facilitated by collection of free-field ground motions at NPPs in Finland. The FennoG16 GMPE attempted such a separation, but the SS σ provided is based on very limited data and thus, for the time being, it is recommended to use the total σ (Fülöp et al. 2020). In the rest of the sensitivity study, the most robust option, the NGA-East GMPE, was used. The justification for the use of NGA-East GMPE can be substantiated from the point of view of the quality and quantity of data used in the calibration, the sophistication and effort of data analysis of the developing team and the transparency of the background of the calibration work.

The next step for Loviisa was to assess the sensitivity to other input parameters. The model cases are given in Table L3. They map the variation of hazard with:

- M_{min} (LSen1 to LSen3),
- GMPE (LSen3 vs. LSen4),
- depth distribution (LSen4 to LSen6),
- M_{max} (LSen6 to LSen8),
- SSA delineation (LSen7 vs. LSen9)
- M_{max} distribution versus postulated value (LSen10 vs. LSen11)
- logic-tree complexity (LSen12 vs. LSen11). In model LSen12 the NGA-East GMPE is used with all its 17 mean prediction branches and 3 ergodic σ estimates, resulting in 17×3=51 logic-

tree branches for the GMPE in the NGAE-51 (ES) model. This arrangement accounts for the epistemic uncertainty of ground motion attenuation. This model is a logic-tree with 9(βλ)×5(M_{max})×51(GMPE)×2(zoning)=4590 branches.

Table L3. *Steps for studying sensitivity of the hazard at Loviisa NPP site.*

Model name	SSAs	Activity param. (β, λ)	Depth distr.	GMPE	SSA variation	M_{min}	M_{max}	No. of branches
The reference here is the LSenBR.								
LSen1	10& 6	Mid β, λ with 100%	-	FennoG16 (TotS)	-	2	5.5	1
LSen2	10 & 6	Mid β, λ with 100%	-	FennoG16 (Tot)	-	3	5.5	1
LSen3	10 & 6	Mid β, λ with 100%	-	FennoG16 (Tot)	-	4	5.5	1
LSen4	10 & 6	Mid β, λ with 100%	-	NGAE-W (ES Cen)	-	4	5.5	1
LSen5	10 & 6	Mid β, λ with 100%	0-13km	NGAE-W (ES Cen)	-	4	5.5	1
LSen6	10 & 6	Mid β, λ with 100%	South	NGAE-W (ES Cen)	-	4	5.5	1
LSen7	10 & 6	Mid β, λ with 100%	South	NGAE-W (ES Cen)	-	4	6.5	1
LSen8	10 & 6	Mid β, λ with 100%	South	NGAE-W (ES Cen)	-	4	7.5	1
LSen9	10 & 6	Mid β, λ with 100%	South	NGAE-W (ES Cen)	Split SSA#10	4	6.5	1
LSen10	10&6	Mid β, λ with 100%, host SSA all β, λ's	South	NGAE-W (ES Cen)	Original (0.66) / Split (1/0.33)	4	6.5	18
LSen11	10&6	Mid β, λ 100%, host SSA all β, λ's	South	NGAE-W (ES Cen)	Original (0.66) / Split (1/0.33)	4	M_{max}	90
LSen12	10&6	Mid β, λ 100%, host SSA#10 all β, λ's	South	NGAE-51 (ES)	Original (0.66) / Split (1/0.33)	4	M_{max}	4590

Notes: The hyphen stands for the original parameter setting for the LBasM according to Saari and Malm (2016) and Malm and Kaisko (2017a). Abbreviations: ***Tot*** the total sigma, ***E*** east, ***W*** weighted average, ***ES*** Ergodic sigma, ***Cen*** central branch of the sigma estimate in NGA-East GMPE.

The results of the sensitivity runs are given as pairs of the hazard curve and the corresponding uniform hazard spectra in Figure L5. The effects are discussed sequentially on the left-hand side of the figures.

LSen1: *Starting model uses the FennoG16 GMPE with total σ, $M_{min}2$, and $M_{max}5.5$. Results demonstrate the level of compatibility of the EZ-FRISK and OpenQuake models.*	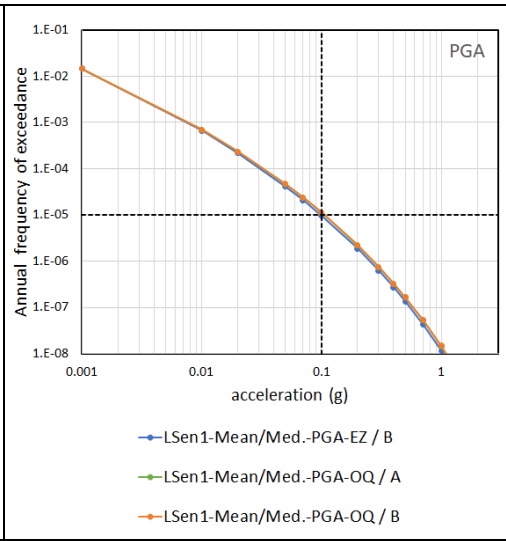	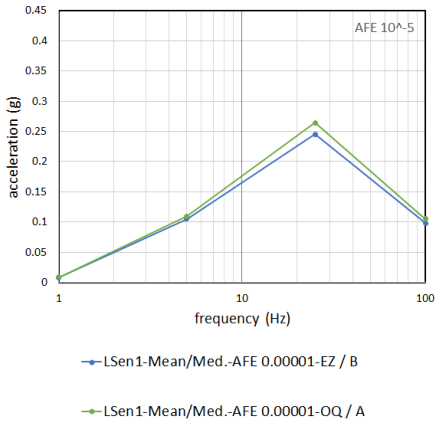
LSen2: *Compared to LSen1 the minimum magnitude was raised from $M_{min}2$ to $M_{min}3$. Results show that PGA hazard decreases, especially at low acceleration levels. No significant effect on AFE 10^{-5} and above.*	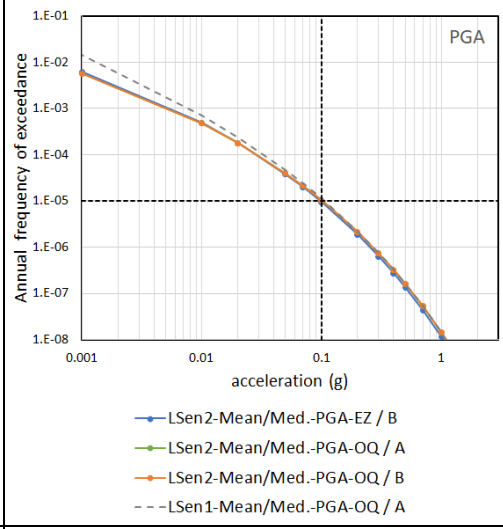	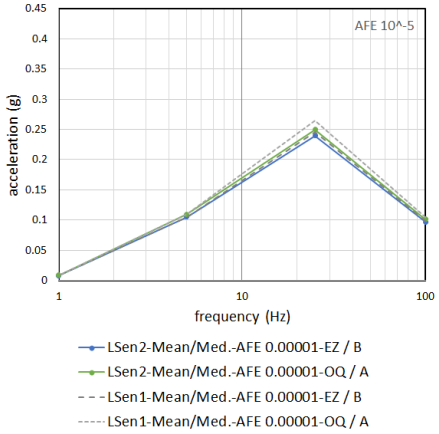
LSen3*: Minimum magnitude raised from $M_{min}3$ to $M_{min}4$. Results show a further decrease in hazards at low acceleration levels. Some effects on AFE 10^{-5}, especially noticeable in the spectra plot.*	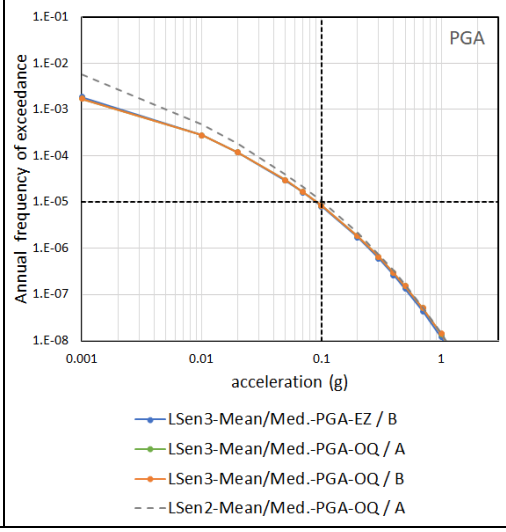	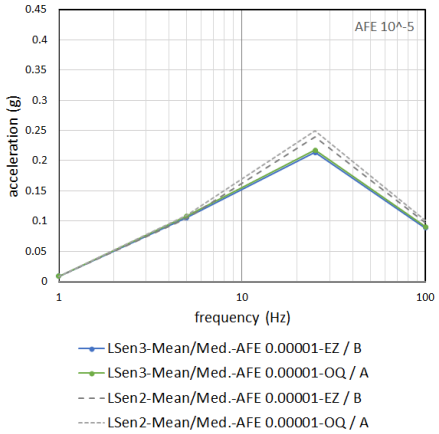

Figure L5. *The Loviisa SENSEI PSHA parameter sensitivity results from Table L3. Note that model LSen12 was revised twice due to small errors uncovered by the expert group of SENSEI. In the table, the final model results LSen12R2 are shown. Additional results are available in the accompanying Excel File of this report. EZ = EZ-FRISK software, OQ = OpenQuake software, A and B = computation by calculation group member "A" or "B".*

LSen4: *GMPE replaced from FennoG16 in LSen3 to the weighted NGA-East GMPE with ergodic σ (central prediction). Results show decrease of hazard, driven by both a lower mean prediction of the GMPE and smaller σ.*	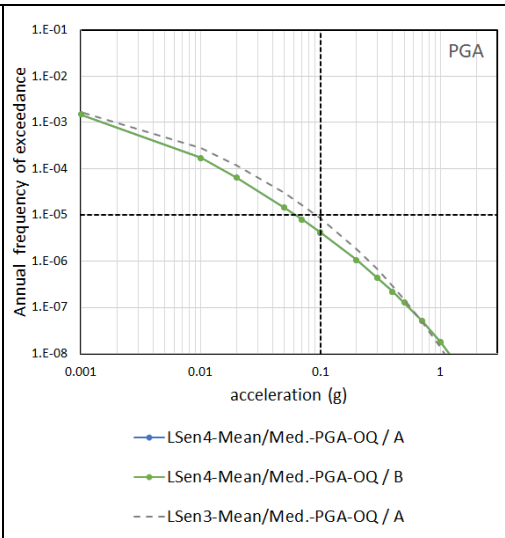	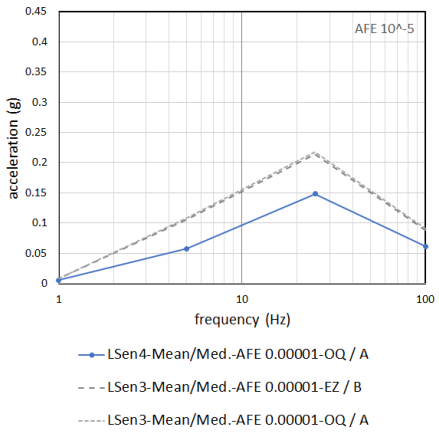
LSen5: *Depth profile changed from uniform 0-35km of earlier models to uniform 0-13km distribution. Hazard increases due to the reduced source volume.*	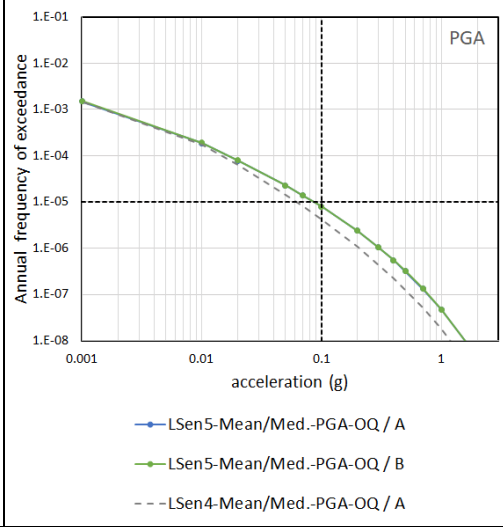	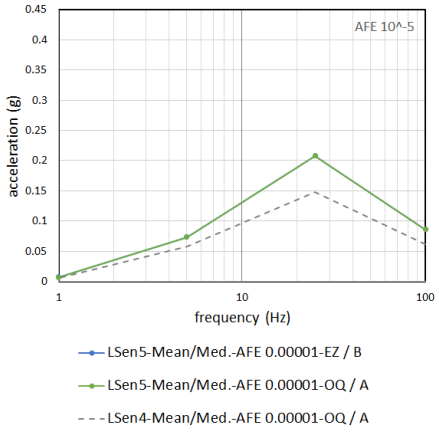
LSen6: *The uniform 0-13km depth profile is replaced with the final "South" depth distribution proposed in SENSEI for the Loviisa and Olkiluoto NPP sites. The hazard remains almost unchanged.*	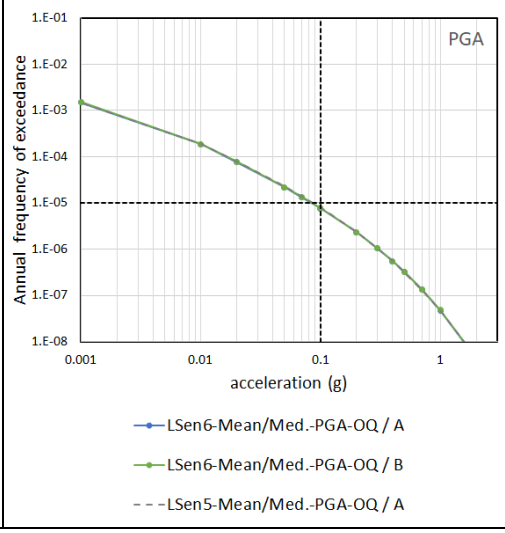	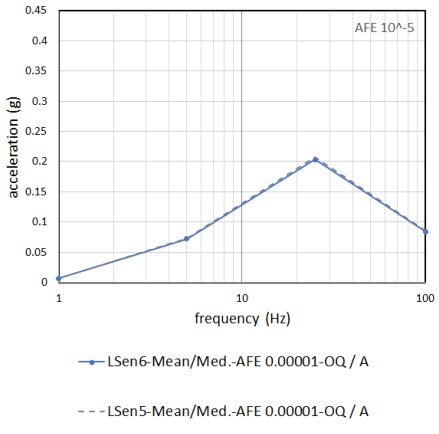

Figure L5 (continued). *The Loviisa SENSEI PSHA parameter sensitivity results from Table L3. Note that model LSen12 was revised twice due to small errors uncovered by the expert group of SENSEI. In the table, the final model results LSen12R2 are shown. Additional results are available in the accompanying Excel File of this report. EZ = EZ-FRISK software, OQ = OpenQuake software, A and B = computation by calculation group member "A" or "B".*

LSen7: *The maximum magnitude is raised from M_w5.5, used in all earlier models to M_{max}=M_w6.5. M_w6.5 is close to the final M_{max} values proposed in the SENSEI project. No significant effect on the hazard.*	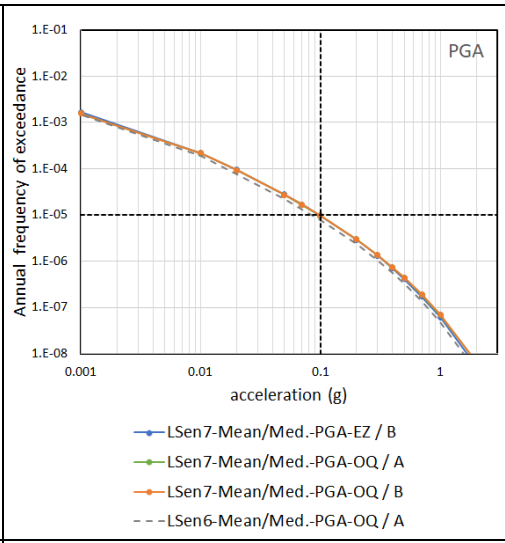	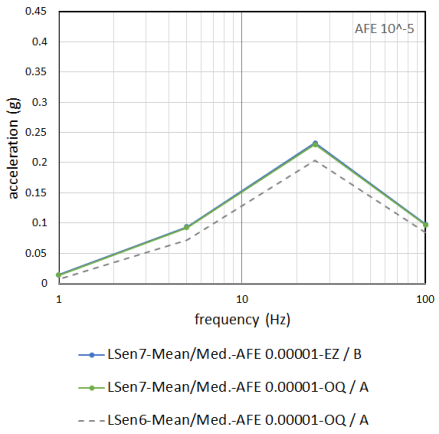
LSen8: *Testing of a hypothetical further increase of M_{max} to M_w7.5 for sensitivity (i.e., value not retained in future models). No significant effect on the hazard.*	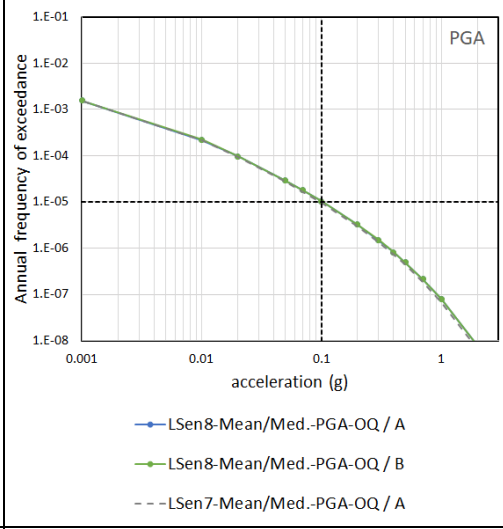	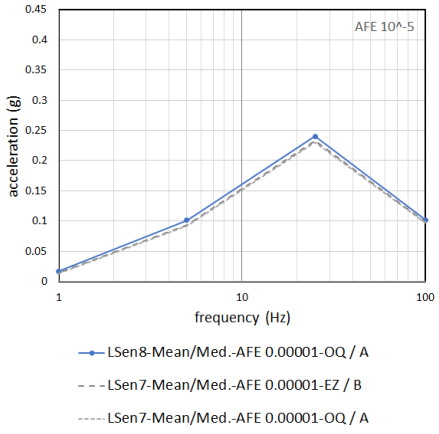
LSen9: *The apparent non-uniformity of seismic activity in the original SSA#10 was noted. SSA#10 was divided, retaining the active part as #SSA10 and assigning the remaining part to SSA#6. The division increases the hazards significantly.*	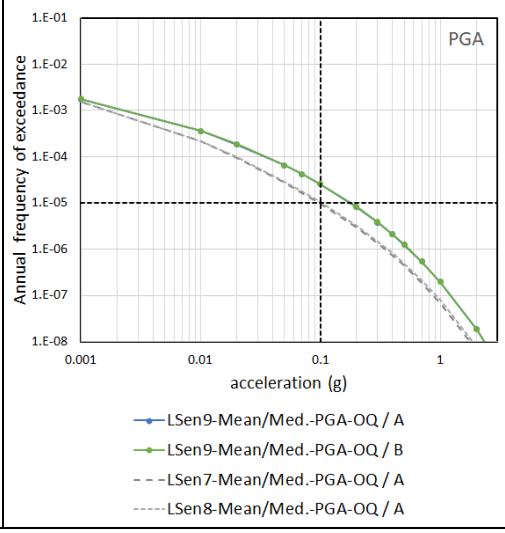	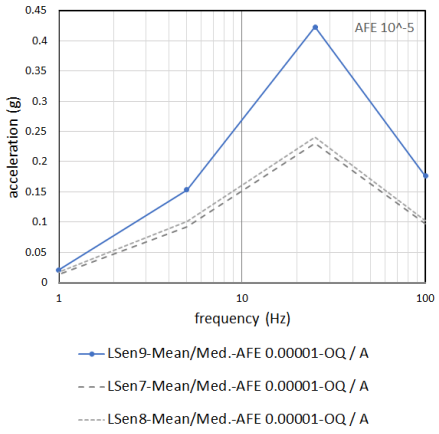

Figure L5 (continued). *The Loviisa SENSEI PSHA parameter sensitivity results from Table L3. Note that model LSen12 was revised twice due to small errors uncovered by the expert group of SENSEI. In the table, the final model results LSen12R2 are shown. Additional results are available in the accompanying Excel File of this report. EZ = EZ-FRISK software, OQ = OpenQuake software, A and B = computation by calculation group member "A" or "B".*

LSen10: *First model with logic-tree. Original SSA#10 included with 66% weight and the divided SSA#10 from LSen9 with 33% weight. The uncertainty in β and λ, reported in the original hazard studies for SSA#10, was included in the model (i.e. 9 branches).*	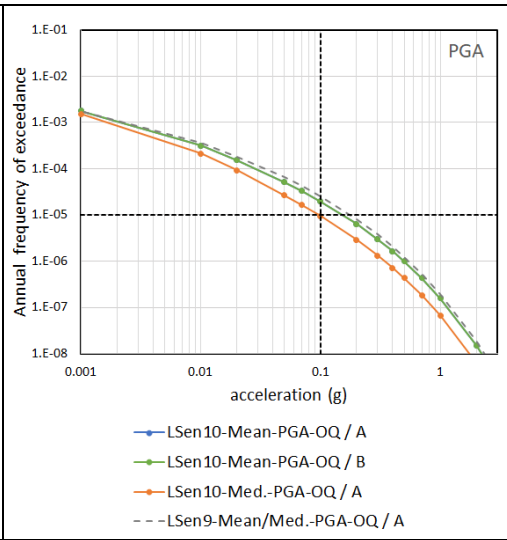	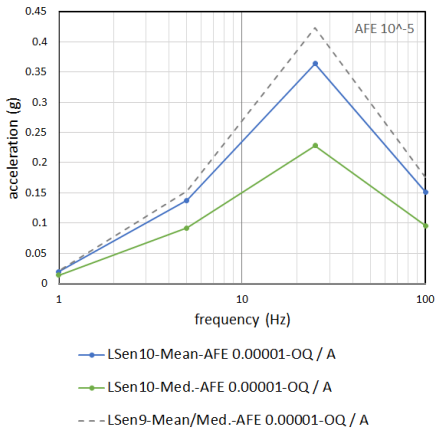
LSen11: *In addition to the branches from LSen10, the M_{max} uncertainty is included. The M_{max} distribution in SENSEI is based on the Bayesian method. The median M_{max} is M_w6.64, not far from M_w6.5 used in earlier models.*	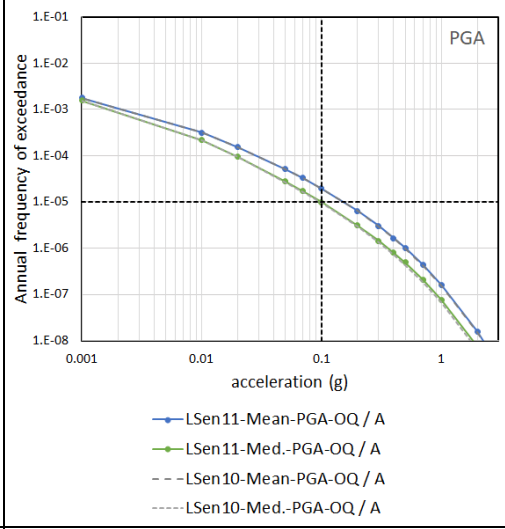	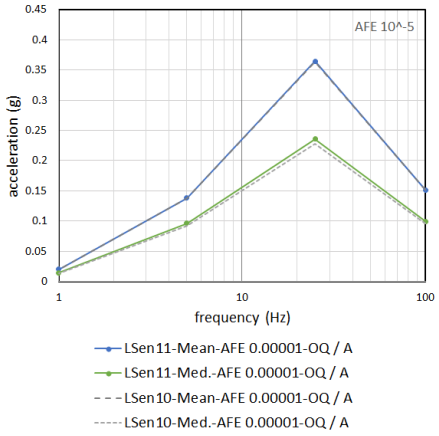
LSen12(R2): *The NGA East GMPE is branched to the 17 branches. The central estimate of ergodic σ is also branched to "high", "central" and "low" predictions. Mean hazard increasingly exceeds the median hazard.*	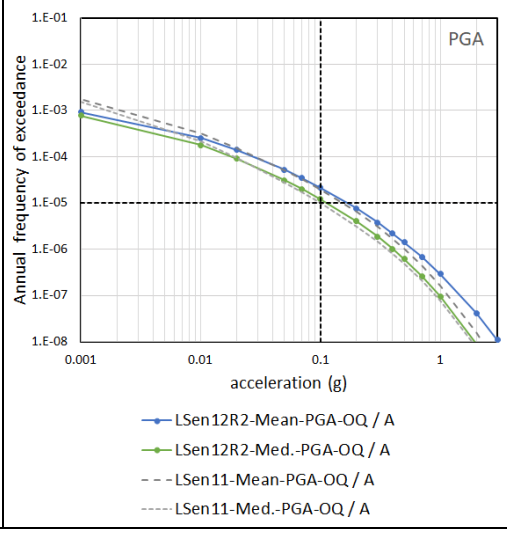	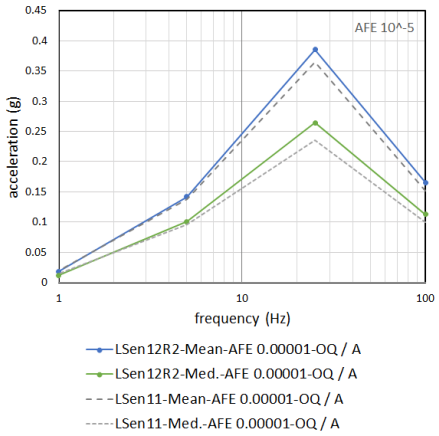

Figure L5 (continued). *The Loviisa SENSEI PSHA parameter sensitivity results from Table L3. Note that model LSen12 was revised twice due to small errors uncovered by the expert group of SENSEI. In the table, the final model results LSen12R2 are shown. Additional results are available in the accompanying Excel File of this report. OQ = OpenQuake software, A and B = computation by calculation group member "A" or "B".*

In addition to the frequencies of the spectra presented in Figure L5, the LSen12 model has been extended to include all the spectral frequencies supported in the NGA-East GMPE. The comparison of the results is shown in Figure L6. While the frequencies chosen for the general analysis appear to be appropriate, there are two important issues to highlight. Firstly, the spectra peaks at between 20Hz and 25 Hz. There appears to be a plateau at these frequencies in the spectra. Secondly, the PGA hazard is generally plotted at 100Hz in the SENSEI project. In reality the NGA-East GMPE differentiates between 100Hz and PGA, and in Figure L6.b the PGA output is plotted at 250Hz differentiating it from the 100Hz output.

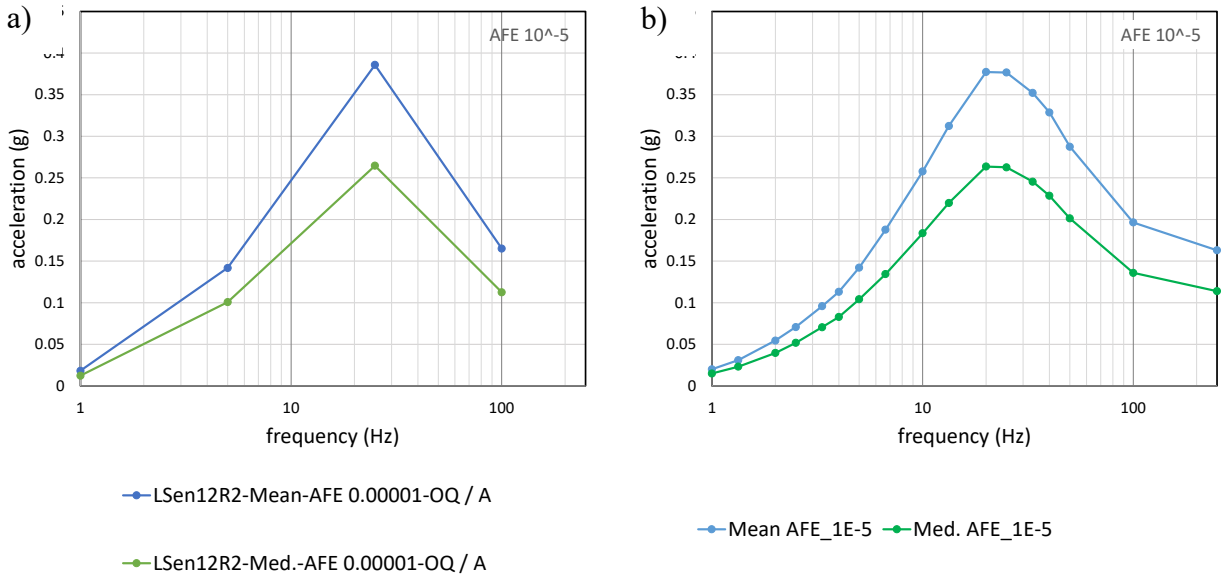

Figure L6. *The Loviisa SENSEI PSHA results using model LSen12(R2). Comparison of the calculated frequencies for the general results (i.e. 1Hz, 5Hz, 25 Hz and PGA) and for the detailed results with all frequencies supported in NGA-East.*

The depth distributions used in the SENSEI project are modified compared to the uniform distributions used in the initial models. The depth profiles used were based on the observed depths of earthquakes in Fennoscandia. The dataset was generically divided to two groups at 63° latitude. The south group had a mean depth of only 4.2km, as it was partly populated with shallow Rapakivi events. The North group had a mean depth of 10.3km. The depth distribution used in the models was lognormal with the parameters given in Table L4.

Table L4. *Depth profile for the SENSEI sensitivity models for the North (Hanhikivi) and South of Finland (Olkiluoto and Loviisa)*

	Earthquakes included in the analysis	Distribution parameter from the data		Depth cutoff (km)
		Mean $\log_{10}$(d)	STD $\log_{10}$(d)	
SENSEI - North	latitude > 63°	1.0122	0.3193	45
SENSEI - South	latitude <= 63° (significant number of Rapakivi events)	0.6221	0.4381	35

5. Calculation sequence for Olkiluoto

The key parameters of the hazard model and the baseline values in PGA hazard for the Olkiluoto PSHA are collected in Figures O1a, O1b, O1c, and O1d.

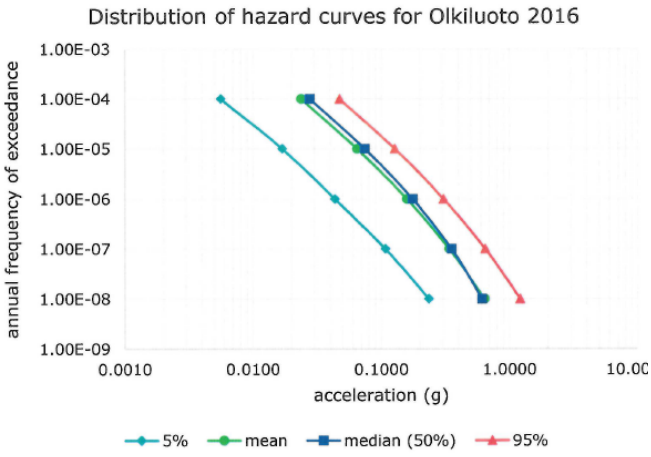

Figure O1a) Median PGA hazard from the "2016" study is the baseline we try to compare to in SENSEI (Figure 3-2 in Saari and Malm 2016).

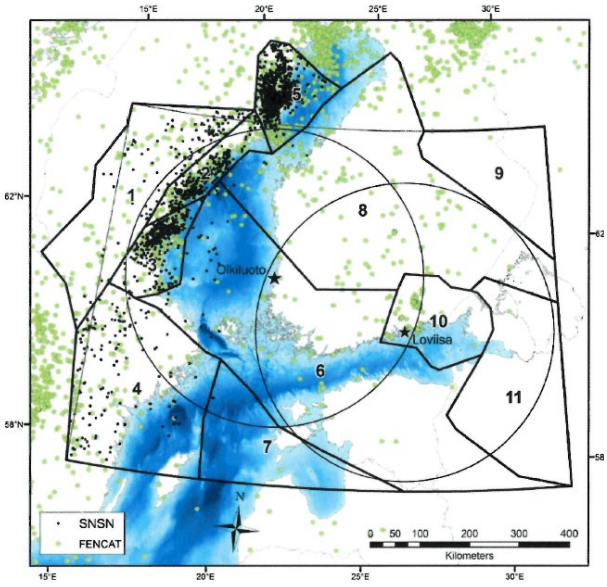

Figure O1b) The result in Figure O1a has been obtained using the source area model shown here (Figure 2-1 in Saari and Malm 2016).

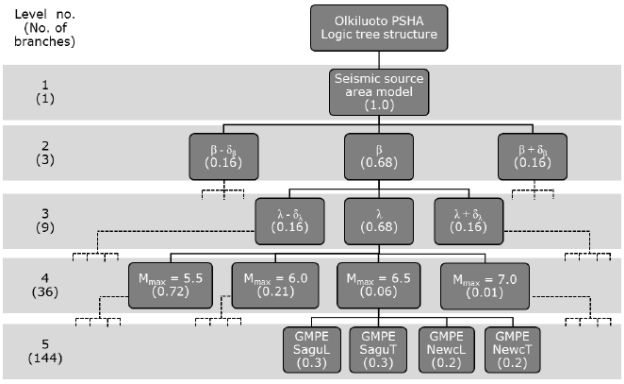

Figure O1c) The logic tree for the results in O1a (Figure 1-2 in Malm and Kaisko 2017a).

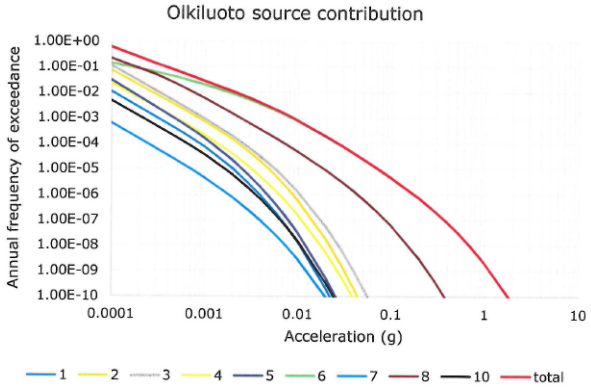

Figure O1d) The contributions of the source areas to the hazard in O1a (Figure 3-4 in Saari and Malm 2016)

The Olkiluoto baseline results (OBasR), the PGA median hazard curve, and median spectral acceleration (in units of g) for AFE of 10^{-5} are presented in Figure O2. The results of the sensitivity computations are compared to the OBasR.

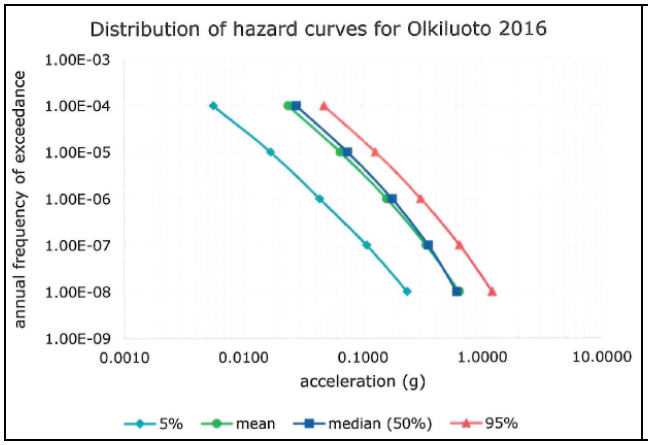

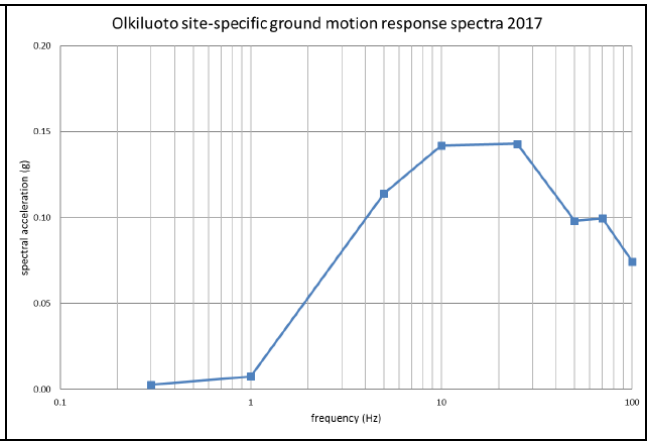

***Figure O2**. The Olkiluoto baseline results (OBasR): PGA median hazard curve (blue line) and median spectral acceleration (in g) for annual frequency of exceedance of 10^{-5} (Saari and Malm 2016; Malm and Kaisko 2017a).*

***Table O1.** Steps to synthetize the Olkiluoto baseline PSHA model (OBasM).*

Model name	SSAs	Activity parameters (β, λ)	Depth distr.	GMPE	SSA variation	M_{min}	M_{max}	No. of branches
The reference results in the synthetizing process are the OBasR (e.g., Figure O2).								
OBasM	-	-	-	-	-	-	-	144
*	6 & 8	Mid branches (β, λ) with 100%	-	-	-	-	-	16
**	6 & 8	Mid branches (β, λ) with 100%	-	-	-	-	5.5/6/6.5 /7	4 (for each M_{max})
OSenBM	*6 & 8*	*Mid β, λ with 100%*	-	-	-	-	*5.5*	*4*
The outcome is the OSenBM with OSenBR								

Note: The hyphen stands for the original parameter setting for the OBasM according to Saari and Malm (2016) and Malm and Kaisko (2017a). The two models (i.e. * and **) are of intermediate complexity. OSenBM was not computed; instead, comparisons in SENSEI are to the OBasM model.

The next step was to compute the sensitivity study models given in Table O2. Since NGA-East has a limited validity range, we could not compute these models without setting up a compatible M_{min}. Similar to the Loviisa site, the first steps in Table O2 constituted a sensitivity study for M_{min}, followed by the effect of GMPE, depth distribution, M_{max} and logic-tree complexity, leading to the most complex model developed, OSen8. The seismic source zones were not altered, but SSA6 and SSA8 were preserved from OBasM.

***Table O2.** Steps for studying sensitivity of the hazard at Olkiluoto NPP site.*

Model name	SSAs	Activity parameters (β, λ)	Depth distr.	GMPE	SSA variation	M_{min}	M_{max}	No. of branches
The reference here is the OSenBR.								
OSen1	6 & 8	Mid β, λ with 100%	0-35km	FennoG16 (Tot)	-	2	5.5	1
OSen2	6 & 8	Mid β, λ with 100%	0-35km	FennoG16 (Tot)	-	4	5.5	1
OSen3	6 & 8	Mid β, λ with 100%	0-35km	NGAE-W (ES Cen)	-	4	5.5	1
OSen4	6 & 8	Mid β, λ with 100%	0-35km	NGAE-W (ES Cen)	-	4	6.5	1
OSen5	6 & 8	Mid β, λ with 100%	South	NGAE-W (ES Cen)	-	4	6.5	1

OSen6	6 & 8	Mid β, λ with 100%, host SSA all β, λs	South	NGAE-W (ES Cen)	-	4	6.5	9
OSen7	6 & 8	Mid β, λ with 100%, host SSA all β, λs	South	NGAE-W (ES Cen)	-	4	M_{max}	45
OSen8	6 & 8	Mid β, λ with 100%, host SSA all β, λs	South	NGAE-51 (ES)	-	4	M_{max}	2295

Notes: The hyphen stands for the original parameter setting for the OBasM according to Saari and Malm (2016) and Malm and Kaisko (2017a). Abbreviations: ***Tot*** total sigma, ***E*** east, ***W*** weighted average, ***ES*** Ergodic sigma, ***Cen*** central branch of the sigma estimate in NGA-East GMPE. The OSen8 model has a logic-tree with 9(βλ)×5(M_{max})×51(GMPE) =2295 branches.

The results of the sensitivity runs are given as pairs of the hazard curve and the corresponding uniform hazard spectra in Figure O3. The effects are discussed sequentially on the left-hand side of the figures.

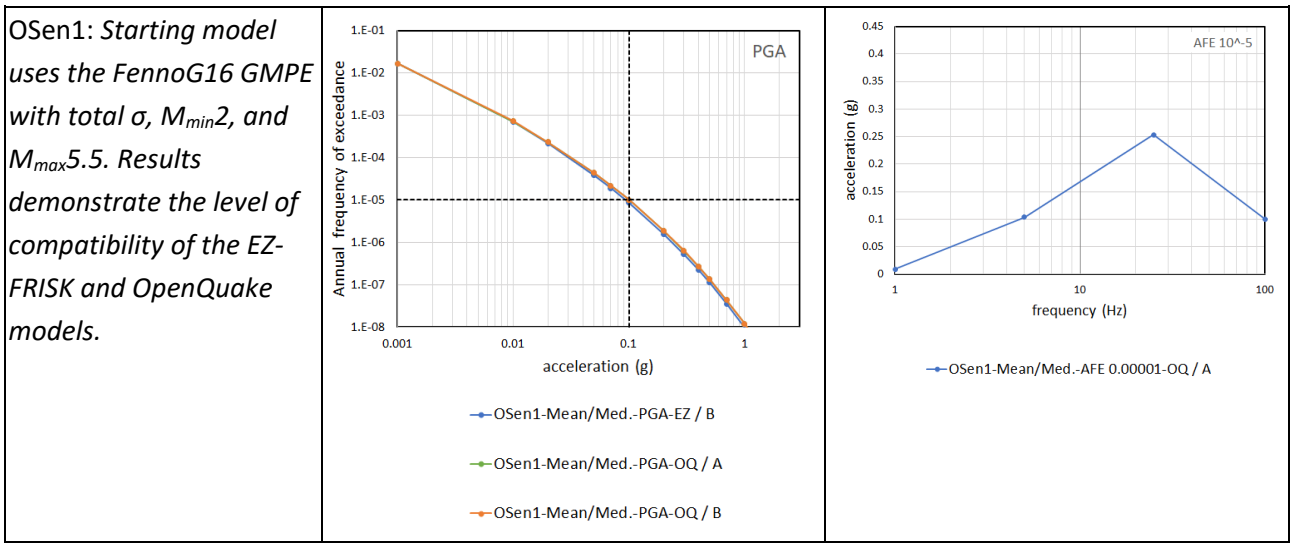

Figure O3. *The Olkiluoto SENSEI PSHA parameter sensitivity results following Table O2. As in the case of the other sites Revision 2 (R2) of the final model is reported. Additional results are available in the accompanying Excel File of this report. EZ = EZ-FRISK software, OQ = OpenQuake software, A and B = computation by calculation group member "A" or "B".*

OSen2: *Compared to OSen1 the minimum magnitude was raised from $M_{min}2$ to $M_{min}4$. Results show that PGA hazard decreases, especially at high AFE levels. Also, a noticeable reduction at AFE 10^{-5} at 25Hz.*	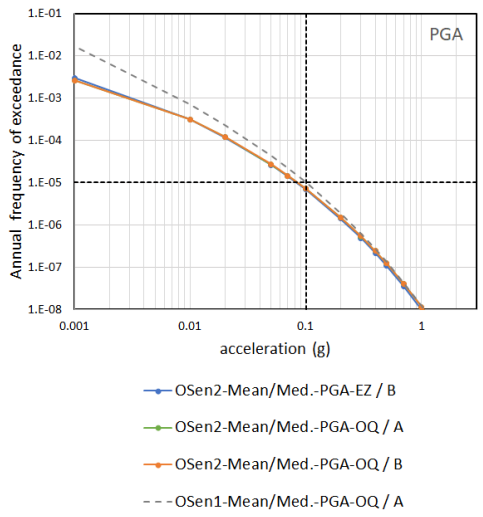	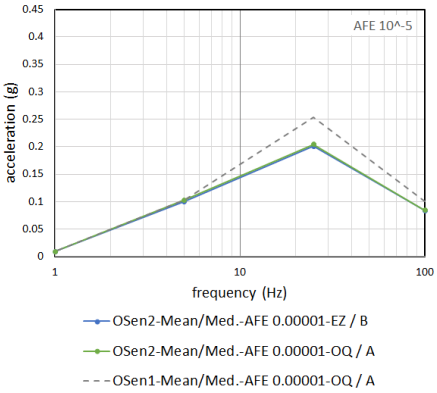
OSen3: *GMPE replaced from FennoG16 in OSen2 to the weighted NGA-East GMPE with ergodic σ (central prediction). Results show decrease of hazard, driven by both a lower mean prediction of the GMPE and smaller σ. The reduction of the 5Hz, 25Hz, and PGA in the spectra can also be noted.*	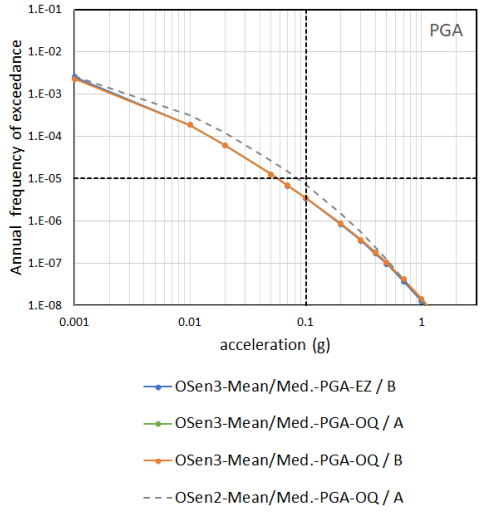	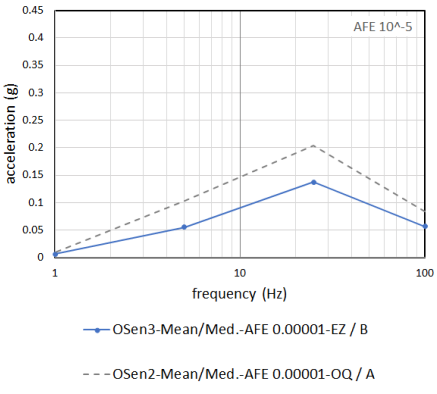
OSen4: *The maximum magnitude is raised from M_w5.5, used in all earlier models to M_{max}=M_w6.5. M_w6.5 is close to the final M_{max} values proposed in the SENSEI project. No significant effect on the hazard curve.*	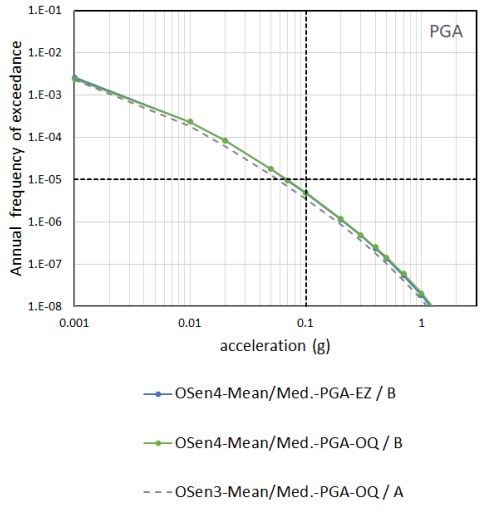	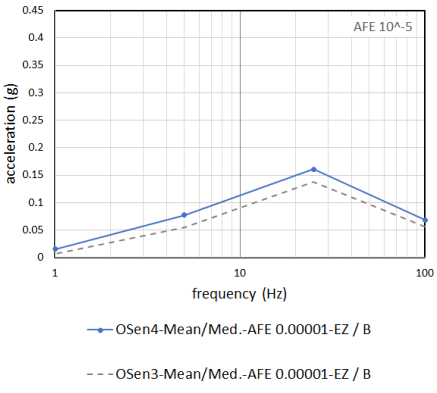

Figure O3 (continued). *The Olkiluoto SENSEI PSHA parameter sensitivity results following Table O2. As in the case of the other sites Revision 2 (R2) of the final model is reported. Additional results are available in the accompanying Excel File of this report. EZ = EZ-FRISK software, OQ = OpenQuake software, A and B = computation by calculation group member "A" or "B".*

OSen5: *The uniform 0-35km depth profile is replaced with the final "South" depth distribution proposed in SENSEI for the Loviisa and Olkiluoto NPP sites. The hazard remains unchanged at low acceleration levels, but starts to differ at 0.01g. Also, some increase throughout the spectra.*	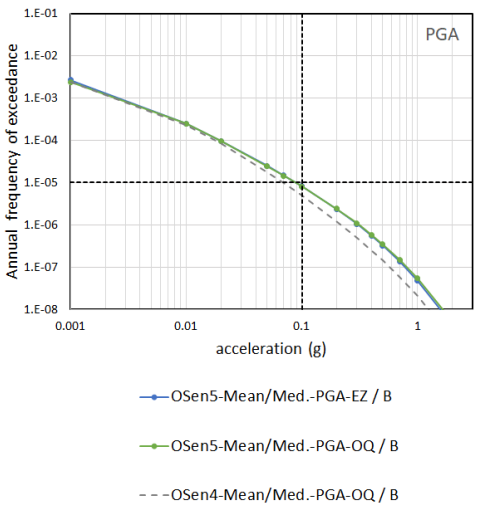	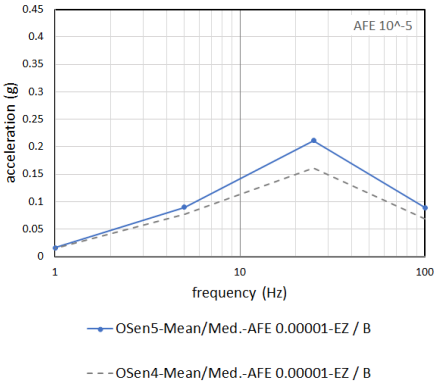
OSen6: *The uncertainty in β and λ, reported in the original hazard studies for SSA#6, was included in the model (i.e., 9 branches). The mean hazard is slightly increased and median hazard slightly decreased.*	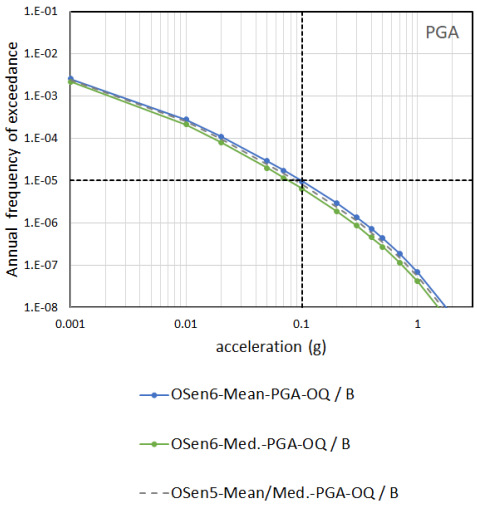	NA
OSen7: *In addition to the branches from OSen6, the M_{max} uncertainty is included. The M_{max} distribution proposed in SENSEI is based on the Bayesian method. The median M_{max} is M_w6.64, not very far from the M_w6.5 used in earlier models. Mean hazard increasingly exceeds the median hazard.*	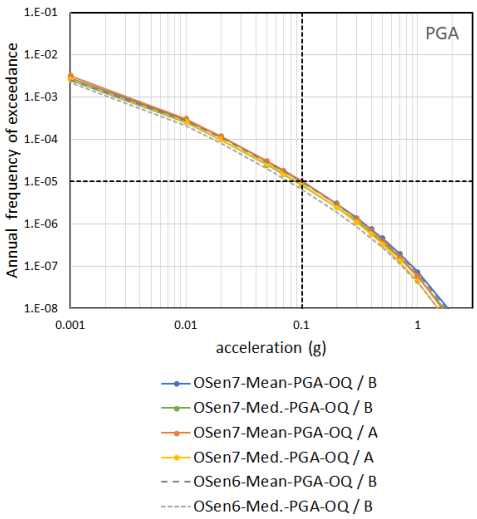	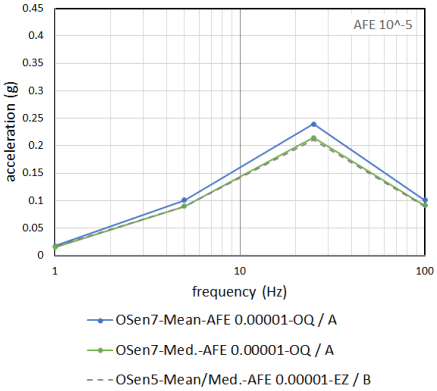

Figure O3 (continued). *The Olkiluoto SENSEI PSHA parameter sensitivity results following Table O2. As in the case of the other sites Revision 2 (R2) of the final model is reported. Additional results are available in the accompanying Excel File of this report. EZ = EZ-FRISK software, OQ = OpenQuake software, A and B = computation by calculation group member "A" or "B".*

OSen8(R2): *The NGA East weighted average GMPE is branched at the 17 branches of the NGA-East GMPE. The central estimate of ergodic σ is also branched to "high", "central" and "low" predictions. Mean hazard increasingly exceeds the median hazard.*	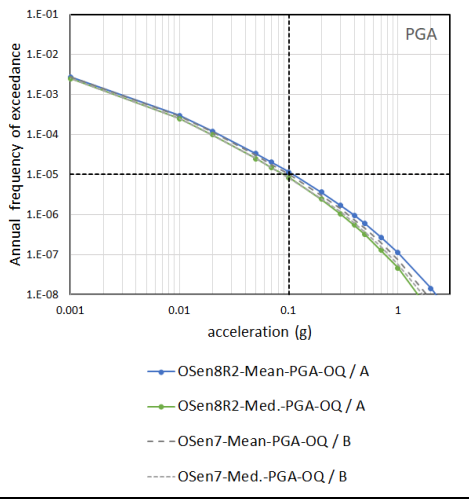	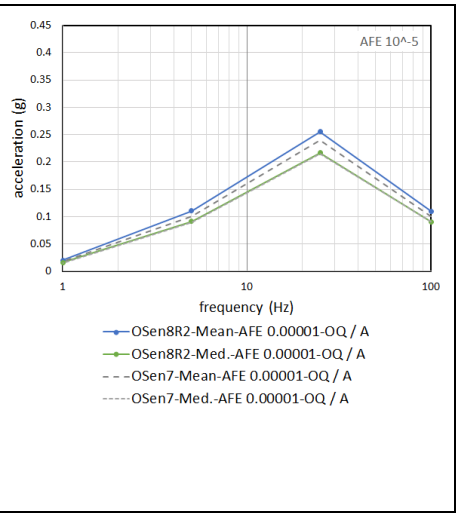

Figure O3 (continued). *The Olkiluoto SENSEI PSHA parameter sensitivity results following Table O2. As in the case of the other sites Revision 2 (R2) of the final model is reported. Additional results are available in the accompanying Excel File of this report. OQ = OpenQuake software, A and B = computation by calculation group member "A" or "B".*

6. Calculation sequence for Hanhikivi

The key parameters of the previous hazard model and the baseline values in PGA hazard for the Hanhikivi PSHA are collected in Figures H1a, H1b, H1c, and H1d.

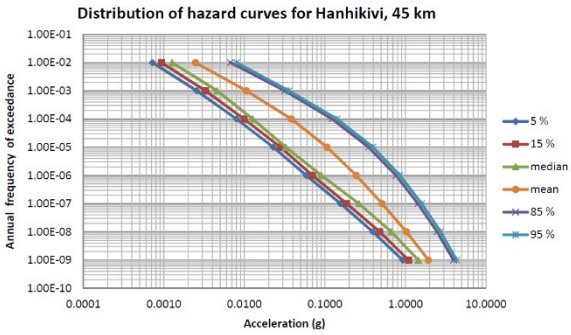

Figure H1a) Median PGA hazard (green line) from the "2015" study is the baseline we try to compare to in SENSEI (Figure 6.1.2 in Saari et al. 2015).

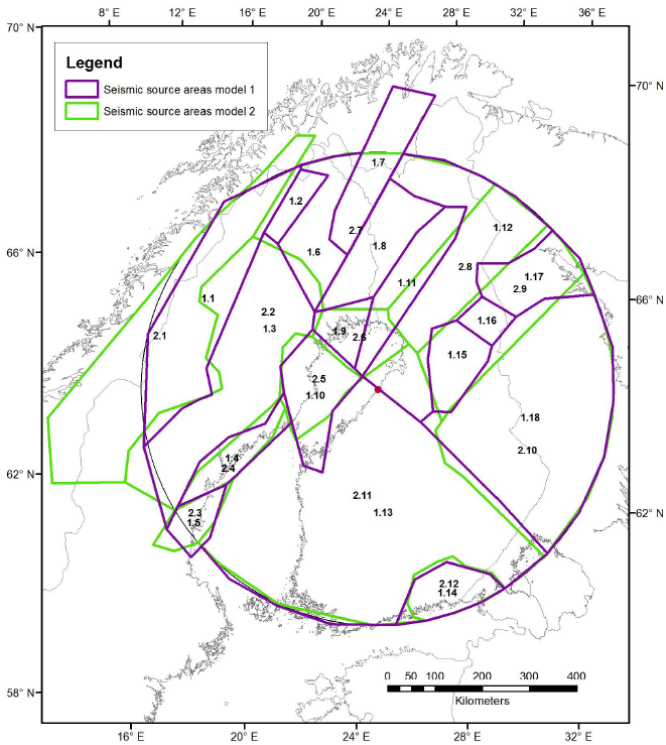

Figure H1b) The result in Figure H1a has been obtained using the source area models 1 (purple) and 2 (green) (Figure 9.5.1 in Korja and Kosonen 2015).

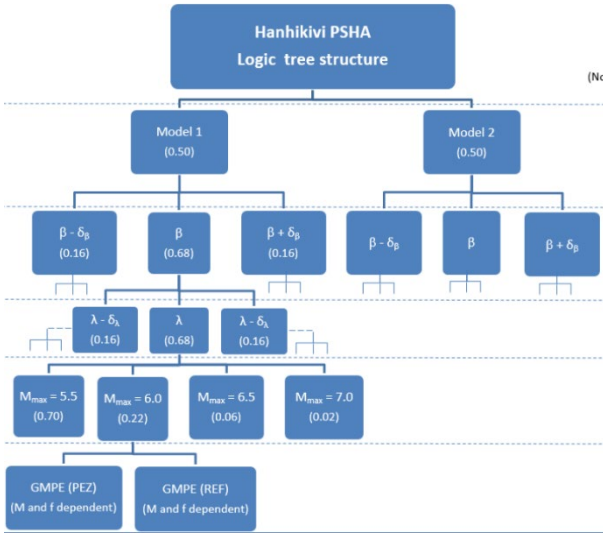

Figure H1c) The logic tree for the results in H1a (Figure 5.1.1 in Saari et al. 2015).

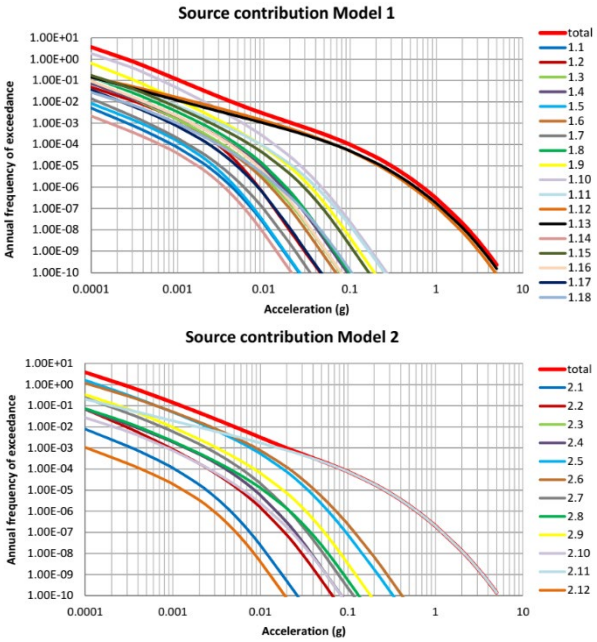

Figure H1d) The contributions of the source areas to the hazard in H1a (Figures 6.1.3a-b in Saari et al. 2015)

The Hanhikivi baseline results (HBasR), PGA median hazard curve, and median spectral acceleration (in g) for AFE of 10^{-5} are presented in Figure H2. The results of the sensitivity computations are compared to HBasR. The synthetized baseline PSHA model is described in Table H1.

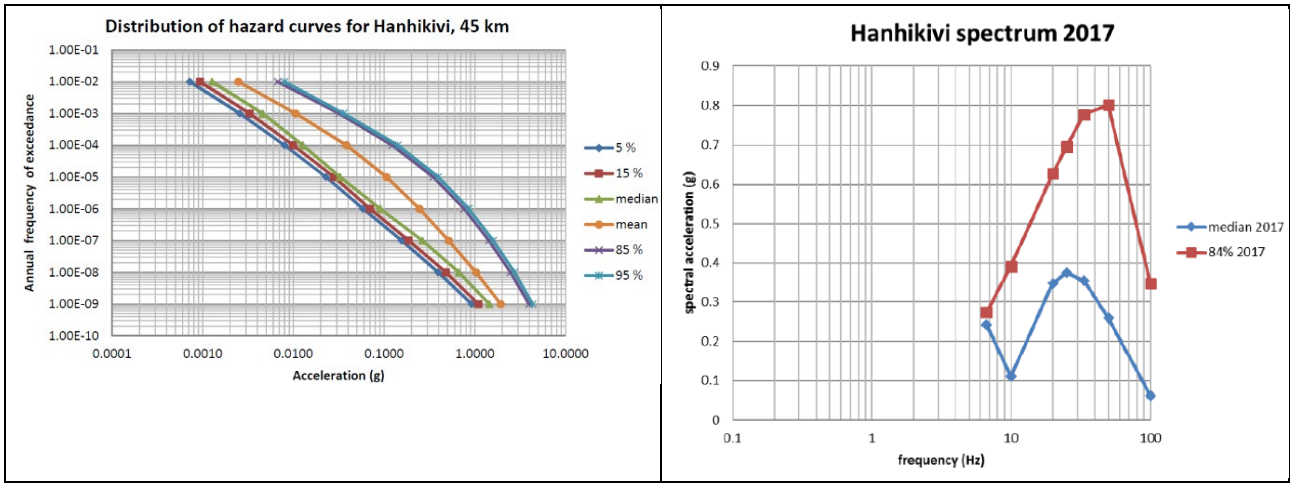

Figure H2*. The Hanhikivi baseline results (HBasR): PGA median hazard curve (green line) and median spectral acceleration (in g, blue line) for annual frequency of exceedance of 10^{-5} (Saari et al. 2015; Malm and Kaisko 2017b).*

An additional complexity of the Hanhikivi model is that two alternative SSA divisions were used in the original study, called Map1 and Map2. In the synthetization process, SSAs 1.10, 1.12 and 1.13 were retained from Map1, and 2.6, 2.7 and 2.11 from Map2.

Table H1. *Steps to synthetize the Hanhikivi baseline PSHA model (HBasM).*

Model name	SSAs	Activity parameters (β, λ)	Depth distr.	M_{min}	M_{max}	No. of branches
The reference results in the synthetizing process are the HBasR (e.g., Figure H2)						
HBasM	-	-	-	-	-	144
*	1.12, 1.13 1.10, 2.11, 2.6, 2.7	Mid branches (β, λ) with 100%	-	-	-	16
**	1.12, 1.13 1.10, 2.11, 2.6, 2.7	Mid branches (β, λ) with 100%	-	-	5.5/6/ 6.5/7	4 (for each M_{max})
HSenBM	*1.12, 1.13 1.10, 2.11, 2.6, 2.7*	*Mid β, λ with 100%*	-	-	*5.5*	*4*
The outcome is the HSenBM with HSenBR						

Note: The hyphen stands for the original parameter setting for the HBasM according to Saari et al. (2015) and Malm and Kaisko (2017b). The two models (i.e. * and **) are of intermediate complexity. HSenBM not computed. HSenBM was not computed; instead, comparisons in SNSEI are to the HBasM model.

The next step was to compute the sensitivity study models of Table H2. The first lines in Table H2 constituted a sensitivity study for M_{min}, followed by sensitivity for GMPE, depth distribution, M_{max} and seismic source zone maps. In addition to the original Map1 and Map2, SENSEI developed a new seismic source zoning called Map4, comprising SSA 2.6 from Map2 and SSAs 5 and 8 from the Loviisa-Olkiluoto seismic source zone map (see Figure L1b or Figure O1b). In Map4, SSA8 became the host zone for the Hanhikivi NPP site, which was not the intention of the developers of the Olkiluoto-Loviisa zoning. Hence, Map 4 models can uncover unintended bias of zoning design.

The depth distribution developed in the SENSEI project for earthquakes in the North is deeper than the South distribution used for Loviisa and Olkiluoto (Table L4). Compared to the original studies, which assumed a uniform probability of earthquake in the depth ranges of 0-35km for most source zones and 0-45km for a few zones, the North distribution has a higher concentration on shallower earthquakes.

Table H2. *Steps for studying different types of sensitivity of the hazard at the Hanhikivi site.*

Model name	SSAs	Activity parameters (β, λ)	Depth distr.	GMPE	M_{min}	M_{max}	No. of branches
The reference for comparing all the results from these models is HSenBR							
HSen1	Map1,2	Mid β, λ	-	FennoG16 (Tot)	2	5.5	2
HSen2	Map1,2	Mid β, λ	-	FennoG16 (Tot)	3	5.5	2
HSen3	Map1,2	Mid β, λ	-	FennoG16 (Tot)	4	5.5	2
HSen4	Map1,2	Mid β, λ	-	NGAE-W (ES Cen)	4	5.5	2
HSen5	Map1,2,4	Mid β, λ	-	NGAE-W (ES Cen)	4	6.5	3
HSen6	Map1,2,4	Mid β, λ	North	NGAE-W (ES Cen)	4	6.5	3
HSen7	Map1,2,4	Mid β, λ	North	NGAE-W (ES Cen)	4	M_{max}	15
HSen8	Map1	Mid β, λ with 100%, host SSA all β, λs	North	NGAE-W (ES Cen)	4	M_{Max}	45
HSen9	Map2	Mid β, λ with 100%, host SSA all β, λs	North	NGAE-W (ES Cen)	4	M_{Max}	45
HSen10	Map4	Mid β, λ with 100%, host SSA all β, λs	North	NGAE-W (ES Cen)	4	M_{Max}	45
HSen11	Map1,2,4 (0.33 each)	Mid β, λ with 100%, host SSA all β, λs	North	NGAE-W (ES Cen)	4	M_{Max}	135
HSen12	Map1,2,4 (0.33 each)	Mid β, λ with 100%, host SSA all β, λs	North	NGAE-51 (ES)	4	M_{Max}	6885

Note: The HSen12 model has a logic-tree with 9(βλ)×5(M_{max})×51(GMPE)×3(zoning)=6885 branches.

The results of the sensitivity runs are given as pairs of the hazard curve and the corresponding uniform hazard spectra in Figure H3. The effects are discussed sequentially on the left-hand side of the figures.

HSen1: *Starting model uses the FennoG16 GMPE with total σ, M_{min}2, and M_{max}5.5. Results demonstrate the level of compatibility of the EZ-FRISK and OpenQuake models. In addition, the difference between Map1 and Map2 can be assessed.*

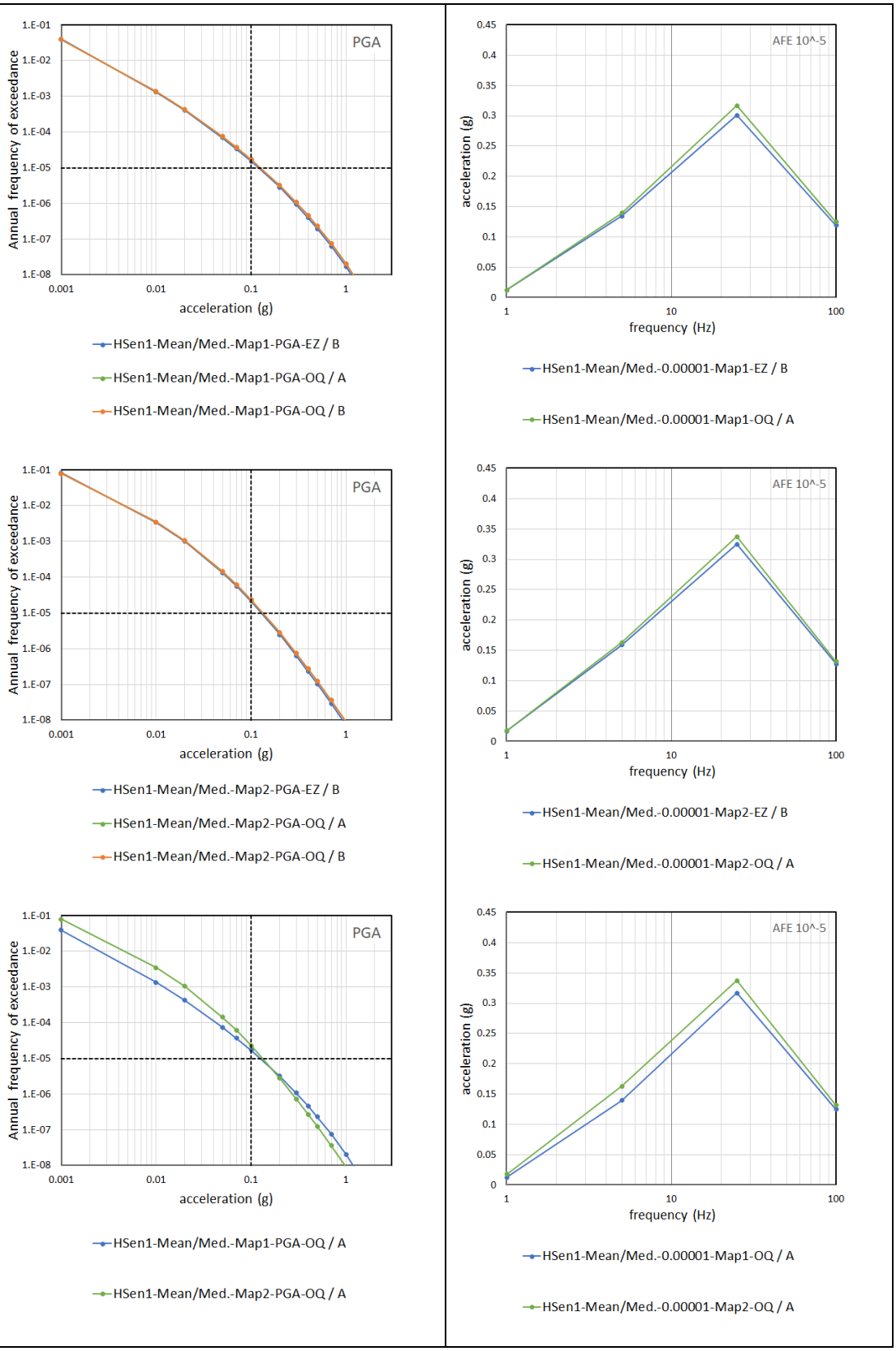

Figure H3. *The Hanhikivi SENSEI PSHA parameter sensitivity results following Table H2. As in the case of the other sites Revision 2 (R2) of the final model (HSen12) is reported. Additional results are available in the accompanying Excel File of this report. EZ = EZ-FRISK software, OQ = OpenQuake software, A and B = computation by calculation group member "A" or "B".*

HSen2: *Compared to HSen1 the minimum magnitude was raised from $M_{min}2$ to $M_{min}3$. Results show that PGA hazard decreases at low acceleration levels. Also, a small reduction at AFE 10^{-5} spectra.*

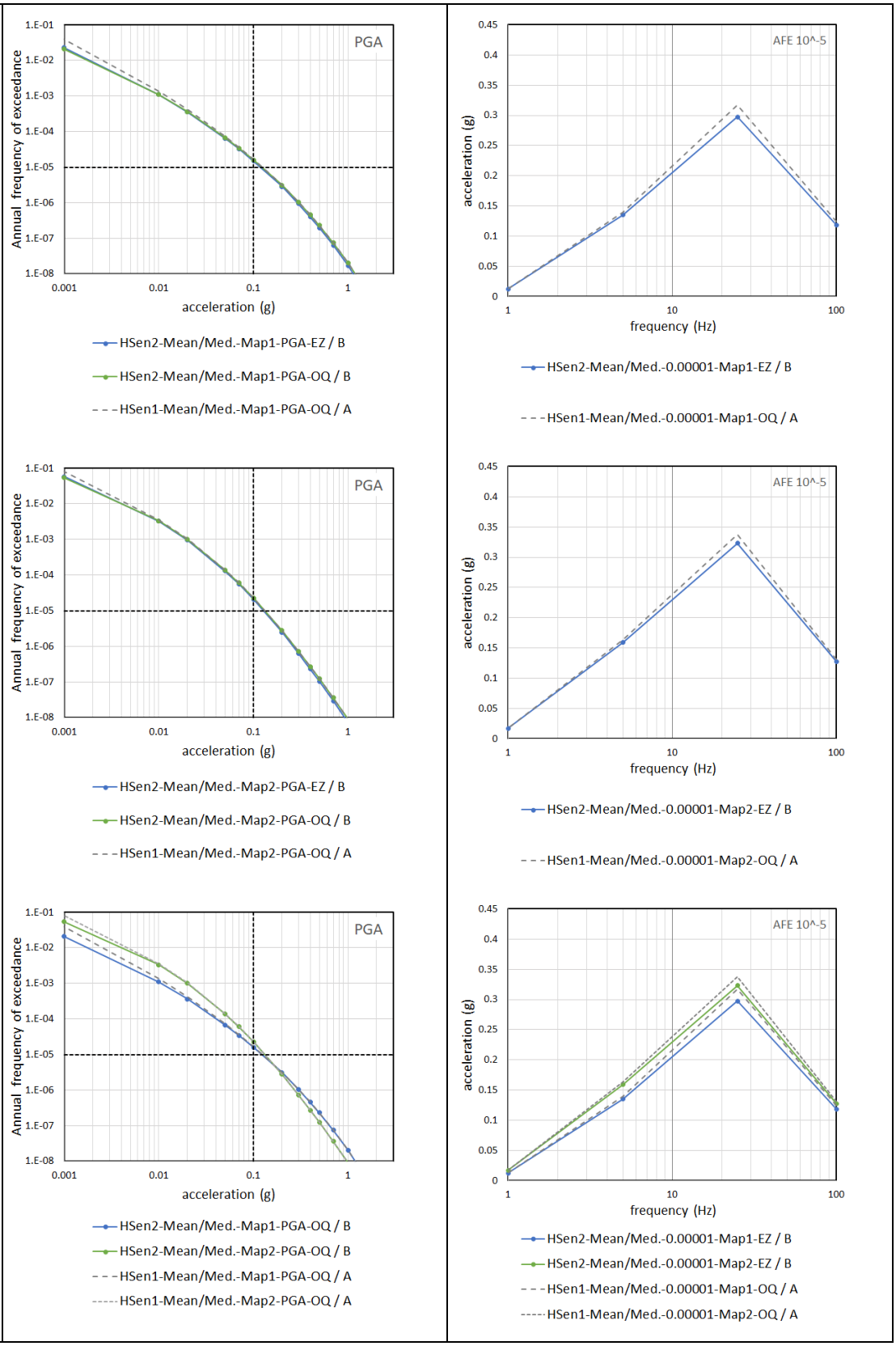

***Figure H3 (continued)**. The Hanhikivi SENSEI PSHA parameter sensitivity results following Table H2. As in the case of the other sites Revision 2 (R2) of the final model (HSen12) is reported. Additional results are available in the accompanying Excel File of this report. EZ = EZ-FRISK software, OQ = OpenQuake software, A and B = computation by calculation group member "A" or "B".*

HSen3: *Compared to HSen2 the minimum magnitude was raised from $M_{min}3$ to $M_{min}4$. Results show that PGA hazard decreases at low acceleration levels. Also, a small reduction on Map1 at AFE 10^{-5} at 25Hz.*

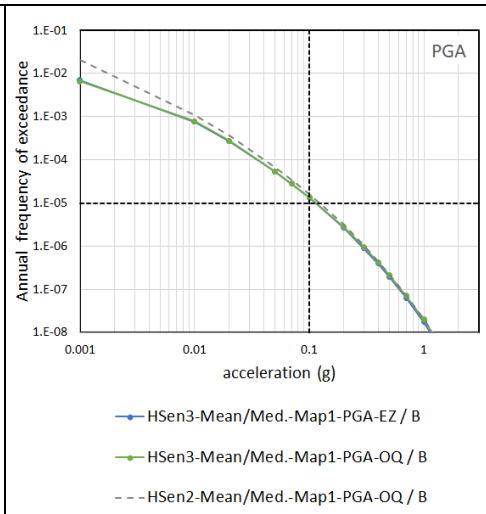

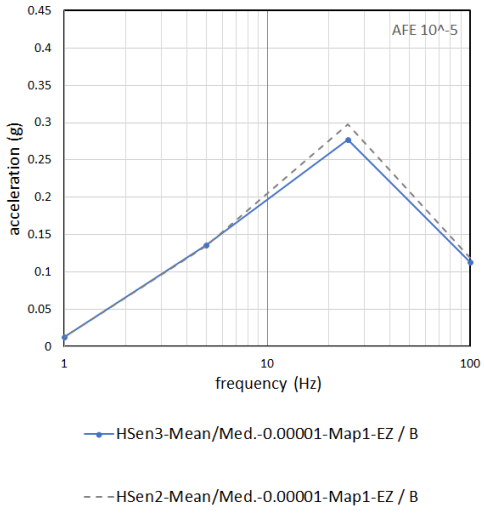

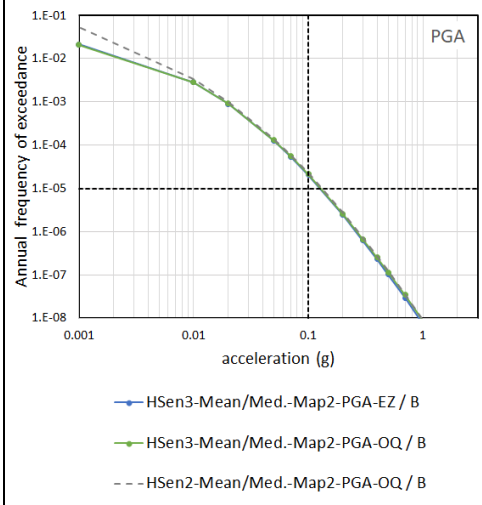

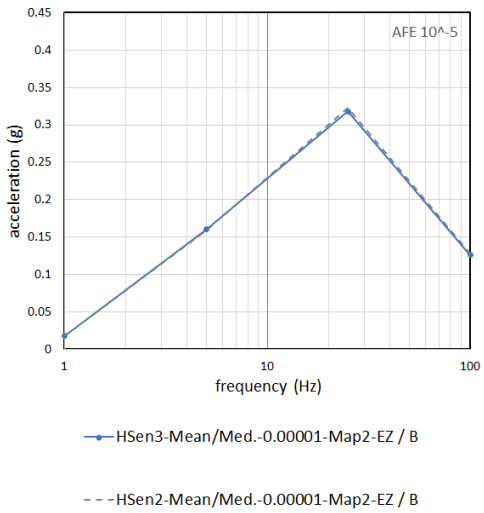

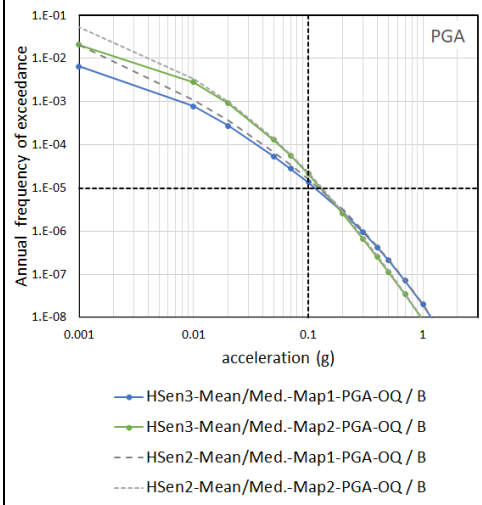

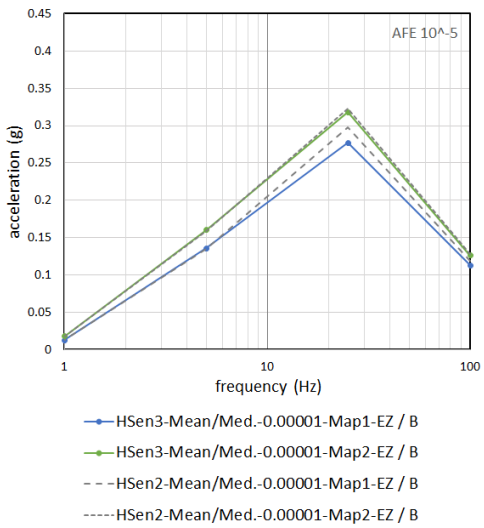

***Figure H3 (continued)**. The Hanhikivi SENSEI PSHA parameter sensitivity results following Table H2. As in the case of the other sites Revision 2 (R2) of the final model (HSen12) is reported. Additional results are available in the accompanying Excel File of this report. EZ = EZ-FRISK software, OQ = OpenQuake software, B = computation by calculation group member "B".*

HSen4: *GMPE replaced from FennoG16 in HSen3 to the weighted average of the 17 NGA-East GMPE branches with ergodic σ (central prediction). Results show decrease of hazard, driven by both a lower mean prediction of the GMPE and smaller σ. The reduction of the 5Hz, 25Hz, and PGA within the spectra can also be noted.*

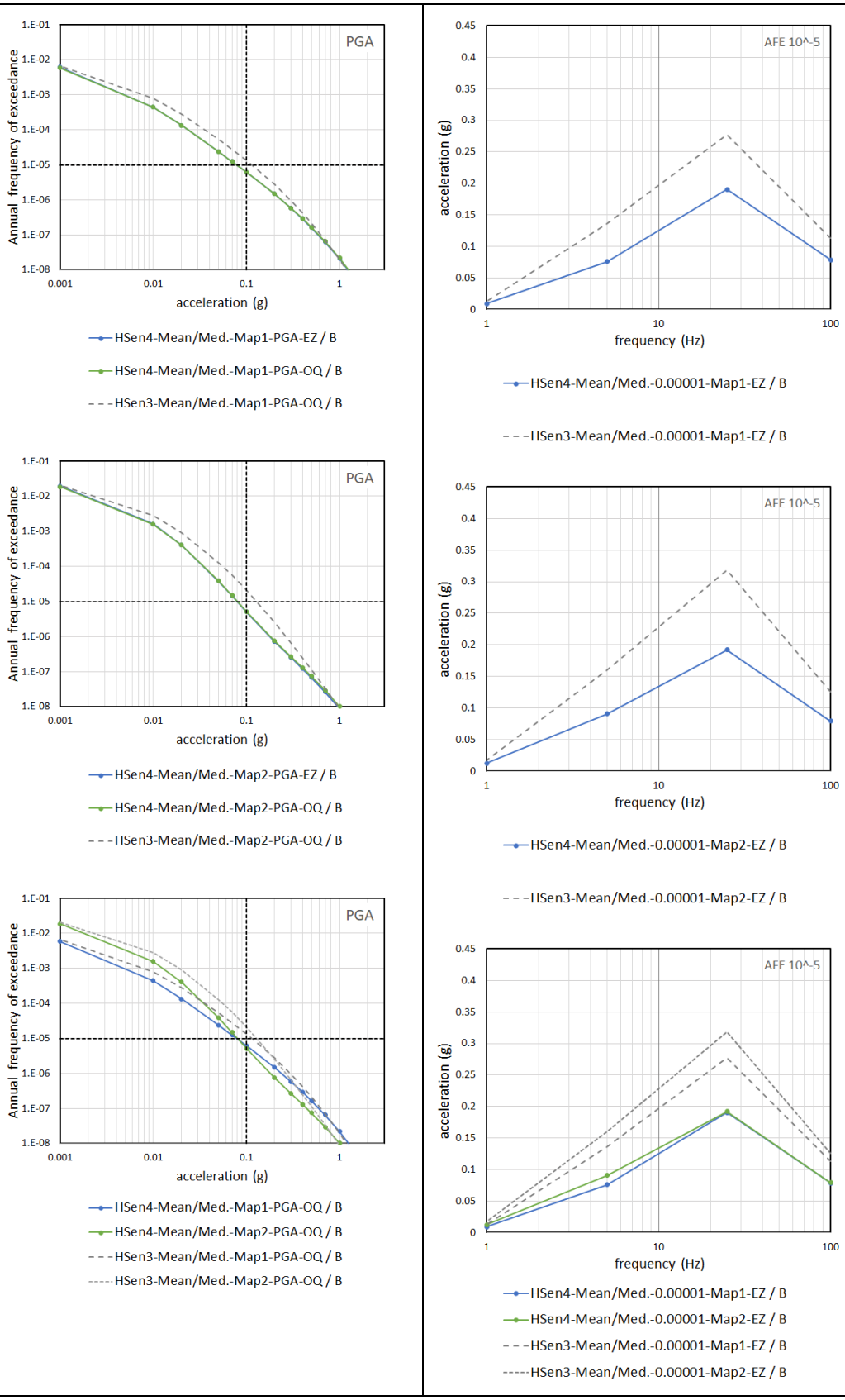

***Figure H3 (continued)**. The Hanhikivi SENSEI PSHA parameter sensitivity results following Table H2. As in the case of the other sites Revision 2 (R2) of the final model (HSen12) is reported. Additional results are available in the accompanying Excel File of this report. EZ = EZ-FRISK software, OQ = OpenQuake software, B = computation by calculation group member "B".*

HSen5: *The maximum magnitude is raised from M_w5.5, used in all earlier models to M_{max}=M_w6.5. M_w6.5 is close to the final M_{max} values proposed in the SENSEI project. A new source area model, Map4, has been used. Some increase in the hazard curves and clear increase throughout the spectra.*	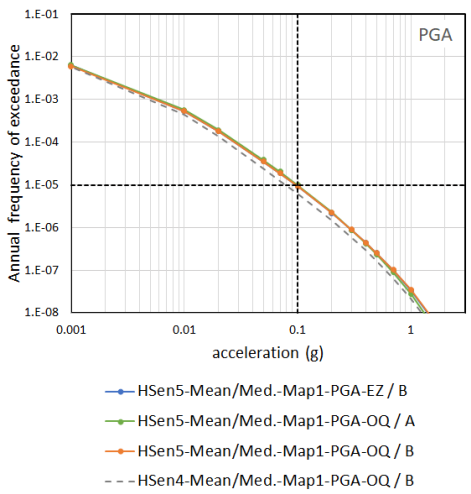 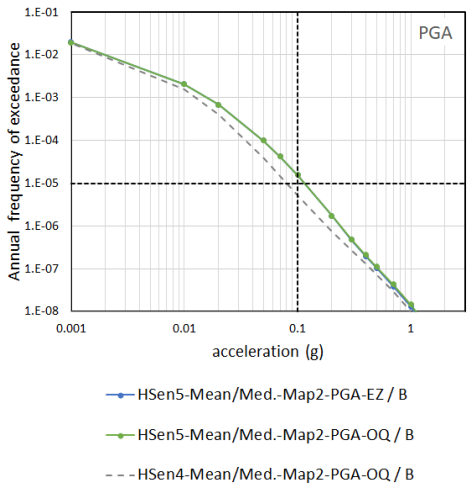 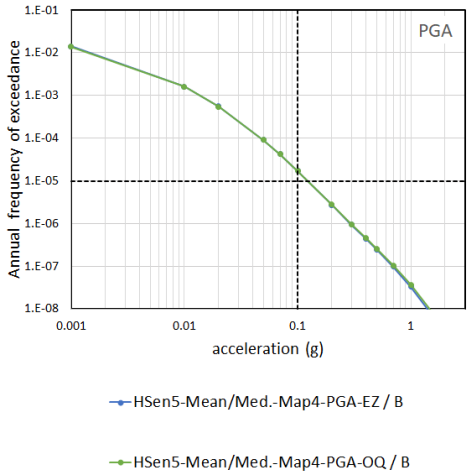	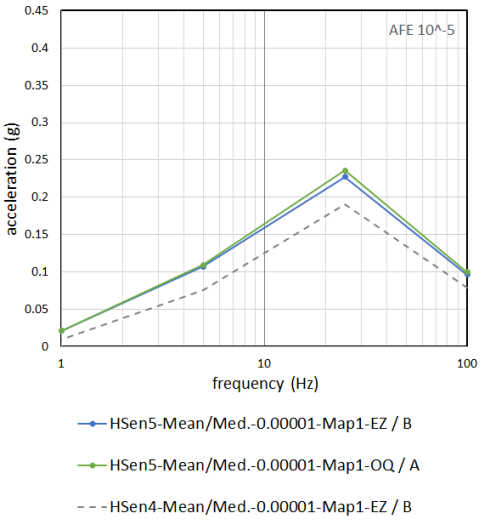 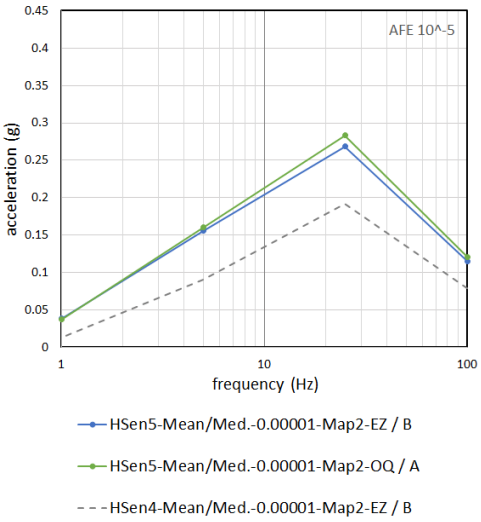 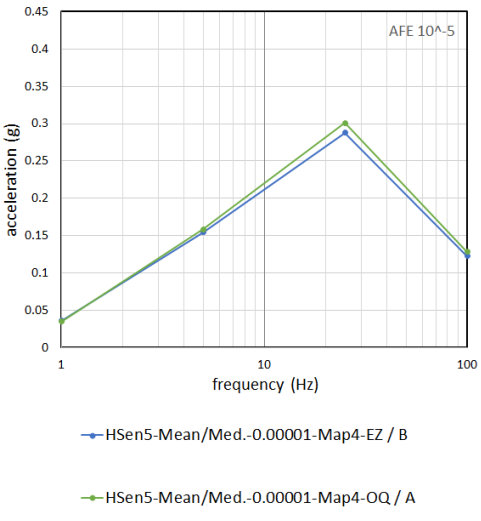

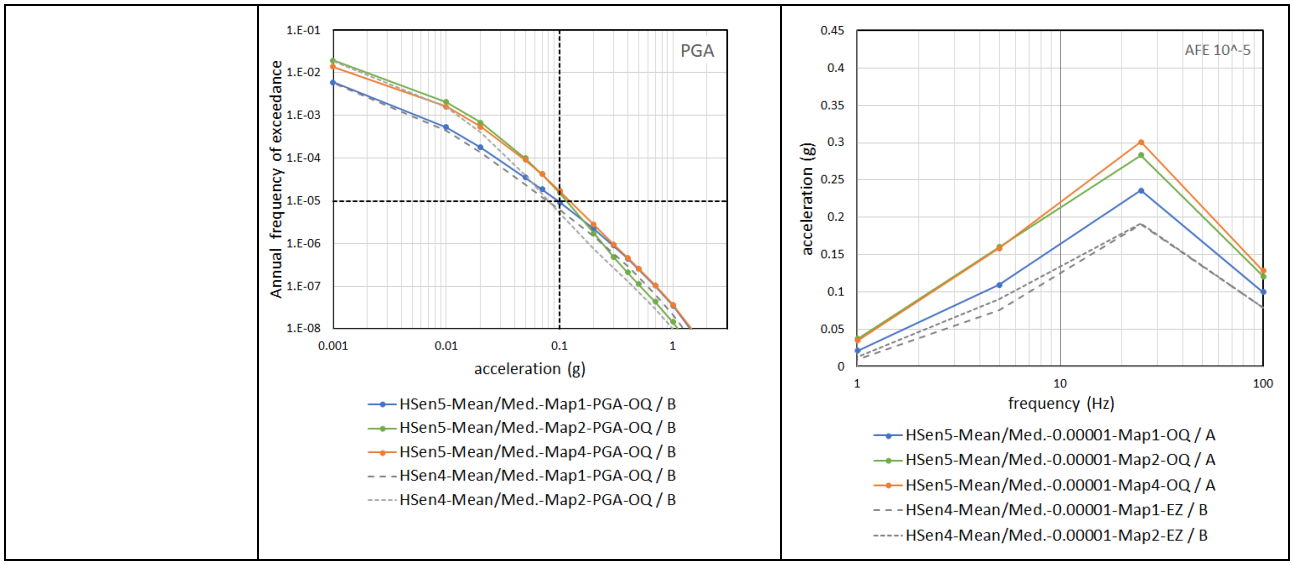

***Figure H3 (continued)**. The Hanhikivi SENSEI PSHA parameter sensitivity results following Table H2. As in the case of the other sites Revision 2 (R2) of the final model (HSen12) is reported. Additional results are available in the accompanying Excel File of this report. EZ = EZ-FRISK software, OQ = OpenQuake software, A and B = computation by calculation group member "A" or "B".*

HSen6: *The uniform 0-35km depth profile is replaced with the final "North" depth distribution proposed in SENSEI for the Hanhikivi NPP site. Hazard remains almost unchanged, but some increase at 25Hz and PGA spectra can be noted.*

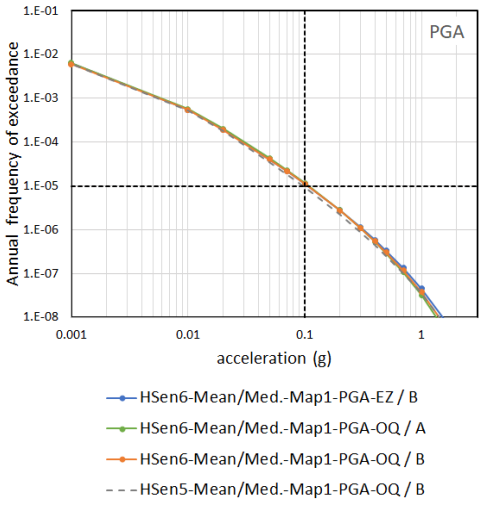

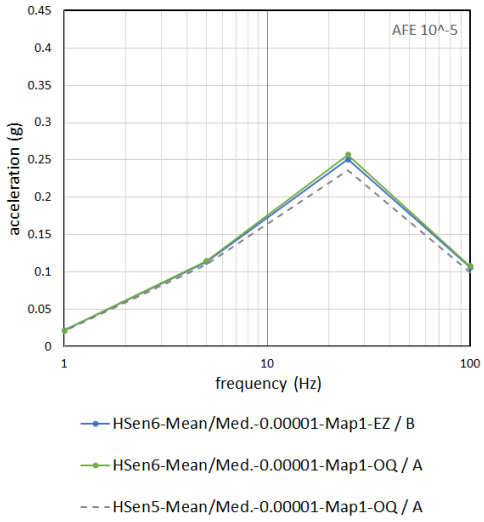

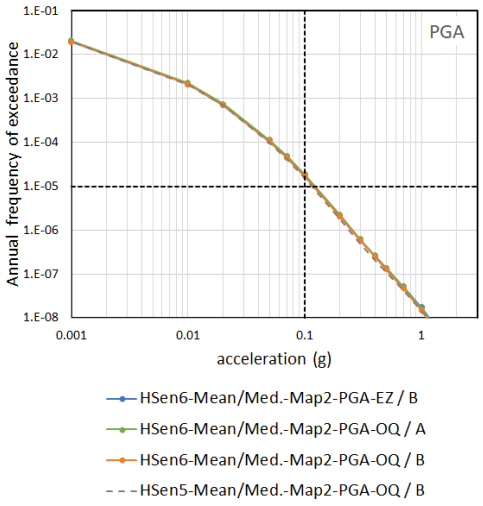

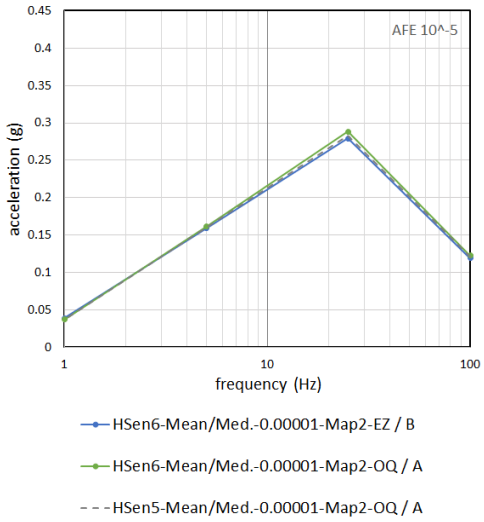

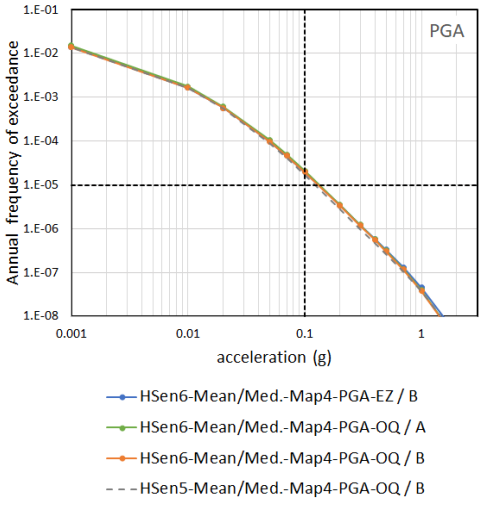

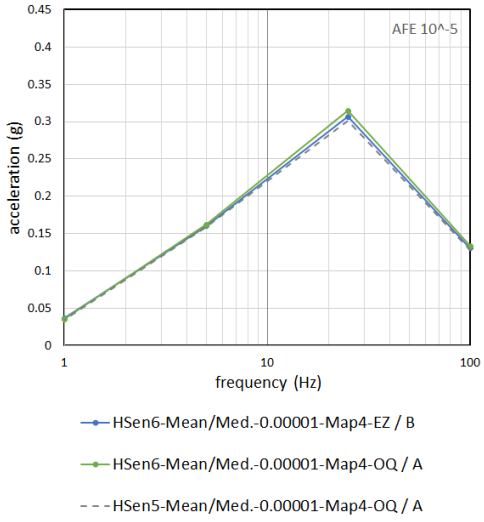

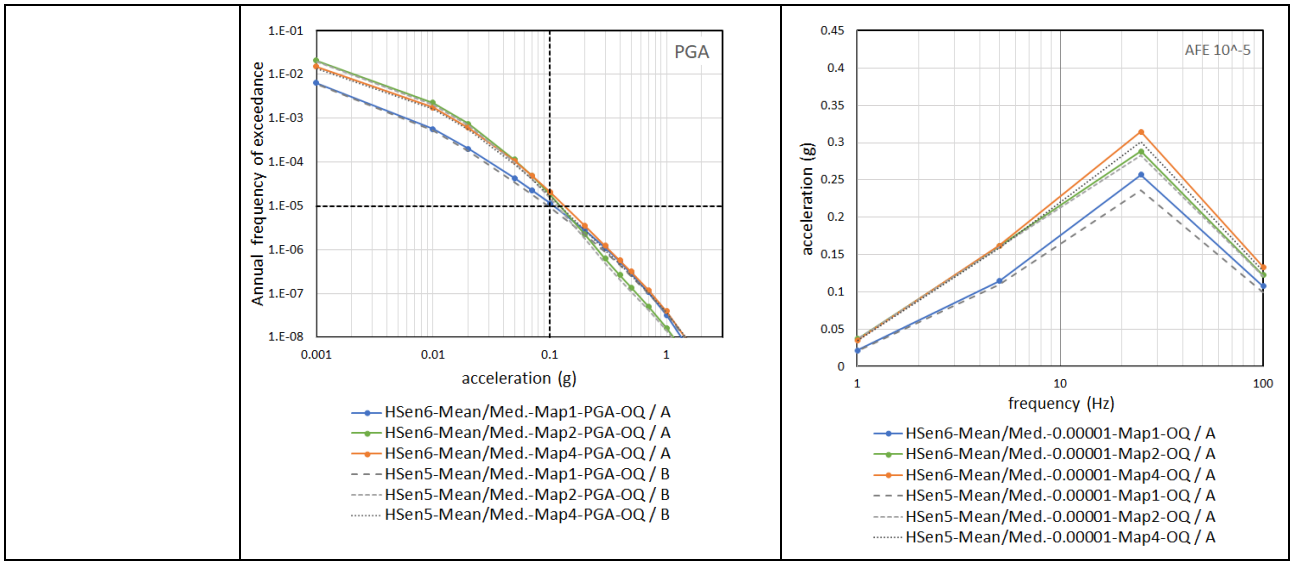

***Figure H3 (continued)**. The Hanhikivi SENSEI PSHA parameter sensitivity results following Table H2. As in the case of the other sites Revision 2 (R2) of the final model (HSen12) is reported. Additional results are available in the accompanying Excel File of this report. EZ = EZ-FRISK software, OQ = OpenQuake software, A and B = computation by calculation group member "A" or "B".*

HSen7: M_{max} *uncertainty is included. The* M_{max} *distribution proposed in SENSEI is based on the Bayesian method. The median* M_{max} *is* M_w*6.64, not very far from the* M_w*6.5 used in earlier models. Mean hazard exceeds the median hazard.* Largest increase at 5Hz spectra.

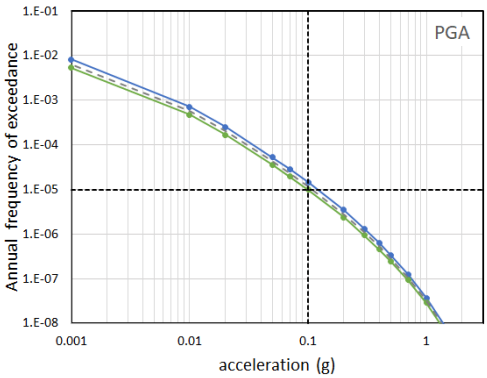

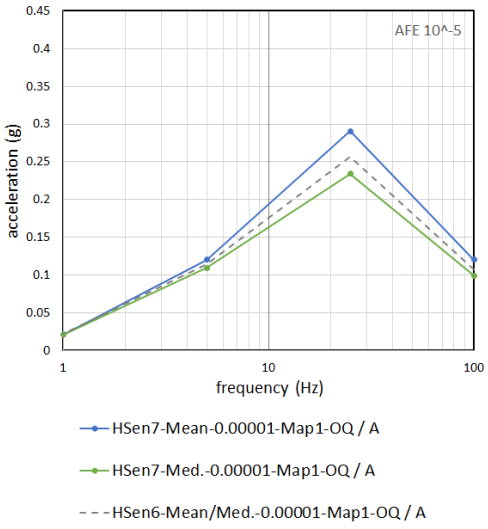

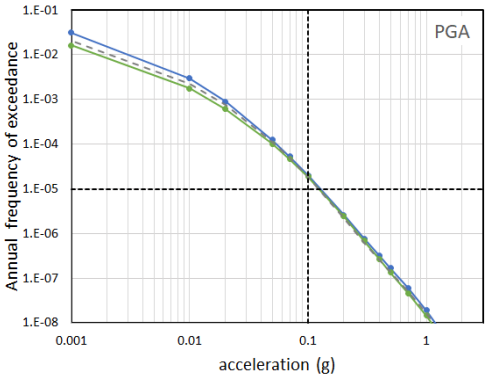

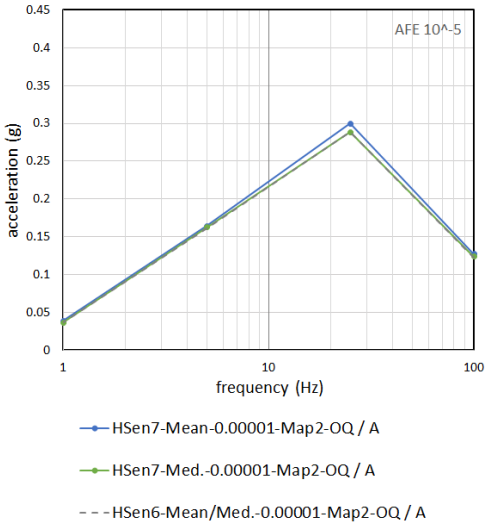

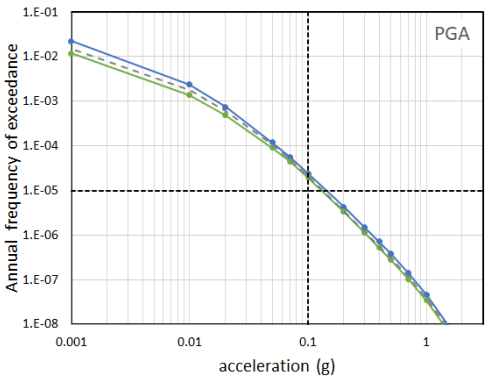

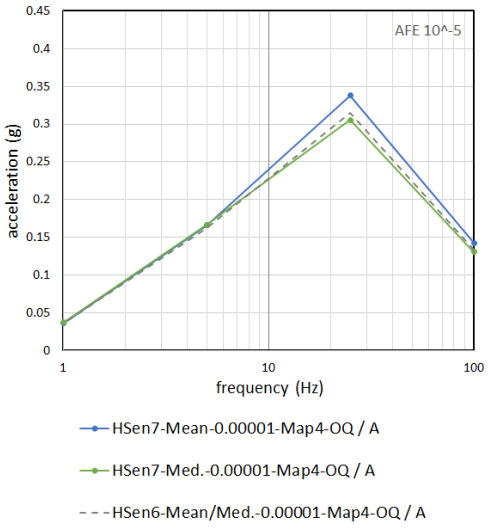

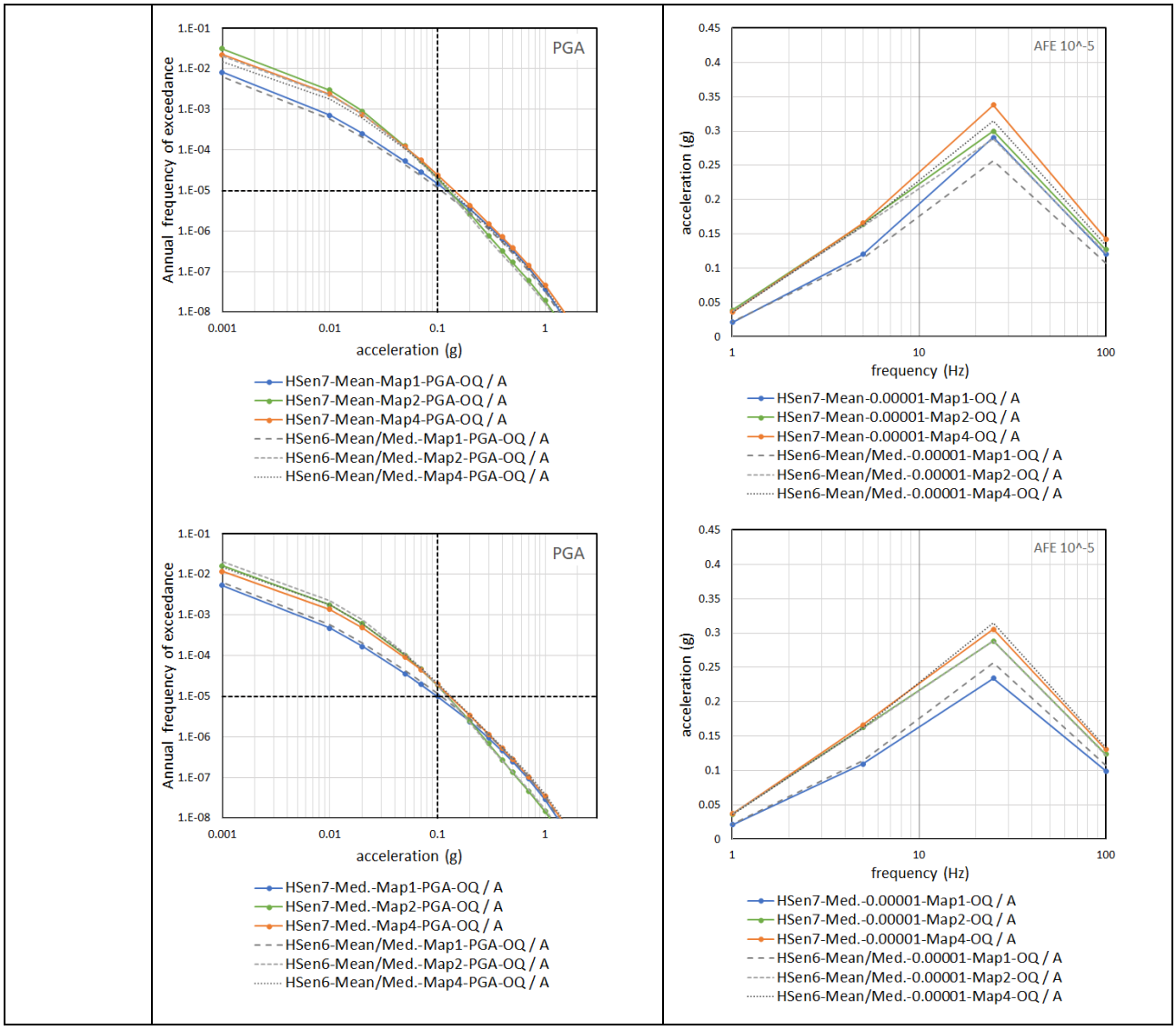

***Figure H3 (continued)**. The Hanhikivi SENSEI PSHA parameter sensitivity results following Table H2. As in the case of the other sites Revision 2 (R2) of the final model (HSen12) is reported. Additional results are available in the accompanying Excel File of this report. OQ = OpenQuake software, A = computation by calculation group member "A".*

HSen8: *Uncertainty in β and λ, for SSA1.13 (Map1) included in (i.e., 9 branches). Mean and median hazards increase.*	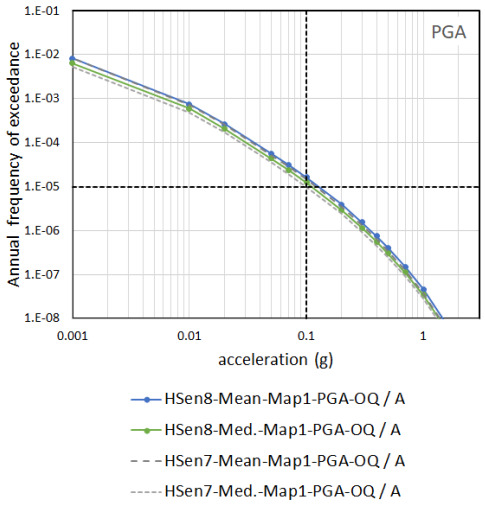	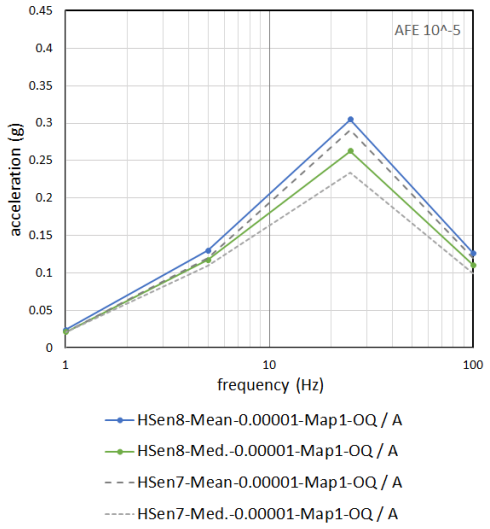
HSen9: *Uncertainty in β and λ, for SSA2.11 (Map2) included (i.e., 9 branches).*	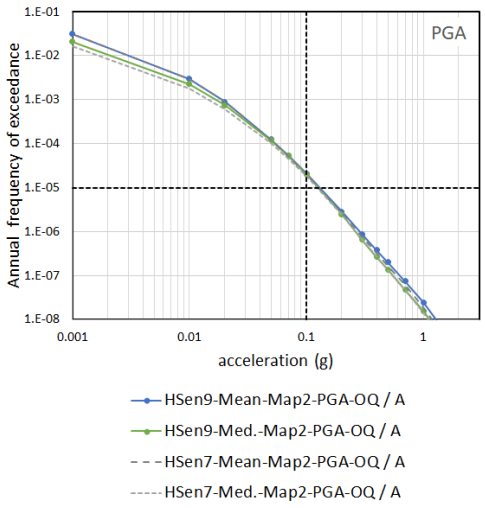	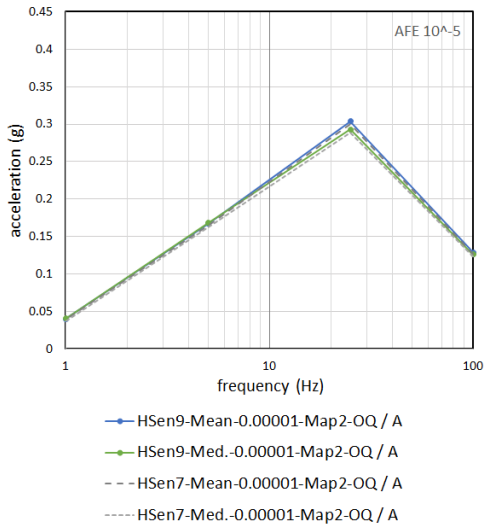
HSen10: *Uncertainty in β and λ, for SSA#8 (Map4) included (i.e., 9 branches). Mean and median hazards increase.*	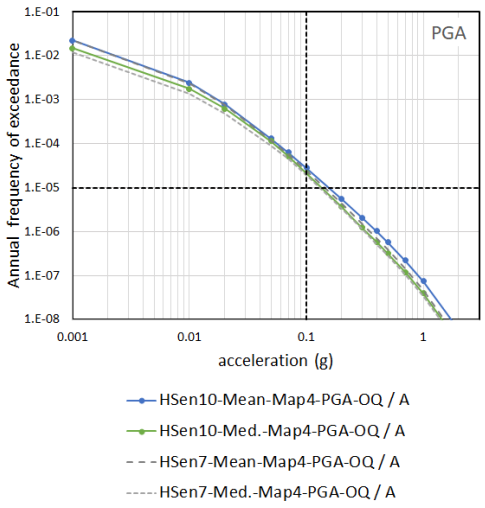	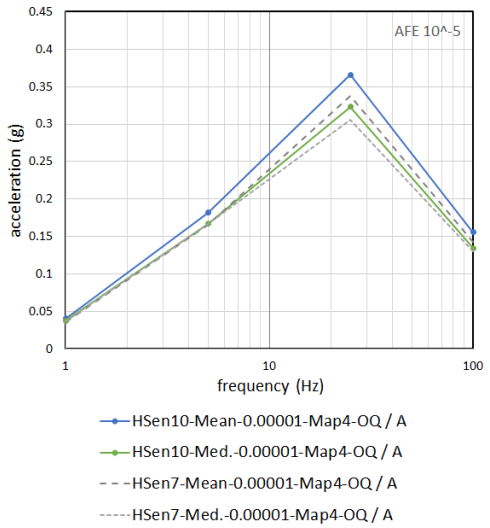

***Figure H3 (continued)**. The Hanhikivi SENSEI PSHA parameter sensitivity results following Table H2. As in the case of the other sites Revision 2 (R2) of the final model (HSen12) is reported. Additional results are available in the accompanying Excel File of this report. OQ = OpenQuake software, A = computation by calculation group member "A".*

HSen11: *All three source area models used as logic tree branches. Mean and median hazard are slightly decreased.*

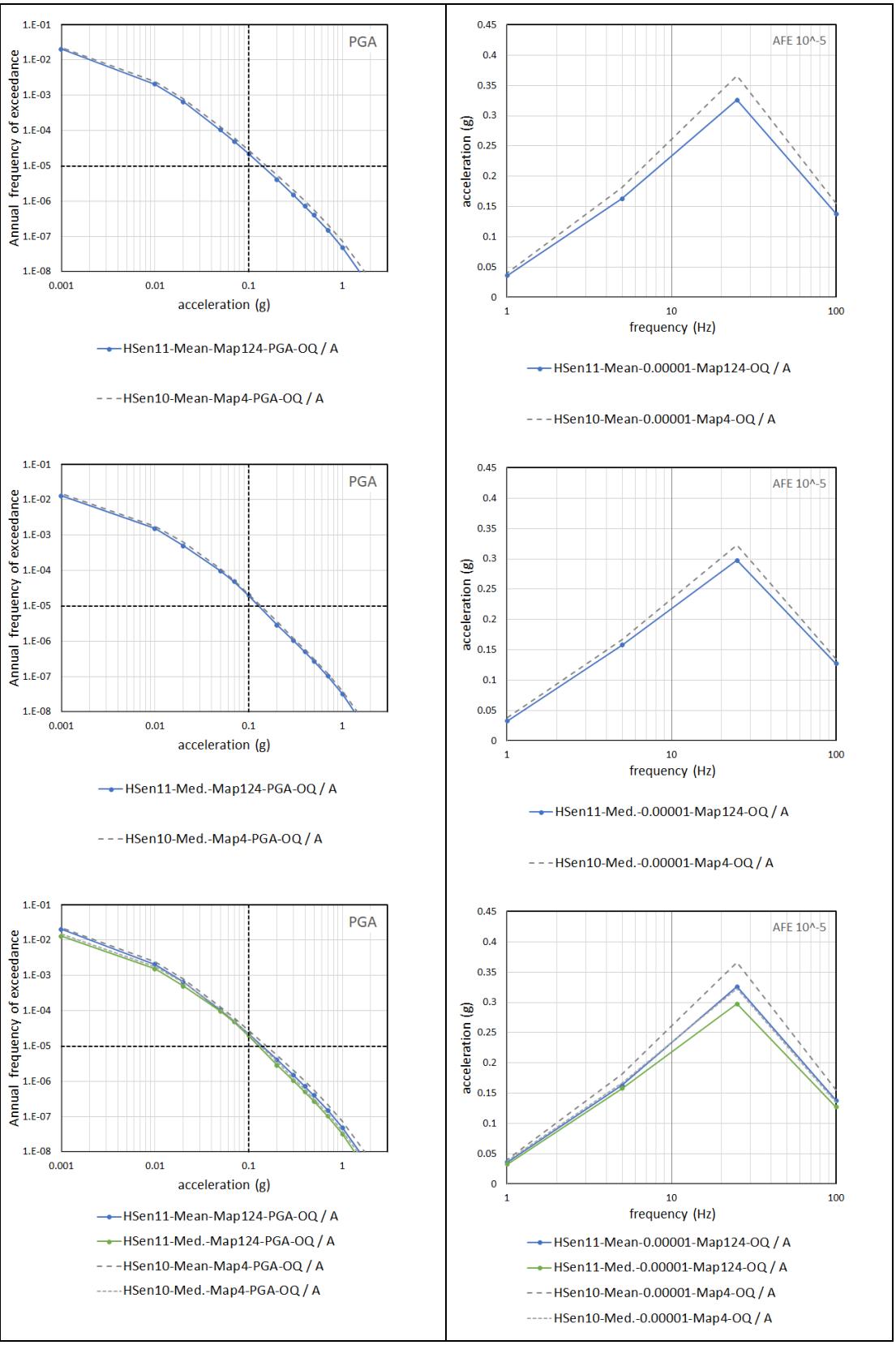

***Figure H3 (continued)**. The Hanhikivi SENSEI PSHA parameter sensitivity results following Table H2. As in the case of the other sites Revision 2 (R2) of the final model (HSen12) is reported. Additional results are available in the accompanying Excel File of this report. OQ = OpenQuake software, A = computation by calculation group member "A".*

HSen12(R2): *The NGA East weighted average GMPE is branched to the 17 branches of the NGA-East GMPE. The central estimate of ergodic σ is also branched to "high", "central" and "low" predictions. Mean hazard increasingly exceeds the median hazard.*

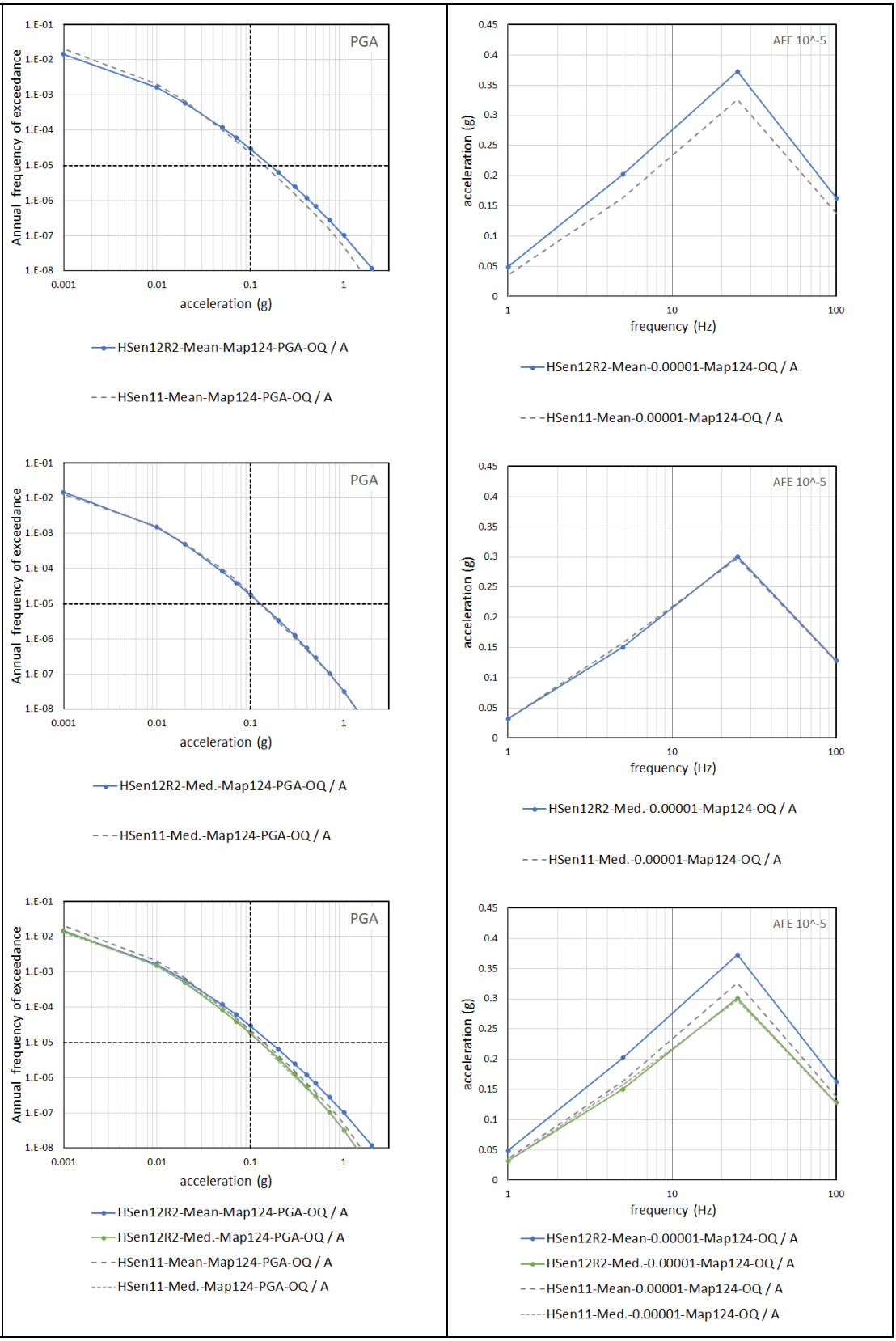

Figure H3. *The Hanhikivi SENSEI PSHA parameter sensitivity results following Table H2. As in the case of the other sites Revision 2 (R2) of the final model (HSen12) is reported. Additional results are available in the accompanying Excel File of this report. OQ = OpenQuake software, A = computation by calculation group member "A".*

7. Sensitivity of the seismic hazard prediction to different input parameters

The one-branch sensitivity calculations described above are discussed further in this section.

7.1. Sensitivity to source area design

7.1.1 Loviisa

Calculations LSen9-LSen12 in Table L3 dealt with the designing of the source area for Loviisa. The seismic source area 10, originally designed in Korja et al. (2016) using data until 2012, covers the geologically uniform Wiborg rapakivi granite batholith, which also extends to offshore areas. SSA10 hosts the NPP and thus dominates the seismic hazard result.

The original design of SSA10 implies that future seismicity can occur anywhere in it with equal probability (i.e., assumption of seismic homogeneity), but the observed seismicity clusters mainly in its westernmost part (Fig. 1). The current geophysical or geological knowledge provides no explanation for the higher rate of observed seismicity there. If SSA10 were situated elsewhere in the country, this feature would suggest pronounced spatial seismicity variations, but it is situated at a border zone. The borderline between Finland and Russia has been positioned differently across the batholith at different times, which implies that the seismicity data are more complete in the west of the batholith which has not belonged to Russia during the era of seismicity observations. In fact, the westernmost third coincides with this area. This notion is also supported by the fact that observations from the Russian territory start to be available only recently, for example December 2016. These thoughts motivated an alternative design of SSA10 in the SENSEI project. Only the westernmost third of SSA10 was retained, and the remaining part was merged with the contiguous SSA6 (Fig. 1).

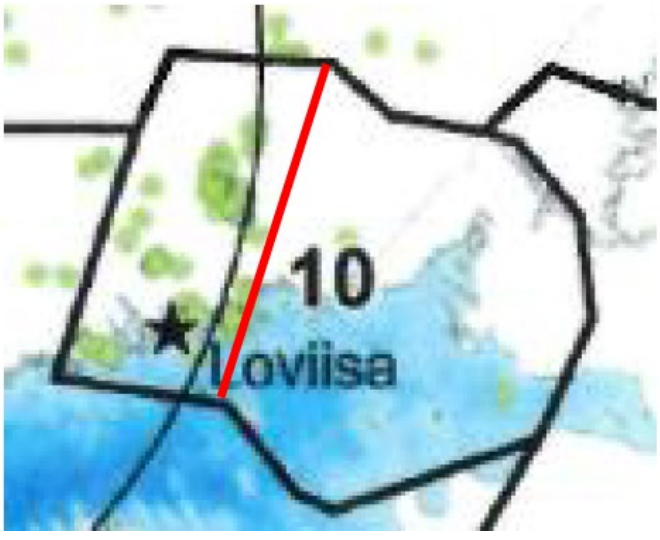

Figure 1. *The alternative design for seismic area source 10 used in the models LSen9 to LSen12. The red line shows how the original SSA10 diminished. The green dots show available earthquake epicenters. The star denotes the Loviisa NPP site.*

Figure LSen9 after Table L3 shows that using the smaller surface area encompassing most of the observed seismicity has a major impact on the hazard and the hazard is substantially increased. An

increase is expected, because the observed seismicity is now distributed over a much smaller surface area. At AFE 10^{-5}, the PGA value is increased from 0.0968*g* (LSen7) to 0.176*g* (LSen9), (when using the NGA-East weighted mean GMPE and maximum magnitude 6.5, and depth distribution South), that is, when the surface area was diminished to one third, the PGA value increased by approximately 82%. At frequency 25 Hz, the increase was from 0.230*g* to 0.423*g* (84%), at 5 Hz from 0.0927*g* to 0.154*g* (almost 66%), and at 1 Hz from 0.014*g* to 0.0206*g* (47%), respectively.

LSen10 was a computation of a logic-tree model, to which the original SSA10 was incorporated with a weight of 2/3 and the new, smaller design with a weight of 1/3. In addition, all the activity parameters of the host zone, SSA10, were incorporated, which resulted in 18 branches. Now that the small-size SSA had less weight, the output decreased, as expected. The median output values of LSen10 are close to those of LSen7 given above. For example, at AFE 10^{-5}, the output value is 0.0957*g* for PGA, 0.228*g* for 25 Hz, 0.0917*g* for 5 Hz, and 0.0139*g* for 1 Hz. The alternative, smaller area has no effect in the logic-tree in practice. The mean values of LSen10 are much larger than the median values, but even so remain below the LSen9 values.

The great value of SENSEI is also seen in initiating the discussion on SSA10 and allowing for tests with new designs. How the non-uniformity of the observed seismicity in SSA10 should be dealt with is not regarded as fully resolved. When attempting to obtain uniformity of seismicity in SSA10, the geological uniformity of the contiguous SSA6 was lost by assigning the eastern parts of the batholith to it. In other words, the new SSA6 comprised parts of different tectonic regimes. An open question is to which extent the observed seismicity is an artifact and to which extent some geophysical and/or geological conditions govern the spatially varying distribution of seismicity in the Wiborg rapakivi granite batholith. The relation between the shallow, low-magnitude swarms to possible larger and deeper earthquakes in the batholith is also an open question, and very relevant to seismic hazard analysis of Loviisa.

7.1.2 Hanhikivi

There were alternative seismic source area designs also for Hanhikivi. Figure H1b shows the two SSA models used in pre-SENSEI computations. The SSAs 1.13 (SSA13 in the first model, below Map1) and 2.11 (SSA11 in the second model, below Map2) are the host source zones, 1.13 alone and 2.11 together with SSA2.8. It was pointed out that SSA8 of the OL-LO design is geometrically very similar. It was suggested at SENSEI WS2 that an additional SSA model (named Map 4) should be constructed for Hanhikivi using the OL-LO SSA8 and other fitting SSAs.

Step HSen5 shows that the source zone model used affects the output. For frequencies 100 Hz (PGA) and 25 Hz, the output value from the model Map1 is the smallest and that of Map4 the largest, whereas for 5 Hz and 1 Hz, the value corresponding to Map2 is the largest and that of Map1 is the smallest. The relative increase from the smallest to the largest value is 27% in the case of PGA and 25 Hz, but 45% for 5 Hz and 80% for 1 Hz.

The output features are similar at step HSen6, except for 5 Hz, which now has the smallest value from Map1 and the largest from Map4. The relative changes are 23%, 22%, 41% and 68% for PGA, 25 Hz, 5 Hz and 1 Hz, respectively. It can also be noted that the absolute values are the largest for 25 Hz, between 0.25*g* and 0.30*g*. The absolute values at 1 Hz are small, between 0.022*g* and 0.036*g*, although the relative increase is large (at AFE 10^{-5}). Steps HSen5 and HSen6 compared the effect of

depth distribution, but the effect of depth is much smaller than that of the different source zone models.

The exercises show that the SSA design can have a major impact on spectral acceleration values. This makes sense, because changing boundaries tends to affect the seismic activity rates. Even if a given zone does not have many epicenters located inside it, changing the surface area affects the seismicity rate per unit area. In particular, the output depends on the extent the seismicity rates of the host SSA are affected by redesigning its boundaries. A relevant question raised in SENSEI regarding Musson's (2000) publication is how to evaluate and rate the different designs available for a given target region: can any of the models be argued to be the best one?

7.2 Sensitivity to assumed depth distribution

In the SENSEI project, considerable effort was devoted to preparing valid depth distributions for the NPP sites in Finland and the respective input files to OpenQuake. Improvements in seismological monitoring and determination of earthquake parameters over the years made it possible to prepare more realistic depth distributions for northern and southern Finland, but the data are too sparse for discerning possible differences between the two southern sites. The new depth distributions were tested for all the sites.

In the case of Loviisa, the steps LSen4 to LSen6 focused on the depths. The shift from the pre-SENSEI model with earthquakes occurring uniformly throughout the entire seismogenic crust (LSen4) to seismicity confined to the uppermost 13 km of the crust (LSen5) increased the output values. For example, PGA values increased from 0.0614*g* to 0.0859*g*, by 40%, 25Hz values from 0.148*g* to 0.208*g*, by 41%, 5Hz values from 0.0577*g* to 0.0737*g*, by approximately 28%, and 1Hz values from 0.00584*g* to 0.00709*g,* which amounts to 21% of increase. The observed seismicity is distributed over a smaller crustal volume in LSen5, and closer to the ground surface, which results in higher hazard estimates. The difference between a depth distribution between 0-13 km and the final southern distribution is small, and thus the output values from LSen6 were very similar to those from LSen5, only slightly below them. The output features are similar at step HSen6, except for 5 Hz, which now has the smallest value from Map1 and the largest from Map4. The relative changes are 23%, 22%, 41% and 68% for PGA, 25 Hz, 5 Hz and 1 Hz, respectively. It can also be noted that the absolute values are the largest for 25 Hz, between 0.25*g* and 0.30*g*. The absolute values at 1 Hz are small, between 0.022*g* and 0.036*g*, although the relative increase is large (at AFE 10^{-5}). Steps HSen5 and HSen6 compared the effect of depth distribution, but the effect of depth is much smaller than that of the different source zone models.

Accordingly, the steps OSen4 and OSen5 shifted the depth distribution from the pre-SENSEI crustal model to the southern distribution, and the effect was similar to LSen4 and LSen5 or LSen6. In contrast, at Hanhikivi, the pre-SENSEI and new depth distributions were not that different, which resulted in minor differences between the output from steps HSen5 and HSen6.

Expanding the database of reliable focal depths remains a challenge for seismic monitoring in southern Finland in particular, because seismicity rates are low and the density of seismic stations is not high there, except temporarily at Kuusaanlampi and more permanently in the capital region. Because of the very scarce seismicity in the south, the depth distribution for this region is considerably influenced by the Wiborg rapakivi seismicity.

It is also debatable if the future distribution of depths, for the hazard prediction, will strictly reflect the observations of current seismicity (i.e., of smaller magnitudes). In any case, deviating from the observed focal depths should be adequately argued.

7.3 Sensitivity to M_{min}

The effect of M_{min} was tested separately in the one-branch calculations for each site. For Loviisa, the steps were LSen1, LSen2, LSen3, with M_{min} values 2, 3 and 4, respectively. As the figures above indicate, the effect was negligible at 5 Hz and 1 Hz on the three steps. At 25 Hz, the increase from M_{min}2 to 4 decreased the output value by almost 18% and at PGA the corresponding decrease was approximately 14%, at AFE 10^{-5}.
At AFE 10^{-6} the behavior followed a similar pattern, but the relative effect was smaller: almost no effect at all at 5 Hz and 1 Hz, but at 25 Hz the decrease was 8% and at PGA almost 6% when M_{min}2 was increased to 4.

Zone model Map1 for Hanhikivi gave output along similar lines: increasing M_{min} from 2 to 3 had no effect at 5 and 1 Hz, and fractions of per cent decrease at 25 Hz and PGA. When increasing M_{min} further to 4, the effect remained small at 5 Hz and 1 Hz, but the decrease at 25 Hz was 8% and at PGA over 5%. The behavior was similar using Map2, but the absolute spectral acceleration values were larger. At 25 Hz, the output for all the M_{min} values exceeded 0.3*g*. In short, the behavior follows that explained by Bender and Campbell (1989); however, they reported larger proportional changes up to a 40% decrease (they investigated M_{min} values 4, 4.5, and 5). The inclusion of small-magnitude earthquakes has an effect on the short return periods of the hazard curve, and the effect is seen in the spectra as well.

7.4 Sensitivity to activity rates including their uncertainty

The slope of the GR relation, the *b* value, is instrumental in transferring observed seismicity rates to magnitude ranges representing non-observed, rare future seismicity, but it was not scrutinized very much in the SENSEI project. One set of calculations with different *b* values was carried out for Loviisa (models LG7-LG9 in Table L2). An unaltered *b* value (1.07), a low *b* value (0.99; standard deviation subtracted) and a high *b* value (1.15; standard deviation added) were used for SSA10, while the *b* value for SSA6 was kept unchanged. The figure below shows that a lower *b* value gave higher output, such that the acceleration values increased by approximately 6 % at 25 Hz, at which the difference is most pronounced. Similarly, a higher *b* value lowered the output by 5 % at 25 Hz.

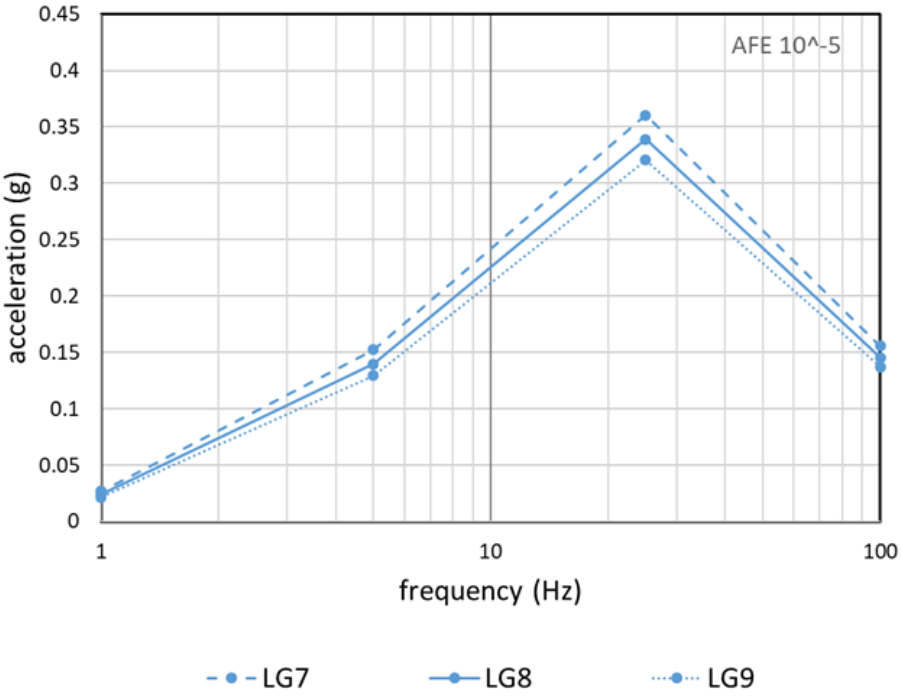

Figure 2. *Effect of the GR* b *value. The solid line (LG8) shows output for unaltered* b *values, the long dashes (LG7) for a low* b *value and the dots (LG9) for a high* b *value for SSA10.*

7.5 Sensitivity to M_{max}

Steps LSen6 to LSen8 in Table L3 were a straightforward, one-branch test of the largest possible magnitude, M_{max}, for the Loviisa site. The M_{max} values used were 5.5, 6.5 and 7.5, respectively. At AFE 10^{-5}, the obtained PGA (100 Hz) values were (using the OQ computation) 0.084*g*, 0.097*g,* and 0.10*g*, respectively. The corresponding values were 0.20*g*, 0.23*g* and 0.24*g* obtained for 25 Hz, 0.073*g*, 0.093*g* and 0.10*g* for 5 Hz, and 0.007*g*, 0.014*g* and 0.017*g* for 1 Hz. The increase from M_{max}5.5 to 6.5 increased PGA by 15% and spectral acceleration at 25 Hz by 13%, 5 Hz by almost 28% and 1 Hz by almost 100%. The shift from M_{max}6.5 to 7.5 increased the PGA output value by a further 5%, the 25 Hz value by 4 %, 5 Hz by almost 10%, and 1 Hz by 23%.

In the case of Olkiluoto, the steps OSen3 and OSen4 compared the output from M_{max} values 5.5 and 6.5. At AFE 10^{-5}, the increase of the spectral accelerations was from 0.057*g* to 0.068*g* (20%) for PGA, 0.14*g* to 0.16*g* (17%) for 25 Hz, from 0.055*g* to 0.077*g* (40%) for 5 Hz and from 0.0065*g* to 0.015*g* (130%) for 1 Hz.

In the case of Hanhikivi, step HSen4 used M_{max}5.5 and HSen5 M_{max}6.5. The relative increases for the frequencies investigated were 22% for PGA, 19% for 25 Hz, 42% for 5 Hz, and 73% for 1 Hz 73% when using Map1 zones and 45% for PGA 40% for 25 Hz, 72% for 5 Hz and over 200% for 1 Hz when using Map2 zones. In all three cases, the proportion of the increase was different for the different frequencies. The largest relative increases were always found at 1 Hz, the second largest at 5 Hz, the third largest at PGA and the smallest relative increases at 25 Hz. The results for Hanhikivi show that the relative increases were different for the two source models used. The proportions were higher in the case of Map2, which also gave higher absolute spectral acceleration values. This

suggests that M_{max}7.5 can give potentially high values, in particular when combined with Map4. It cannot be concluded that the effect of M_{max} is small in general. The absolute spectral acceleration values were in reverse order; the smallest absolute values were found at 1 Hz and the largest at 25 Hz.

7.6 Sensitivity to GMPE and the sigma of GMPE

Two alternative GMPEs emerged from the stepwise comparison of the GMPEs available for the intraplate, hard-rock conditions in Fennoscandia. Table L2 above focuses on the Loviisa site, but the final choices, the NGA-East and Fenno-G16 GMPEs, were taken into use for the other two sites as well. Epistemic uncertainty of ground motion is typically incorporated in PSHA logic trees by a set of alternative GMPE branches with associated weights. In that respect, the two final alternatives appear rather disparate. The NGA-East model is a suite of 17 median GMPEs developed for Central and Eastern North America in a large project framework (Goulet et al. 2018), while Fenno-G16 is adapted to the G16 backbone curve of the equation proposed by Graizer (2016) and was developed as a small-scale effort (Fülöp et al. 2020). However, the Fenno-G16 model is of special interest in SENSEI, because data recorded at seismic stations in Finland were also used to calibrate it. It is expected to be subject to further inspection and development in the coming years.

An obvious measure of the selected GMPEs is their effect on PSHA results at individual sites. Steps LSen3 and LSen4 in Table L3 and the corresponding figures show the higher hazard values from the Fenno-G16 model at AFE 10^{-5}. The PGA (OQ) values are 0.0903*g* and 0.0614*g* from Fenno-G16 and NGA-East weighted average (WA) of the 17 GMPEs, respectively, indicating a 32% reduction. The corresponding reduction at 25 Hz is from 0.2177*g* to 0.1483*g*, i.e., 32%, and at 5 Hz from 0.1086*g* to 0.05772*g*, almost 47%. At 1 Hz, the absolute values are small, 0.008824*g* and 0.005836*g*, but the reduction is proportionally of the same order of magnitude as at PGA and 25 Hz, almost 34%.

Steps OSen2 and OSen3 provided a similar one-branch comparison for the Olkiluoto site. The depth range used extended down to 35 km, so the absolute values are lower than those from the new depth distribution "south", and interest is in the proportional changes. When replacing Fenno-G16 by NGA-East WA, the PGA (EZ) value at AFE 10^{-5} was reduced by 32%, at 25 Hz by 32%, at 5 Hz by 45% and at 1 Hz by almost 26%.

For the Hanhikivi site, the corresponding steps were HSen3 and HSen4, with two branches for the source areas. For Map1 and AFE 10^{-5}, the reduction at PGA, 25 Hz, and 1 Hz (EZ values) was approximately 30%, and at 5 Hz approximately 44%. The reductions were 37%, 40%, 44%, and 30% for 100, 25, 5, and 1 Hz, respectively. In the case of Map2, the corresponding values were 37%, 40%, 40% and 30%, i.e., identical except for a lower value at 5 Hz.

In summary, when replacing Fenno-G16 by NGA-East WA, the proportions of reductions at the three sites range from 26% to 47%. In all cases, except for Hanhikivi Map2, the proportional change was largest at 5 Hz. The Hanhikivi example also reconfirms that seismic source design may affect the hazard results.

Fülöp et al. (2020) showed that Fenno-G16 gives higher results than the NGA-East suite of 17 GMPEs. Figure 3 shows that Fenno-G16 gives higher results than the NGA-East WA over the entire

range where the two models apply and are of interest to PSHA in the case of moment magnitude **M**4 and rupture distance 50 and 100 km. Only one or two NGA-East GMPEs produce equally high or individual higher values. At 10 km and below 5 Hz the two GMPEs yield rather similar values. The comparison is overall interpreted to reflect the low attenuation of seismic waves in the crystalline bedrock of Fennoscandia.

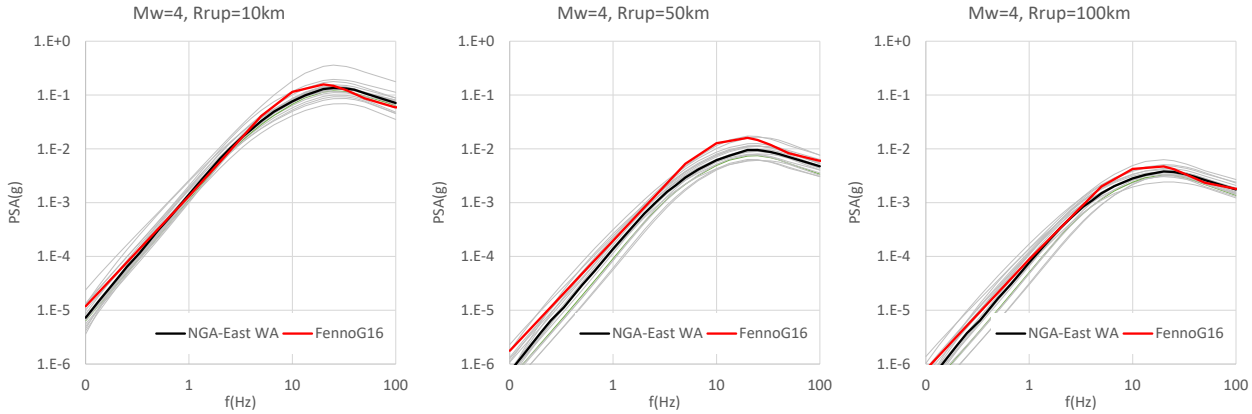

Figure 3. *Comparison of FennoG16 GMPE (red solid line) with the suite of NGA-East GMPEs (gray lines, mean black solid line) for moment magnitude **M**4 and rupture distance 10km, 50km and 100km.*

At higher magnitudes, the FennoG16 model relies entirely on NGA-East data and follows the NGA-East WA curve quite closely. This raises the concern of getting too low ground-motion values from using NGA-East WA, and clearly demonstrates the problems posed by sparse data in Fennoscandia.

7.7 Summary of the one-branch calculations

The one-branch calculations explained in the previous subsections are briefly summarized below by incorporating some of the calculations together into single figures.

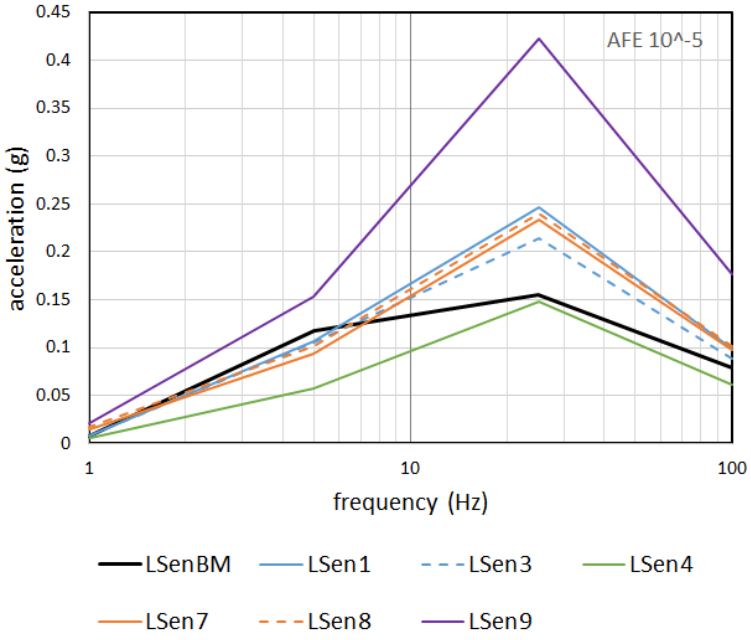

Figure 4. *Comparison of the one-branch models LSen1, 3, 4, 7, 8 and 9 for Loviisa. The thick black line marks the pre-SENSEI baseline, the blue lines show the effect of changing M_{min} from 2 (solid blue) to 4 (dashed blue) with Fenno-G16 GMPE, and the green line shows the NGA-East WA GMPE result for $M_{min}4$. The orange lines show the effect of increasing M_{max} from 6.5 (solid orange) to 7.5 (dashed orange). The purple line shows the effect of diminishing SSA10 into one third of the original surface area.*

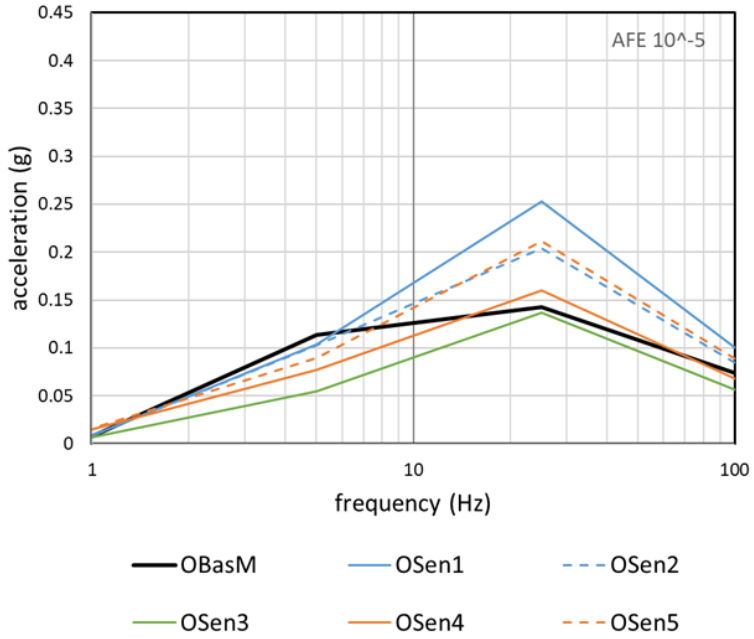

Figure 5. *Comparison of the one-branch models OSen1, 2, 3, 4 and 5 for Olkiluoto. The thick black line marks the pre-SENSEI baseline, the blue lines show the effect of changing M_{min} from 2 (solid blue) to 4 (dashed blue) with Fenno-G16 GMPE, and the green line shows the NGA-East WA GMPE result for $M_{min}4$. The orange lines show the effect of changing the depth distribution from 0-35 km (solid line) to the southern distribution (dashed line).*

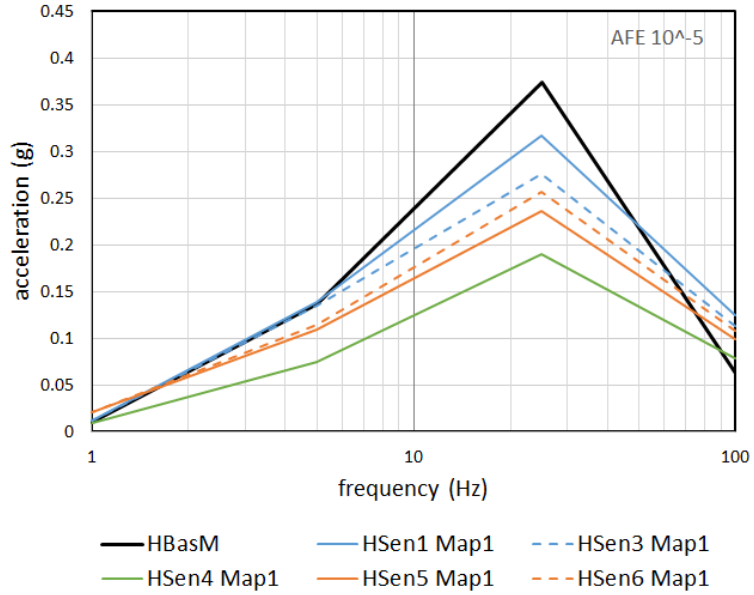

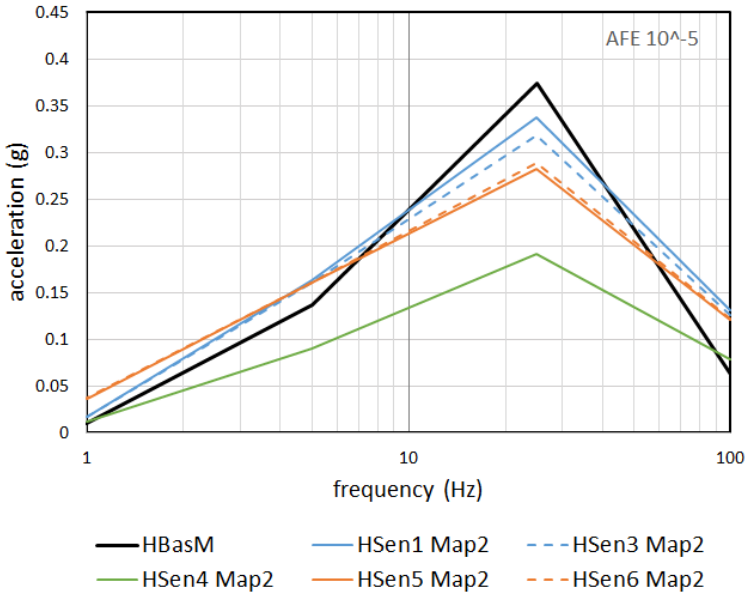

Figure 6. *Comparison of the one-branch models HSen1, 3, 4, 5 and 6 for Hanhikivi. The thick black line marks the pre-SENSEI baseline, the blue lines show the effect of changing M_{min} from 2 (solid blue) to 4 (dashed blue) and the green line shows the NGA-East WA GMPE result for $M_{min}4$. The orange lines show the effect of changing the depth distribution from 0-35 km (solid orange) to the northern distribution (dashed orange). Upper figure: Map1, lower figure: Map2.*

In all figures 4-6, the lowest output values shown are for the NGA-East WA GMPE with $M_{max}5.5$. When it was increased to 6.5, the corresponding results were substantially increased, as described in subsection 7.5. $M_{max}7.5$ was only calculated for Loviisa, and the increase from 6.5 to 7.5 was not as significant as from 5.5 to 6.5. However, it is not known whether the other two sites follow the same pattern.

8. Magnitude-distance disaggregation of the SENSEI logic-tree models

The one-branch stepwise computations constituted a large part of the SENSEI project. However, the performance of logic-trees is important when striving towards full PSHA. This section presents the magnitude-distance disaggregation of the hazards from the LSen12(R2), OSen8(R2), and HSen12(R2) models. They were the most mature hazard models for the three sites developed in the SENSEI project.

Magnitude bins M_w4-5, M_w5-6, M_w6-7, and M_w7-8 are used. These bins are centered on M_w **4.5**, **5.5**, **6.5** and **7.5**, used as legend of the figures. The distance bins have an increment of 20 km until the 300 km maximum calculation distance. Every second bin-centre distance is used as legend in the plots (i.e., **10**, **50**, **90**, etc. kilometres).

The results are given in Figures 7 – 9. They show that most of the hazard originates from nearby earthquakes, especially in the high-frequency range of the spectra (25Hz and PGA). At lower frequencies, especially 1Hz, the contribution of larger earthquakes at longer distances increases. This effect is especially significant for the Hanhikivi site, where it also extends to the 5Hz spectral frequency (Fig. 9).

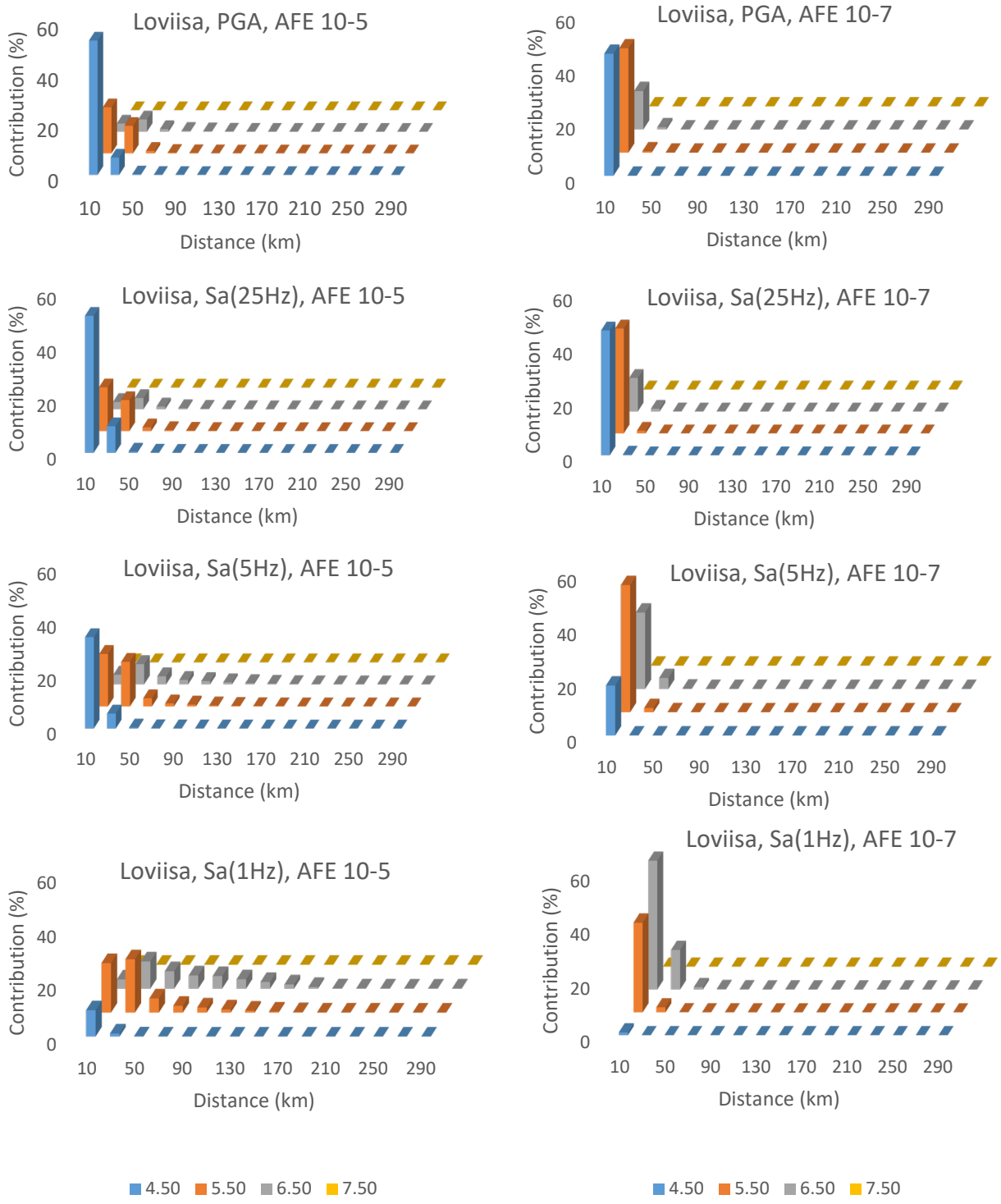

***Figure** 7. Loviisa disaggregation results by magnitude and hypocenter distance for PGA, 25Hz, 5Hz and 1Hz. The contribution of the magnitude-distance bins is given relative to the total hazard at each intensity measured (e.g., PGA) and AFE.*

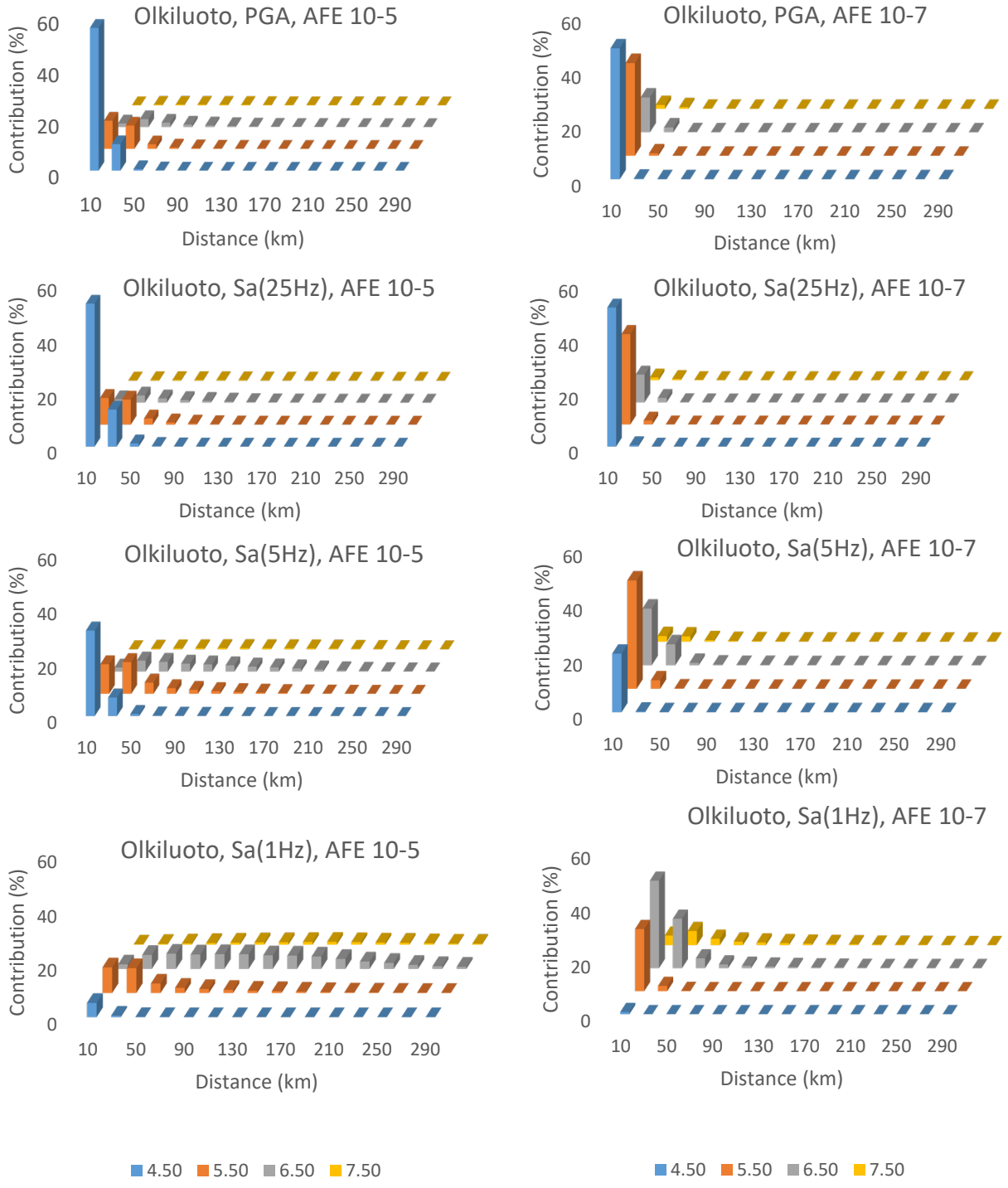

Figure 8. *Olkiluoto disaggregation results by magnitude and hypocenter distance for PGA, 25Hz, 5Hz and 1Hz. The contribution of the magnitude-distance bins is given relative to the total hazard at each intensity measured (e.g., PGA) and AFE.*

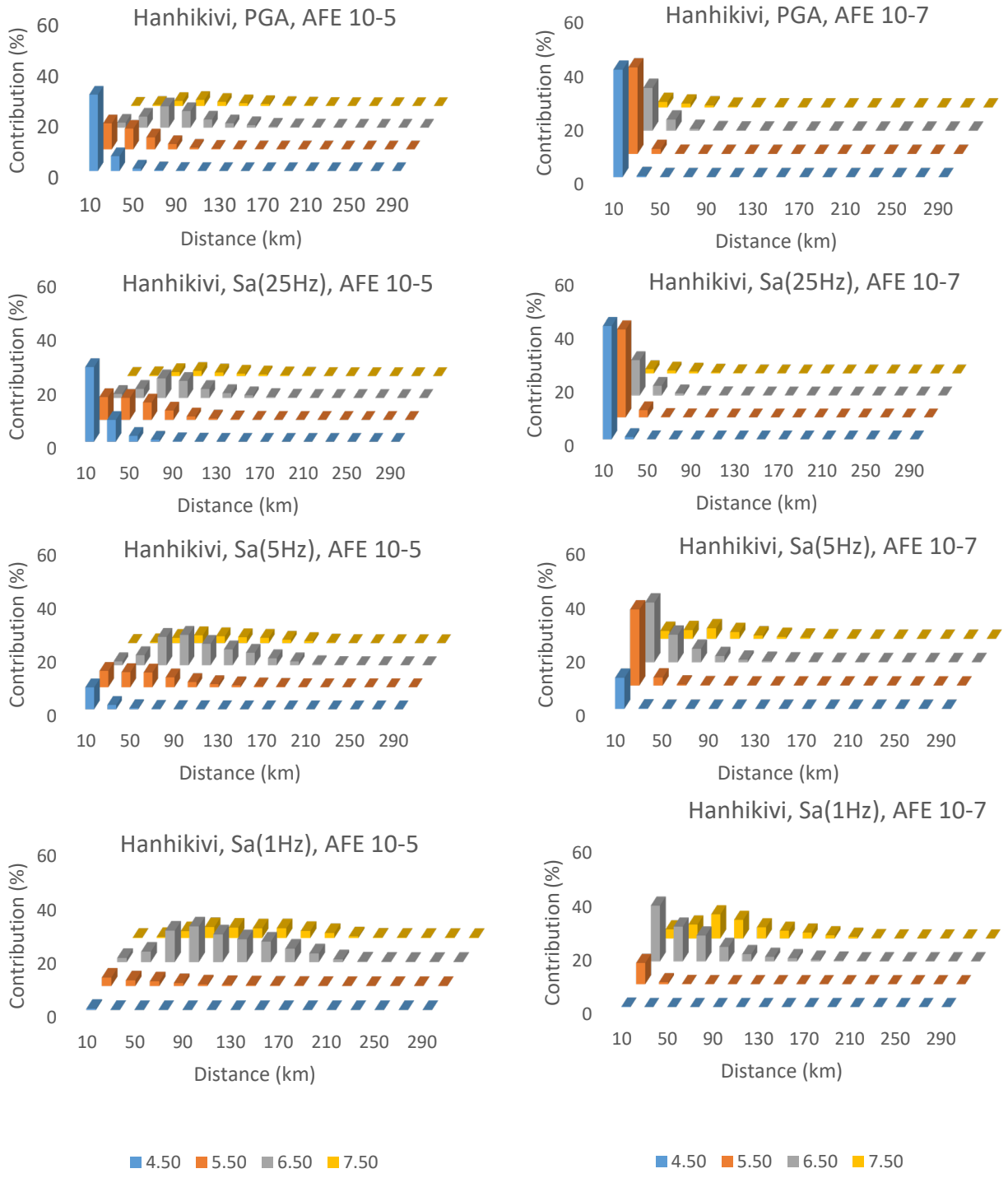

Figure 9. *Hanhikivi disaggregation results by magnitude and hypocenter distance for PGA, 25Hz, 5Hz and 1Hz. The contribution of the magnitude-distance bins is given relative to the total hazard at each intensity measured (e.g., PGA) and AFE.*

9. Analysis of the logic-tree models LSen12(R2), OSen8(R2), and HSen12(R2)

9.1 Significant logic-tree branches at AFE 10^{-5} and AFE 10^{-7}

This section presents an analysis of the influence of different parameters on the hazard results of the LSen12(R2), OSen8(R2) and HSen12(R2) models. The figures explore the path within the logic-tree to the smallest and largest values of intensity measures (IMs). Weighting of the logic-tree branches is ignored in this representation.

The legend to the plots is shown in Figure 10. The horizontal axis corresponds to the branching levels of the logic-tree: (1) seismic source area (SSA) map, (2) M_{max}, (3) GR parameters *a* and *b,* (4) GMPE mean prediction, and (5) GMPE aleatory variability (σ).

The LSen12(R2) model has two SSA map options, OSen8(R2) one, and HSen12(R3) three. Each model has a five-branch discretization of the M_{max} distribution with different weights. The GR parameters are cross-correlated. They correspond to the mid-value of *b* (**b0**) together with lower (**b-**) and upper (**b+**) estimates. A lower *b* in the GR relationship corresponds to a more gently decreasing activity rate. Each b value is associated with a low, mid, and high estimate of *a*. E.g., for *b*-, these are **a9**, **a8** and **a7**, respectively (Fig. 3). Hence, the median estimate for activity rate is **a5**, **b0**, the highest estimate is **a8**, **b-** and the lowest is **a2**, **b+** (Fig. 3). The next levels of branching correspond to the 17 mean predictions of the NGA-East GMPE and the randomness σ.

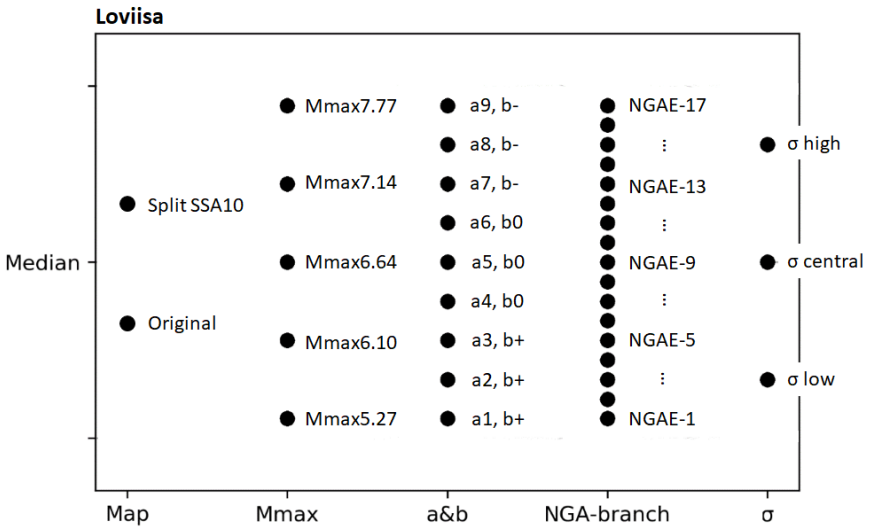

***Figure 10**. Legend for different NPP sites. Maps are different depending on the site and number of models used. M_{max} shows the EPRI M_{max} model options. The a & b are the Gutenberg-Richter activity parameters. The NGA-branch shows the 17 GMPE mean prediction options for the NGA-East model. The σ are the low, central, and high prediction for ergodic sigma model.*

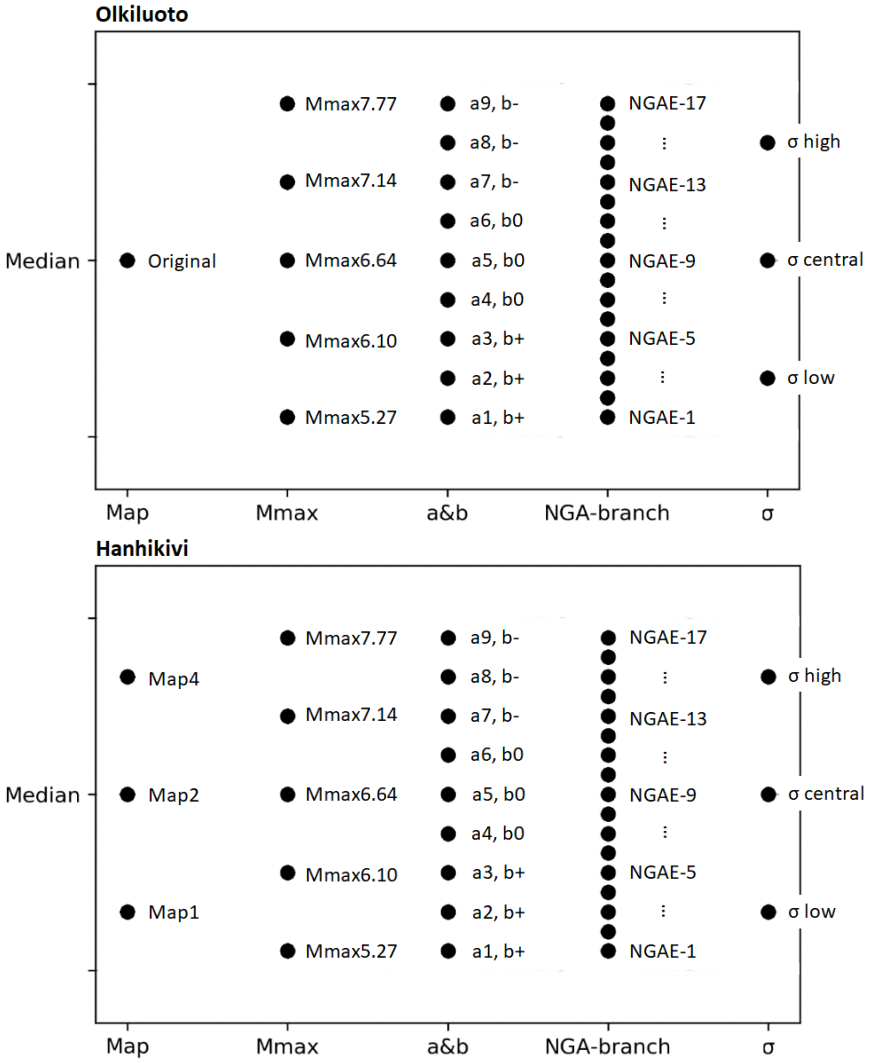

***Figure 10 (continued)**. Legend for different NPP sites. Maps are different depending on the site and number of models used. M_{max} shows the EPRI M_{max} model options. The a & b are the Gutenberg-Richter activity parameters. The NGA-branch shows the 17 GMPE mean prediction options for the NGA-East model. The σ are the low, central, and high prediction for ergodic sigma model.*

The results of the analysis are presented in Figure 11 for PGA, Figure 12 for 25Hz, Figure 13 for 5Hz and Figure 14 for 1Hz spectral acceleration (SA), on the two extremes of the frequency range calculated. In the plots, each line represents a path of the logic-tree leading to a hazard result. The value of result scales the color of the line, from white for the smallest value to black for the largest. One can notice, for example, that many darker lines originate from seismic source zoning option *Split SSA10* for Loviisa (Fig. 11a). This means that logic-tree branches leading to larger PGA outputs initiate from it.

Similarly, it can be noticed that most dark lines intersect in the **b-**, **a7** node of the logic-tree. This corresponds to a slower pace of decrease of activity rates for higher magnitudes in the GR relationship. The effect of the *b* value is generally stronger than the effect of the *a* value (i.e., dark lines concentrate in the **b-** branches). Hence, establishing the slope parameter of the GR relationship with high confidence is of primary importance.

Finally, it can be noticed that certain NGA-East GMPE branches for mean prediction result (e.g., NGA-East 10) in higher PGA outputs. And, perhaps not surprisingly, larger aleatory uncertainty of the GMPE is also a driver for higher PGA results.

The smallest (**Min**), largest (**Max**) and median (**Med**) branch results is given under each plot. The median results are in the expected range for AFE 10^{-5}, but the range of values hint to a significant uncertainty of the prediction. The AFE 10^{-7} prediction is comparatively high, perhaps due to reasons described at the GMPE sensitivity section of this document (Table L2).

It is interesting to note, however, that the picture of most influencing logic-tree branches changes for the low frequency range of the spectra, specifically 1Hz (Fig. 14).

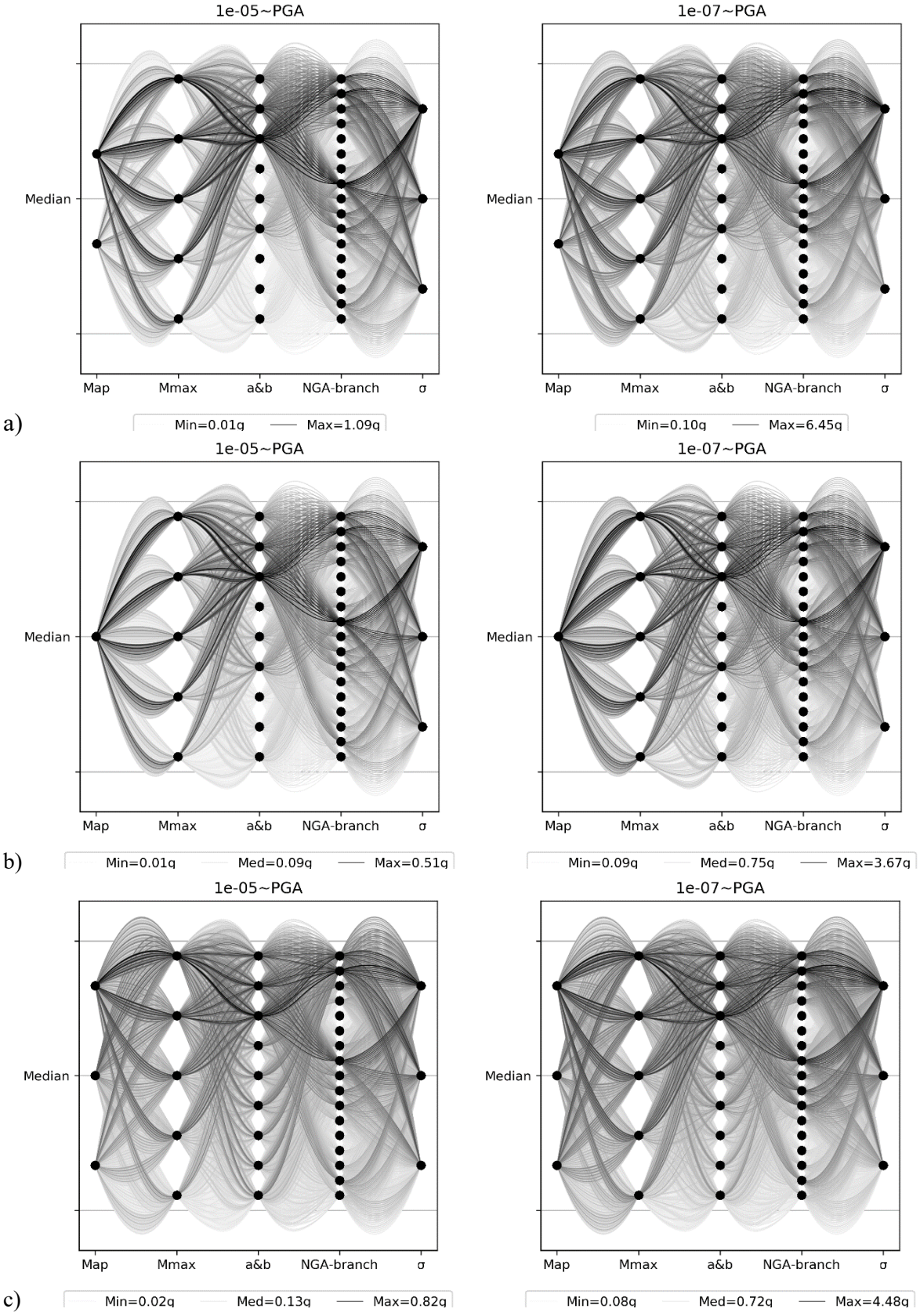

Figure 11. *Influence lines of PGA output. Line tone is given by the normalized intensity measure (i.e., PGA/PGA$_{max}$) of the individual branch. Scale is from PGA=0 white to PGA=PGA$_{max}$ black. (a) Loviisa, (b) Olkiluoto and (c) Hanhikivi, with 10^{-5} and 10^{-7} AFE. PGA$_{min}$, PGA$_{max}$ and the median value are given.*

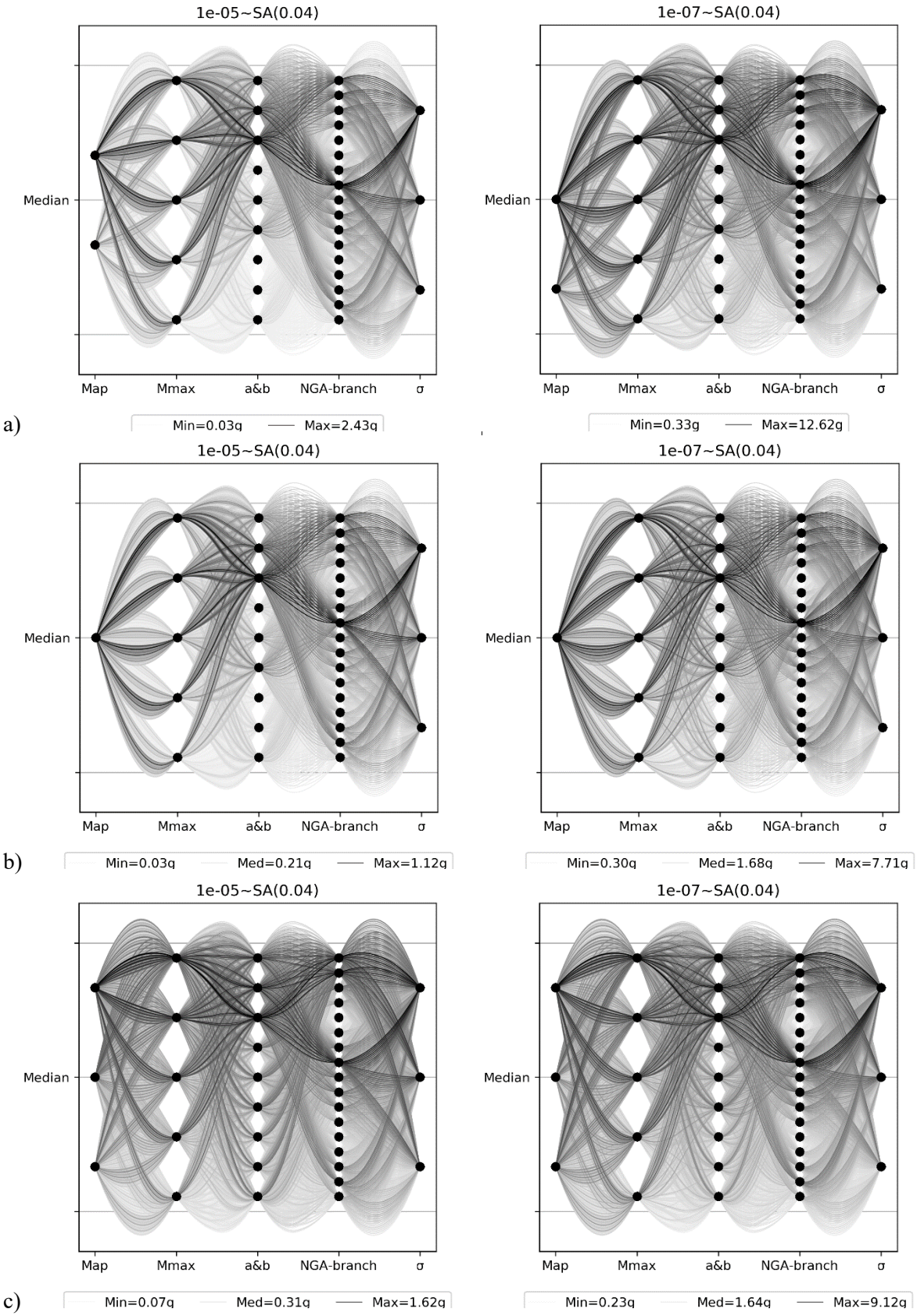

***Figure 12**. Influence lines of the SA_{25Hz} output. Line tone is given by the normalized intensity measure (i.e., PGA/PGA_{max}) of the individual branch. Scale is from SA_{25Hz}=0 white to SA_{25Hz}= SA_{25Hz_max} black. (a) Loviisa, (b) Olkiluoto and (c) Hanhikivi, with 10^{-5} and 10^{-7} AFE. SA_{25Hz_min}, SA_{25Hz_max} and the median value are given.*

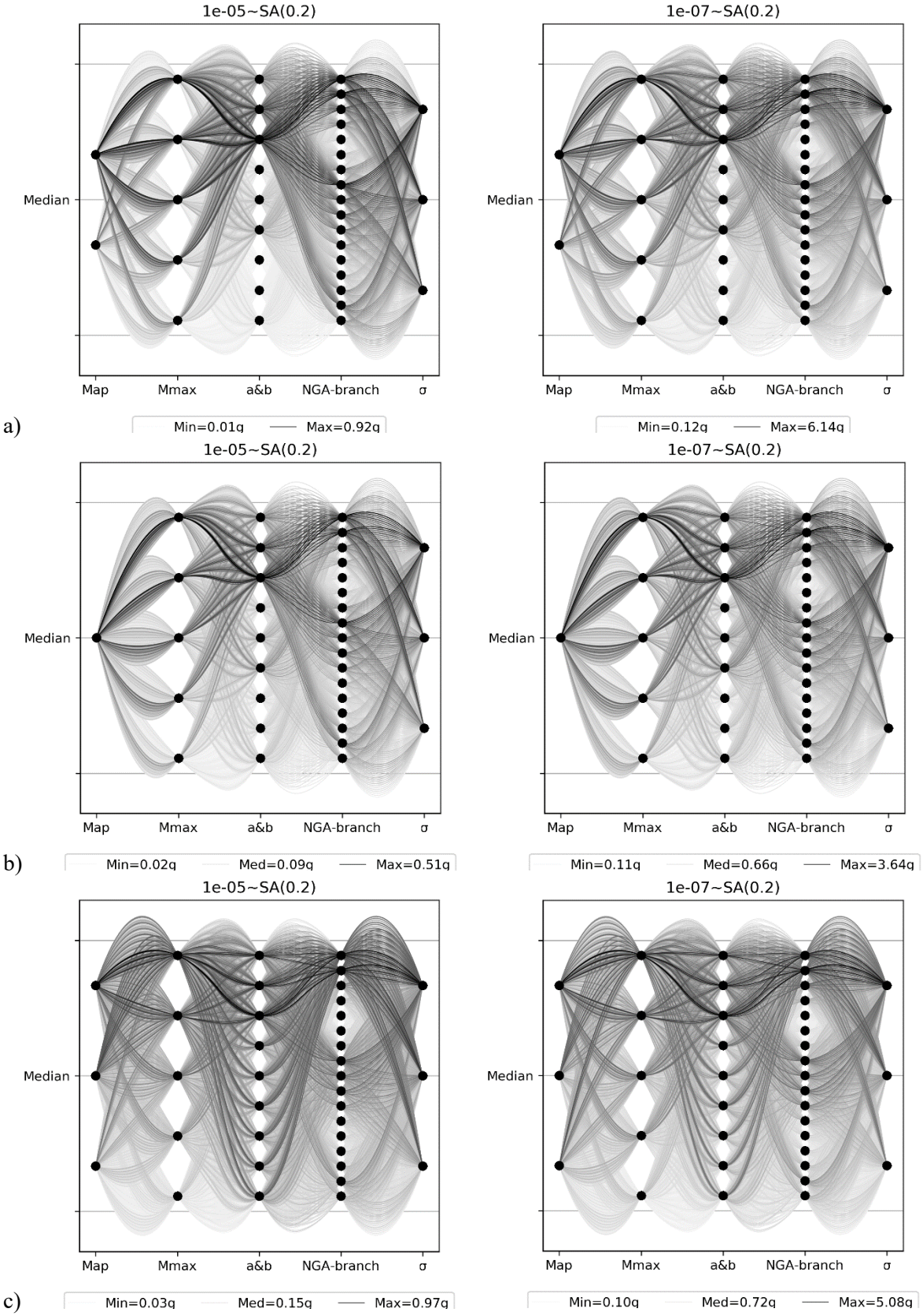

***Figure 13**. Influence lines of the SA_{5Hz} output. Line tone is given by the normalized intensity measure (i.e., SA_{5Hz}/ SA_{5Hz_max}) of the individual branch. Scale is from SA_{5Hz}=0 white to SA_{5Hz}= SA_{5Hz_max} black. (a) Loviisa, (b) Olkiluoto and (c) Hanhikivi, with 10^{-5} and 10^{-7} AFE. SA_{5Hz_min}, SA_{5Hz_max} and the median value are given.*

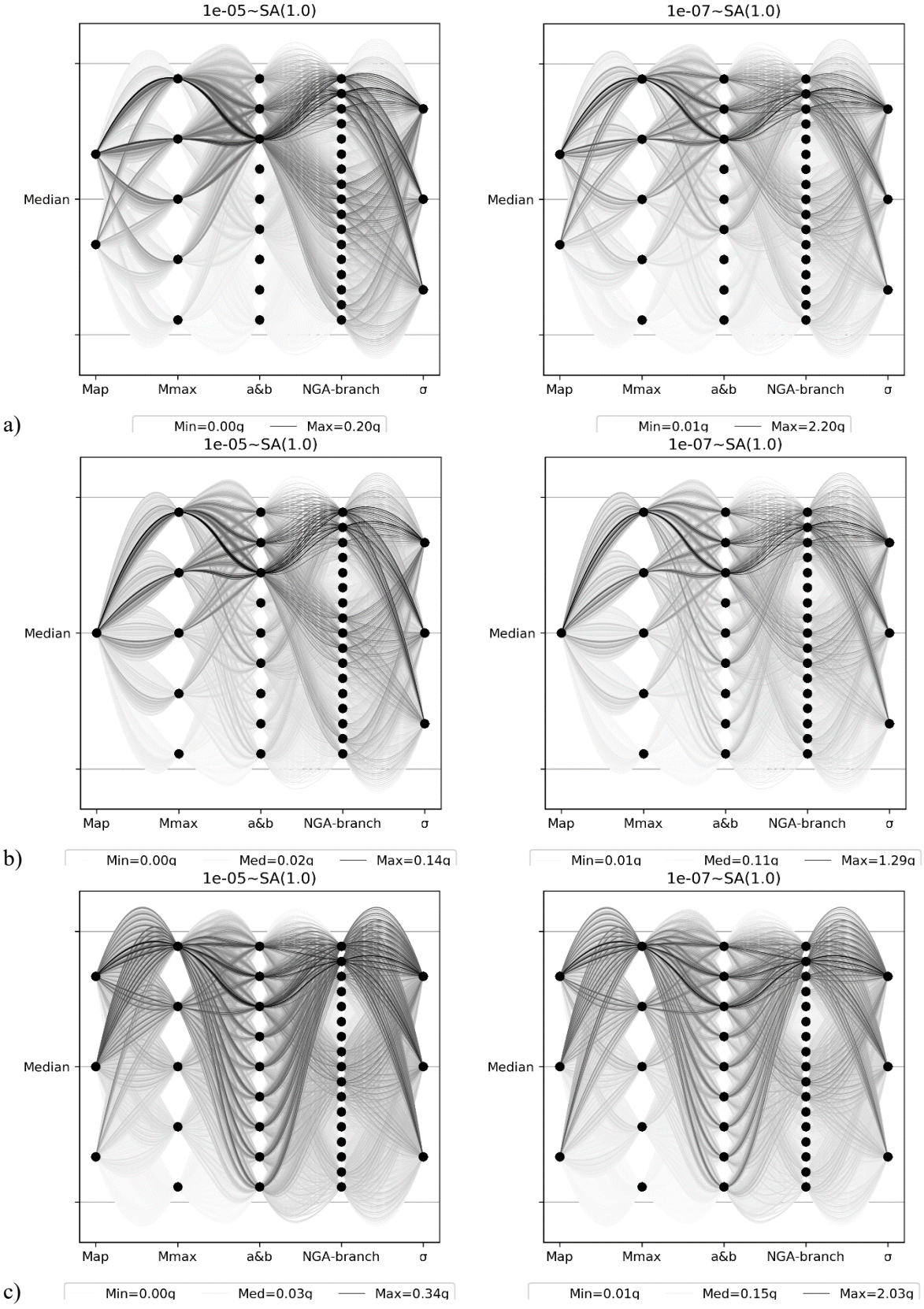

Figure 14. *Influence lines of SA_{1Hz} output. Line tone is given by the normalized intensity measure (i.e. SA_{1Hz} / SA_{1Hz_max}) of the individual branch. Scale is from SA_{1Hz}=0 white to SA_{1Hz}= SA_{1Hz_max} black. (a) Loviisa, (b) Olkiluoto and (c) Hanhikivi, with 10^{-5} and 10^{-7} AFE. SA_{1Hz_min}, SA_{1Hz_max} and the median value are given.*

9.2 Variation of the influence of logic-tree branches in the hazard curves

The PGA hazard curves of the LSen12(R2), OSen8(R2), and HSen12(R2) models are analyzed in Figure 15. In each figure, the hazard curves obtained from all the branches of the logic-tree are plotted with grey. These line clouds represent the range of hazard curves in the model. The weighted median hazard curve of all the branches is shown with blue. Finally, the median hazard curves were calculated for all the logic-tree branches associated with a set of input parameters, in order to illustrate the influence on the hazard of these parameters. For example, the first line of Figure 15 for Loviisa represents the SSA map sensitivity of the hazard curves. One green line represents the median of all the hazard curves from branches that use Map1 and the second green line the median of the hazard curves from Map 2 branches. The distance between the green lines gives the range of hazard, influenced by the epistemic uncertainty related to SSAs.

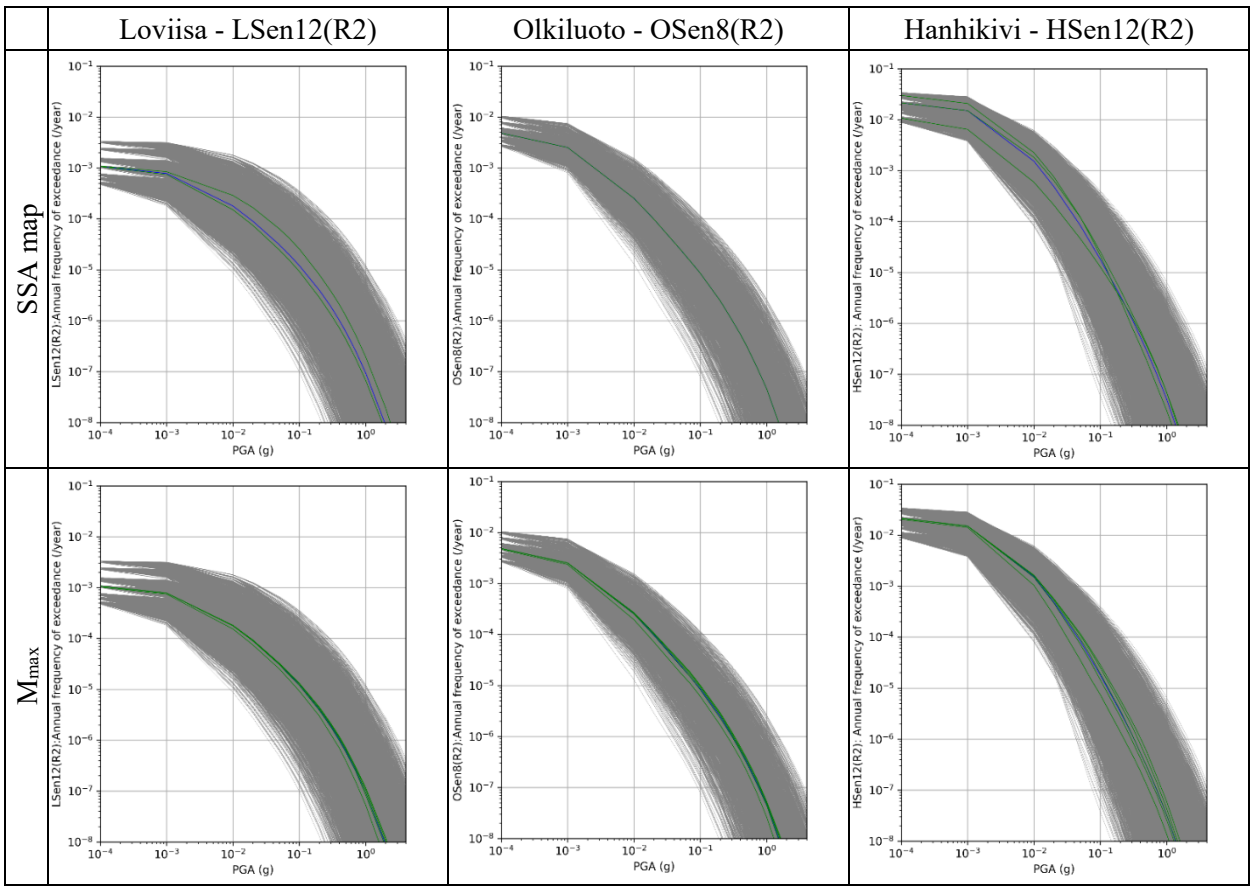

***Figure 15**. Influence of input parameters on the PGA hazard curves for Loviisa, Olkiluoto and Hanhikivi.*

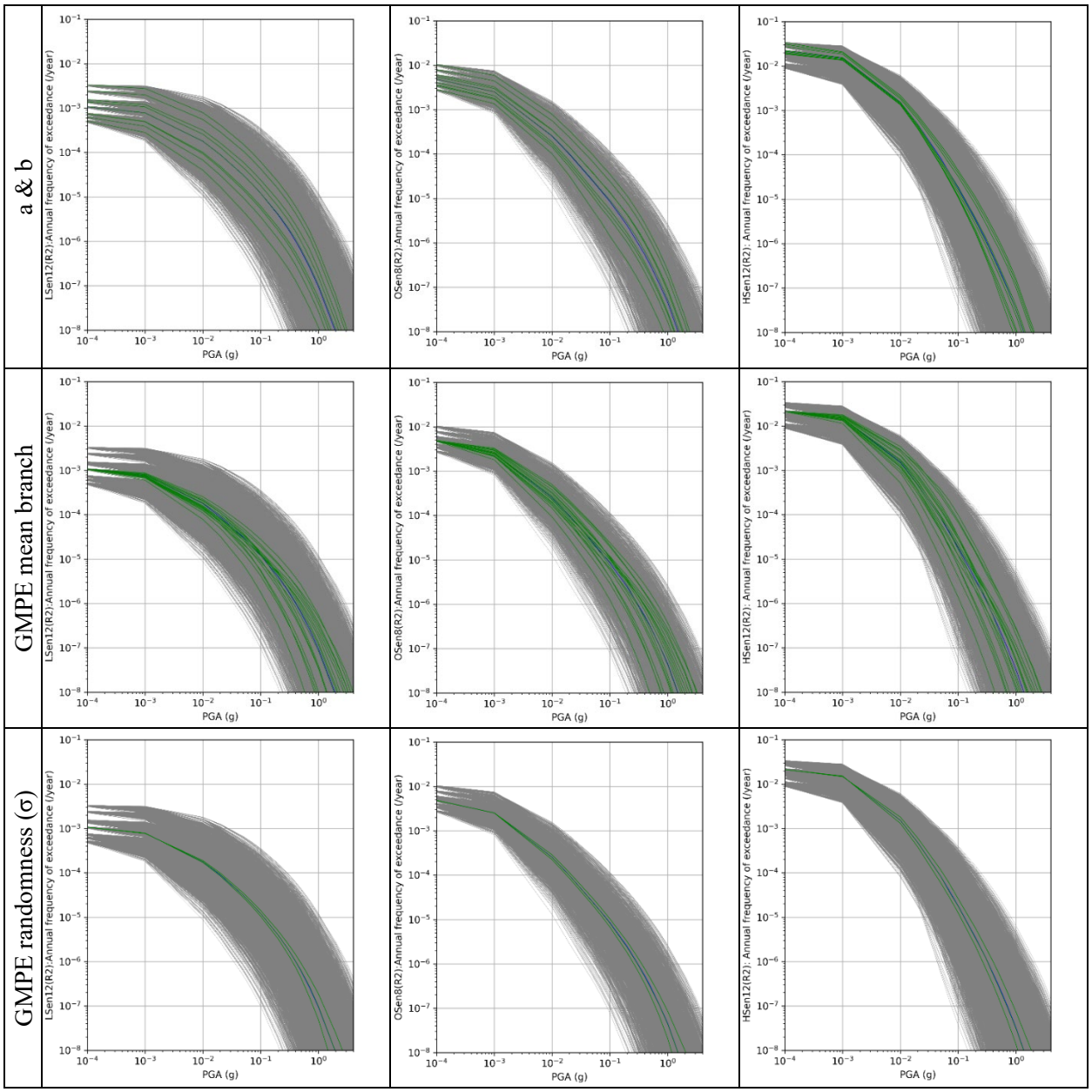

Figure 15(continued). *Influence of input parameters on the PGA hazard curves for Loviisa, Olkiluoto and Hanhikivi.*

	Loviisa - LSen12(R2)	Olkiluoto - OSen8(R2)	Hanhikivi - HSen12(R2)
SSA map	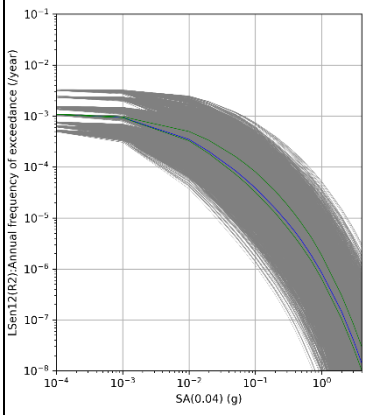	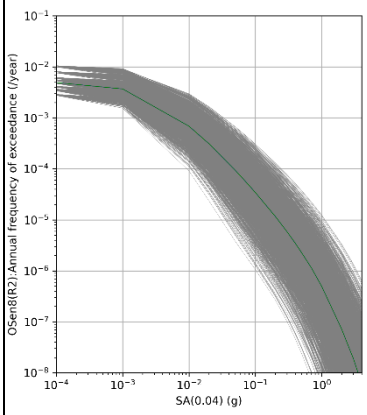	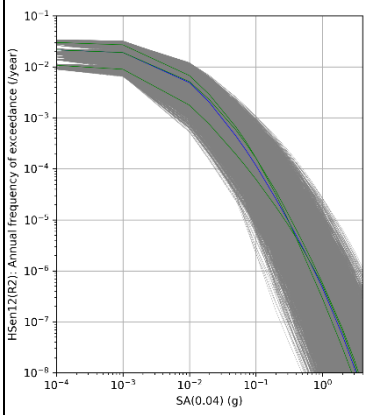
M_{max}	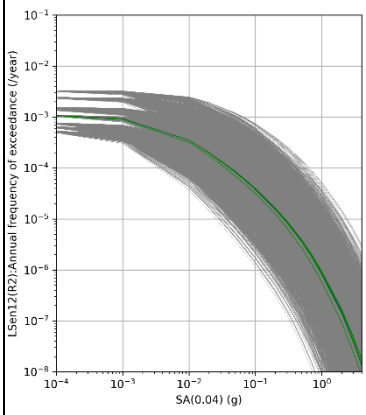	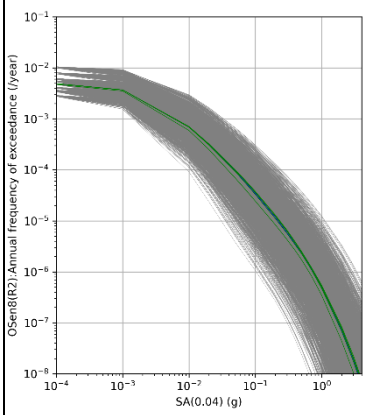	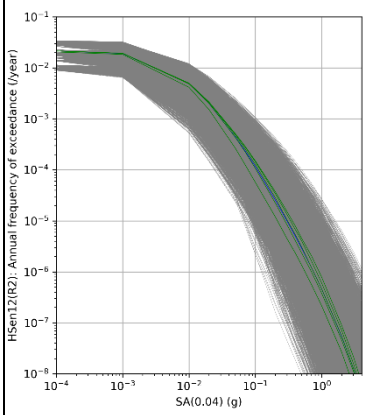
a & b	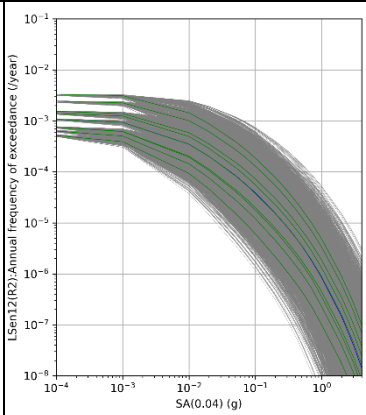	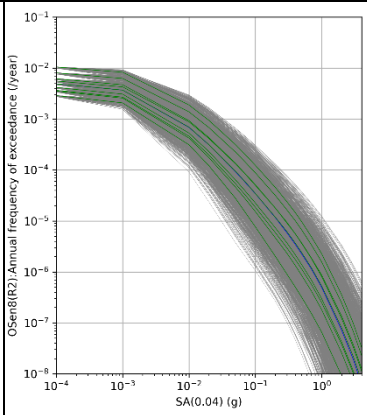	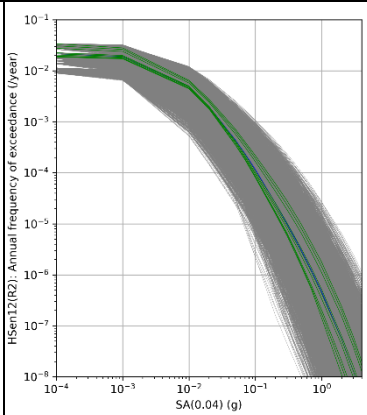
GMPE mean branch	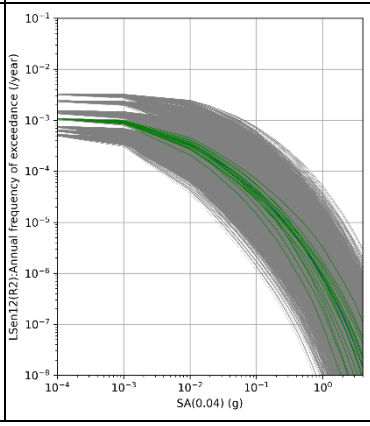	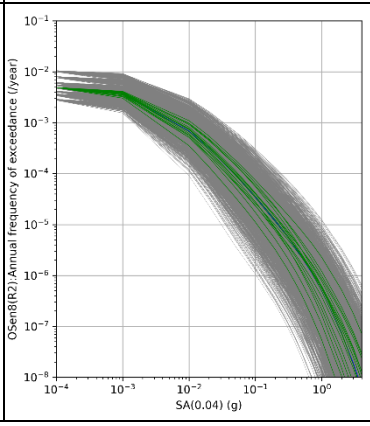	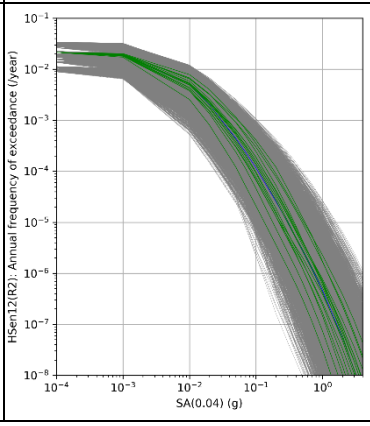

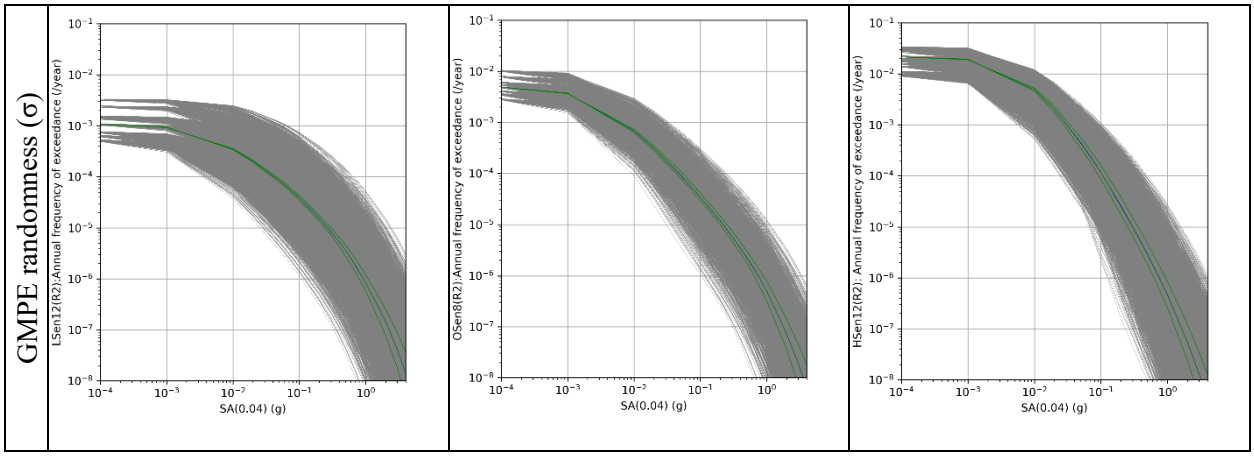

***Figure 16**. Influence of input parameters on the SA_{25Hz} hazard curves for Loviisa, Olkiluoto and Hanhikivi.*

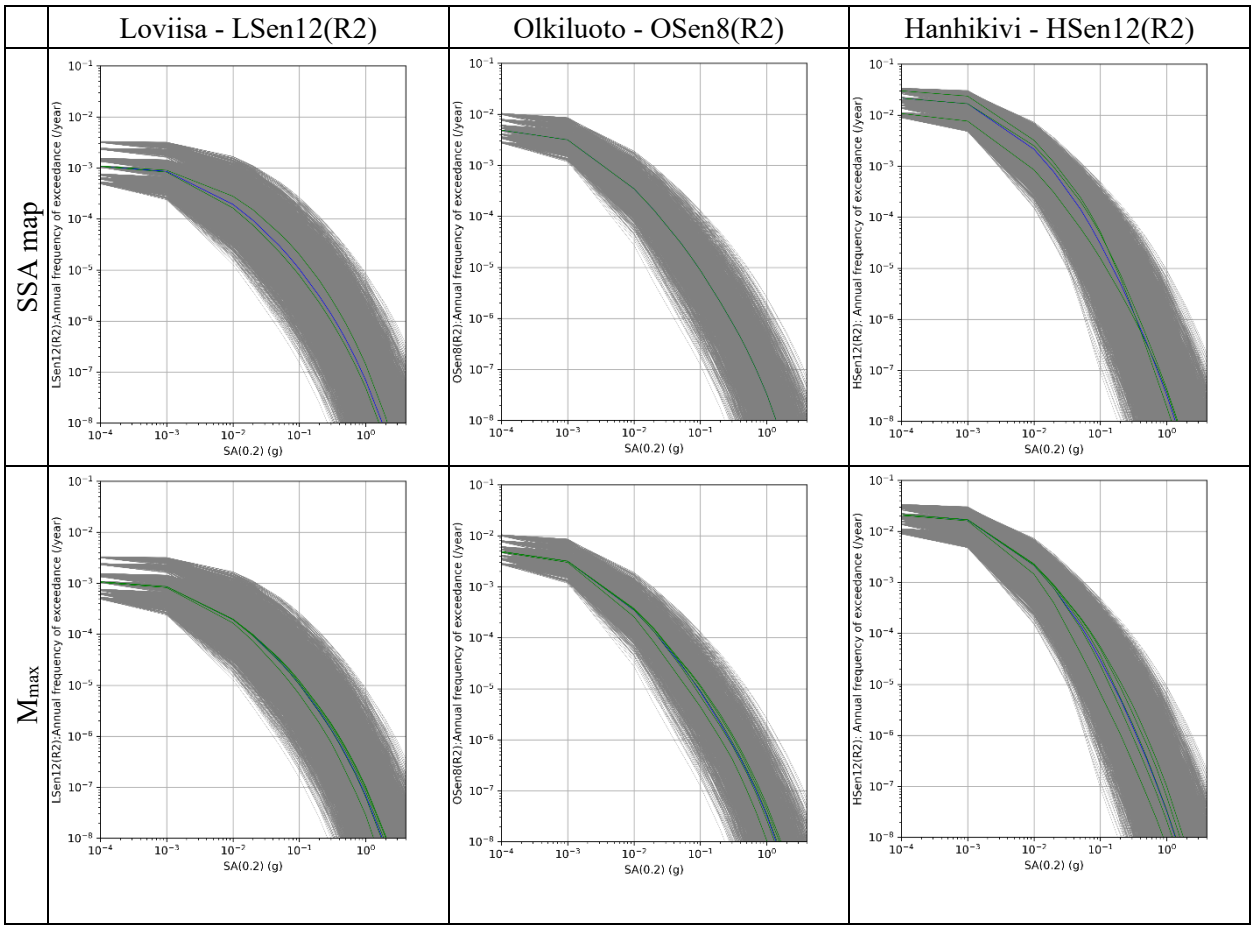

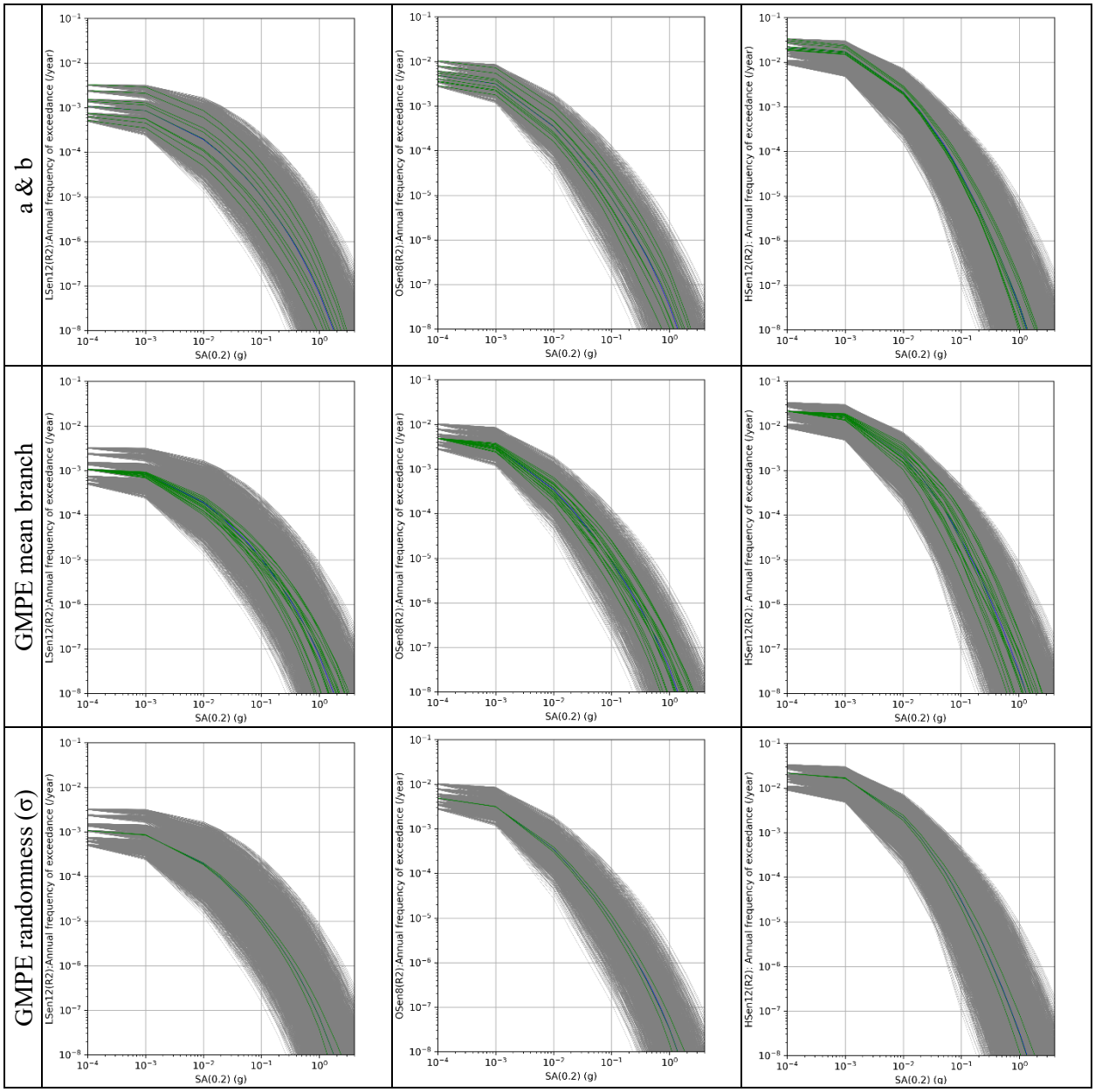

Figure 17*. Influence of input parameters on the SA_{5Hz} hazard curves for Loviisa, Olkiluoto and Hanhikivi.*

	Loviisa - LSen12(R2)	Olkiluoto - OSen8(R2)	Hanhikivi - HSen12(R2)
SSA map	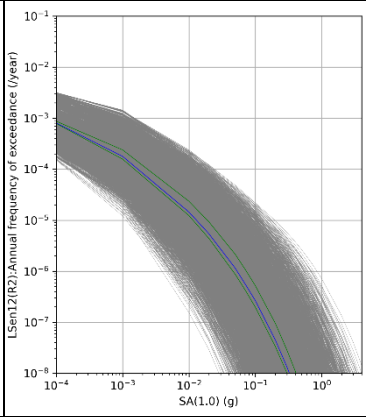	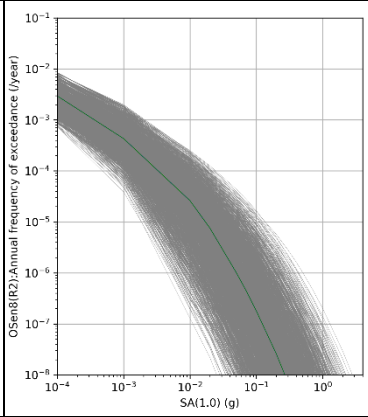	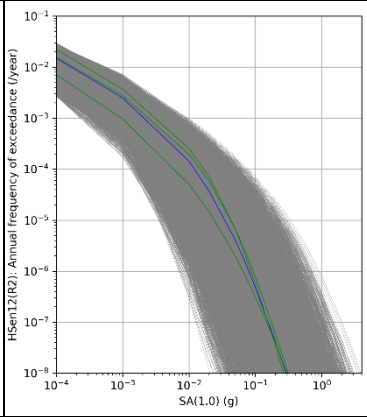
M_{max}	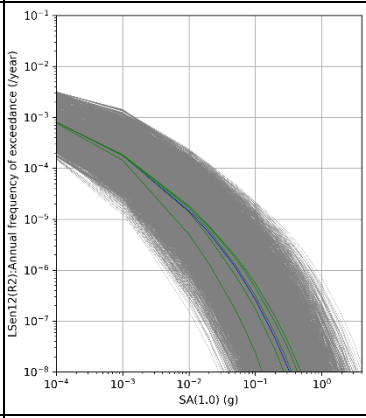	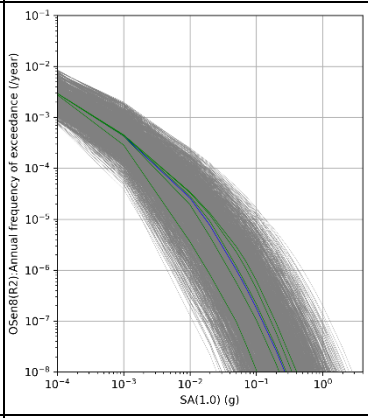	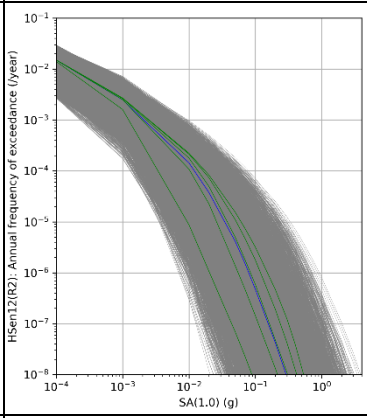
a & b	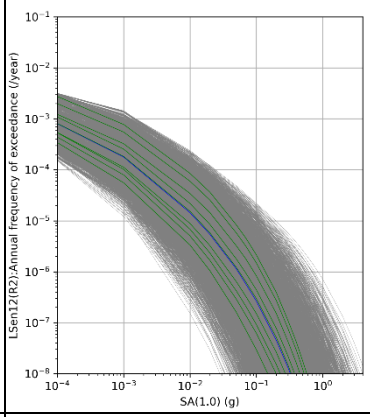	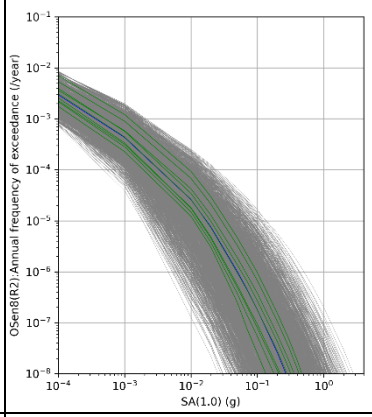	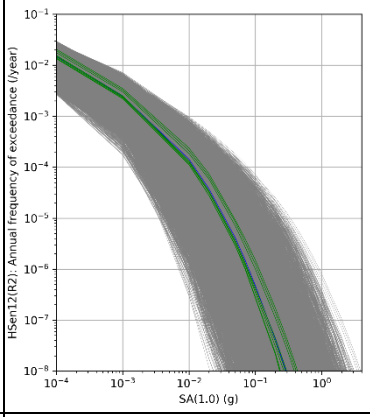
GMPE mean branch	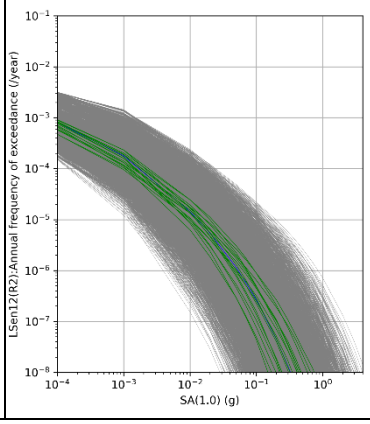	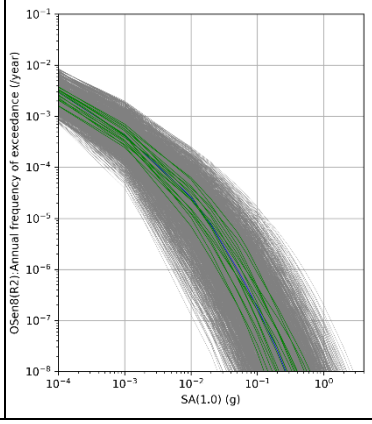	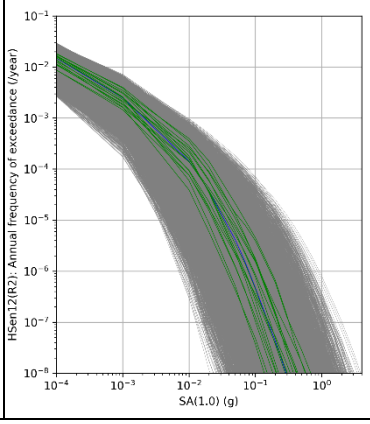

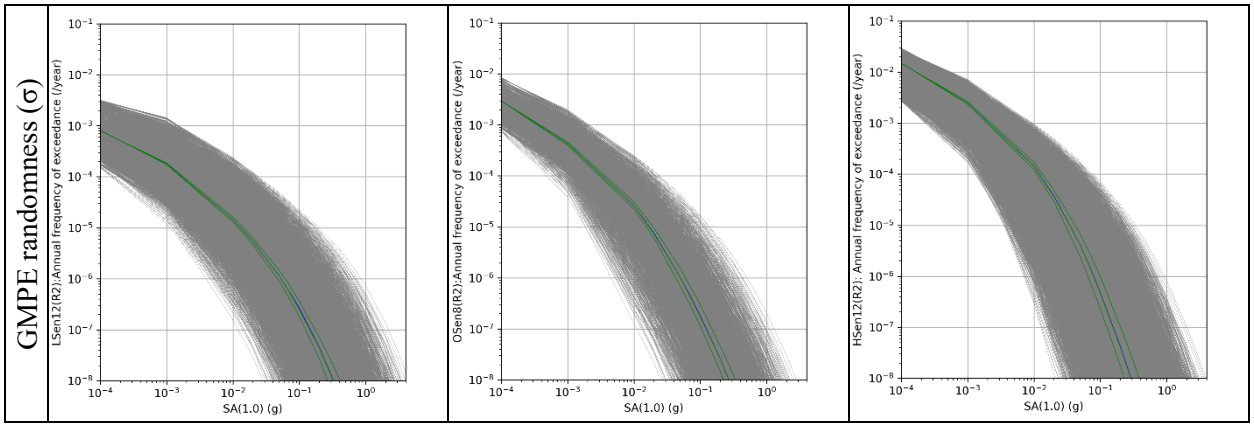

***Figure 18**. Influence of input parameters on the SA_{1Hz} hazard curves for Loviisa, Olkiluoto and Hanhikivi.*

The results show that different inputs may control different ranges of the hazard curves. $\mathbf{M_{max}}$ and **σ** seem to influence lower AFE values. The largest uncertainty is related to the **GMPE** median prediction and the **a** & **b** values of the Gutenberg-Richter relationship. While the GMPE median is mostly influencing the hazard at low AFE, the activity parameters have an overall effect for all ranges of AFE. Finally, **SSA maps** may or may not have a significant role. For Hanhikivi, for example, the different maps produce significantly different hazard for high values of AFE.

9.3 Quantification of the effect at AFE 10^{-5} and 10^{-7}

In this section, the AFE ranges of interest to nuclear safety are analysed. Figures 19 to 22 were obtained by extracting the AFE 10^{-5} and AFE 10^{-7} PGA hazard values from the curves in Figure 15. The overall weighted median hazard, calculated from all logic-tree branches, is shown with the grey vertical line. The weighted median hazard from sub-group of branches corresponding to different input parameters are shown with coloured rectangles. For instance, in the LSen12(R2) logic-tree the first level of branching is for SSA maps, with two map options. The median of branches crossing Map1 and Map2, at this branching level corresponds to the two red rectangles. One is above the overall median, the other below. The size of the rectangles shows the total weight of the branches for Map1 and Map2, 66.7% and 33.3% in this case. The branching levels in Figure 19 are: Level 1 for SSA maps, Level 2 for M_{max}, Level 3 for *a* and *b* parameters, Level 4 for GMPE mean prediction, and Level 5 for GMPE σ.

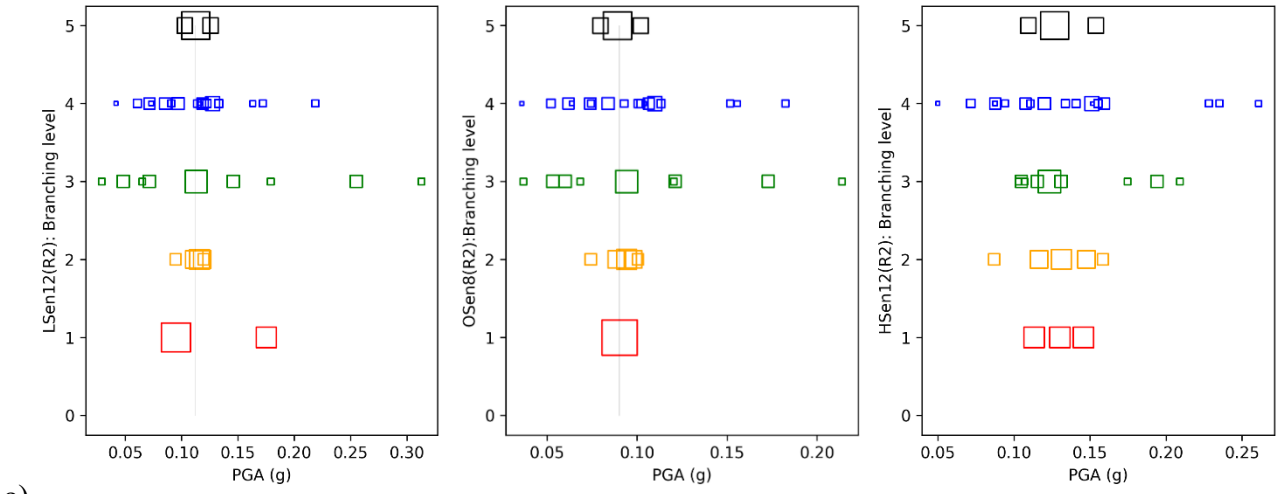

a)

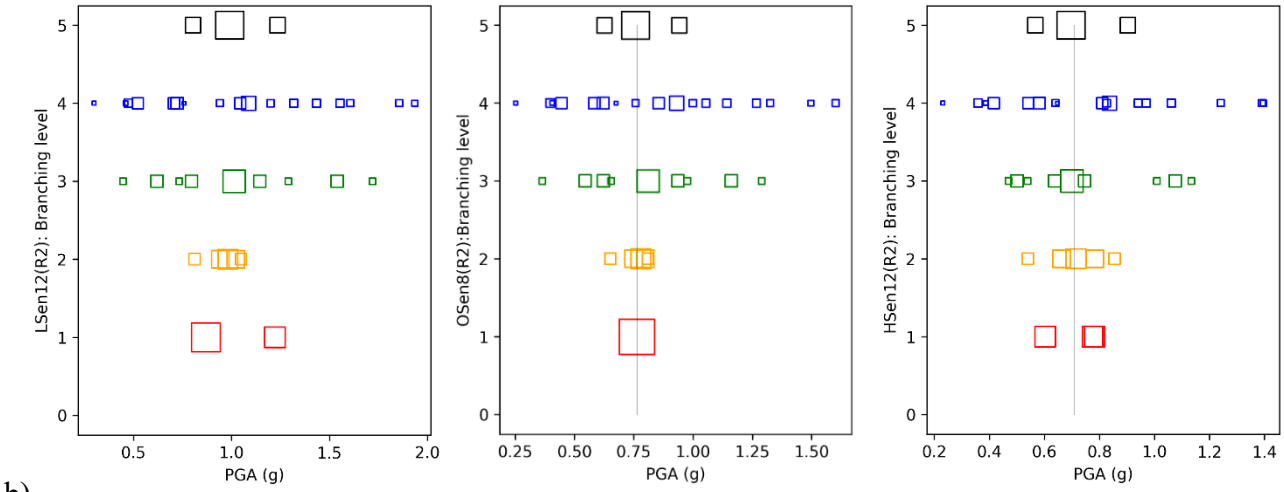

b)

Figure 19. *Summaries of sensitivity of PGA hazard with input parameters at (a) AFE 10^{-5} and (b) AFE 10^{-7}. LSen12(R2) for Loviisa, OSen8(R2) for Olkiluoto, and HSen12(R2) for Hanhikivi. Level 1 (red) for SSA maps, Level 2 (orange) for M_{max}, Level 3 (green) for a and b parameters, Level 4 (blue) for GMPE mean prediction, and Level 5 (black) for GMPE σ. Gray line shows the overall weighted median hazard.*

It can be noticed in Figure 19 that the most important parameter for sensitivity, at this AFE levels, are the mean GMPE and the Gutenberg-Richter parameters *a* and *b*. M_{max} plays a more prominent role only in the case of the Hanhikivi model, HSen12(R2). Seismic zoning maps also play some role, in the case of Loviisa / LSen12(R2) it is highlighted.

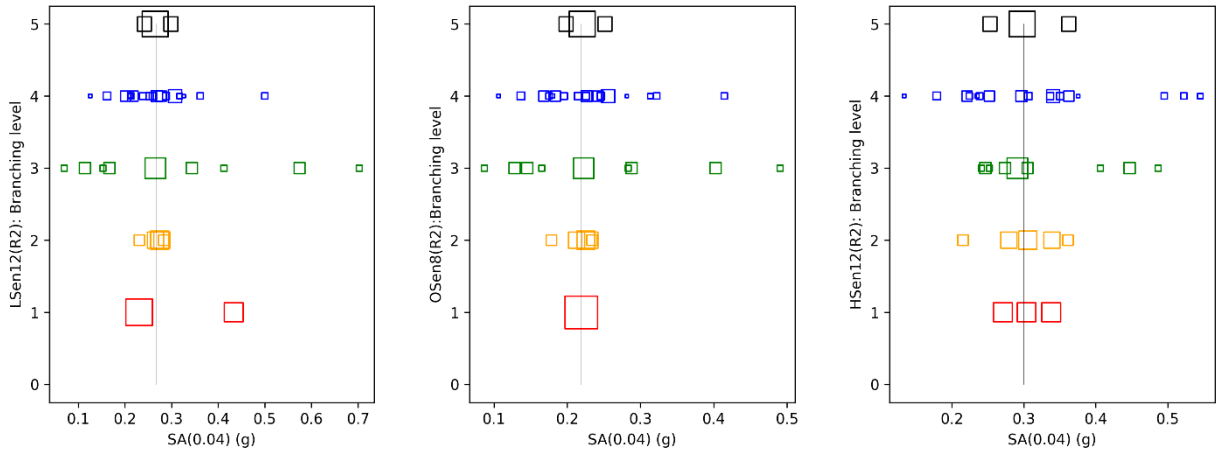

a)

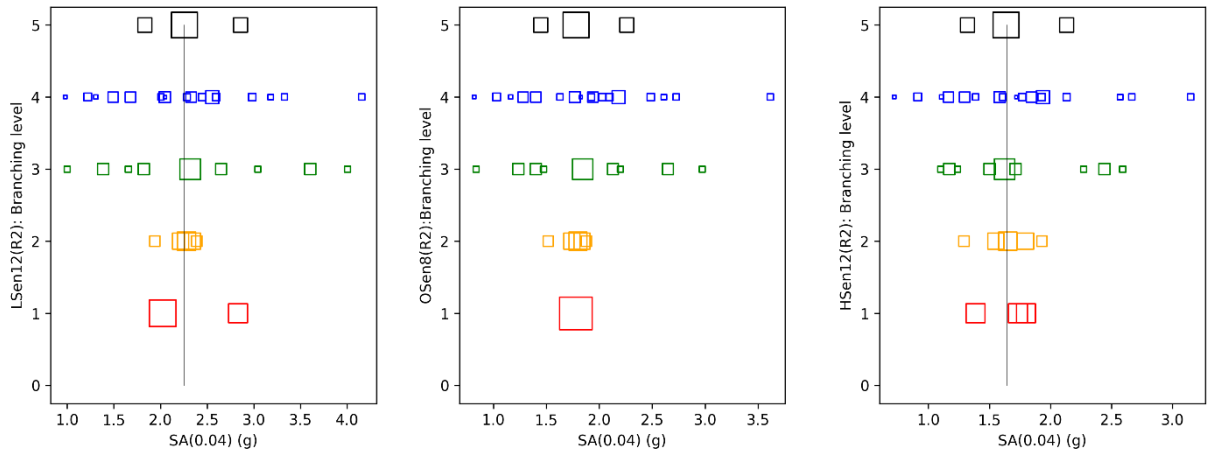

b)

Figure 20. *Summaries of sensitivity of SA_{25Hz} hazard with input parameters at (a) AFE 10^{-5} and (b) AFE 10^{-7}. LSen12(R2) for Loviisa, OSen8(R2) for Olkiluoto, and HSen12(R2) for Hanhikivi. Level 1 (red) for SSA maps, Level 2 (orange) for M_{max}, Level 3 (green) for a and b parameters, Level 4 (blue) for GMPE mean prediction, and Level 5 (black) for GMPE σ. Gray line shows the overall weighted median hazard.*

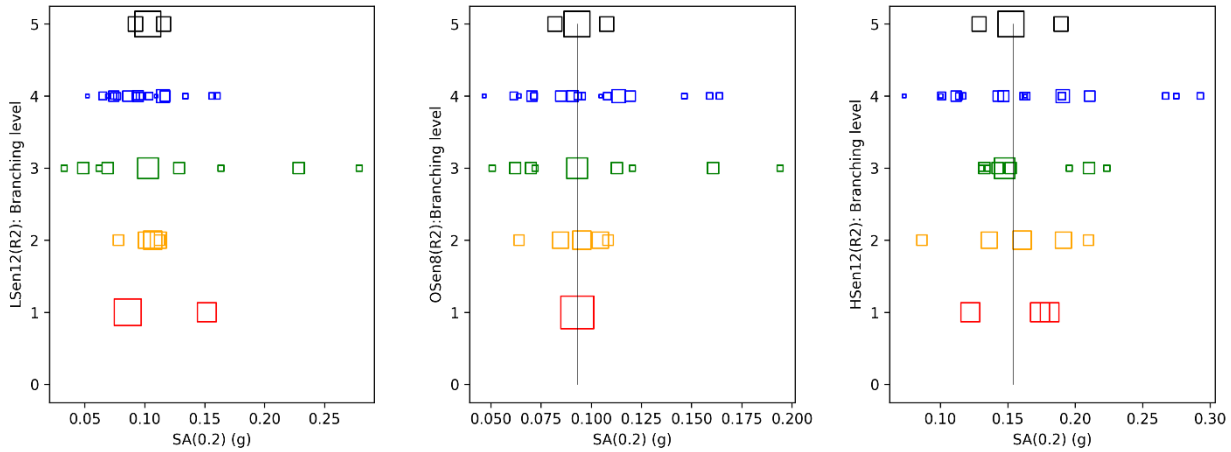

a)

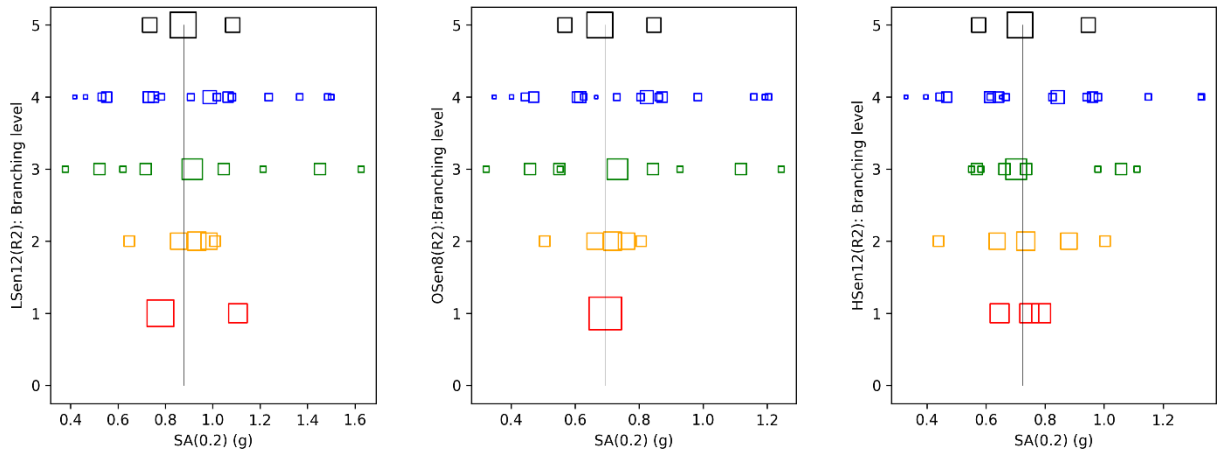

b)

Figure 21. *Summaries of sensitivity of SA_{5Hz} hazard with input parameters at (a) AFE 10^{-5} and (b) AFE 10^{-7}. LSen12(R2) for Loviisa, OSen8(R2) for Olkiluoto, and HSen12(R2) for Hanhikivi. Level 1 (red) for SSA maps, Level 2 (orange) for M_{max}, Level 3 (green) for a and b parameters, Level 4 (blue) for GMPE mean prediction, and Level 5 (black) for GMPE σ. Gray line shows the overall weighted median hazard.*

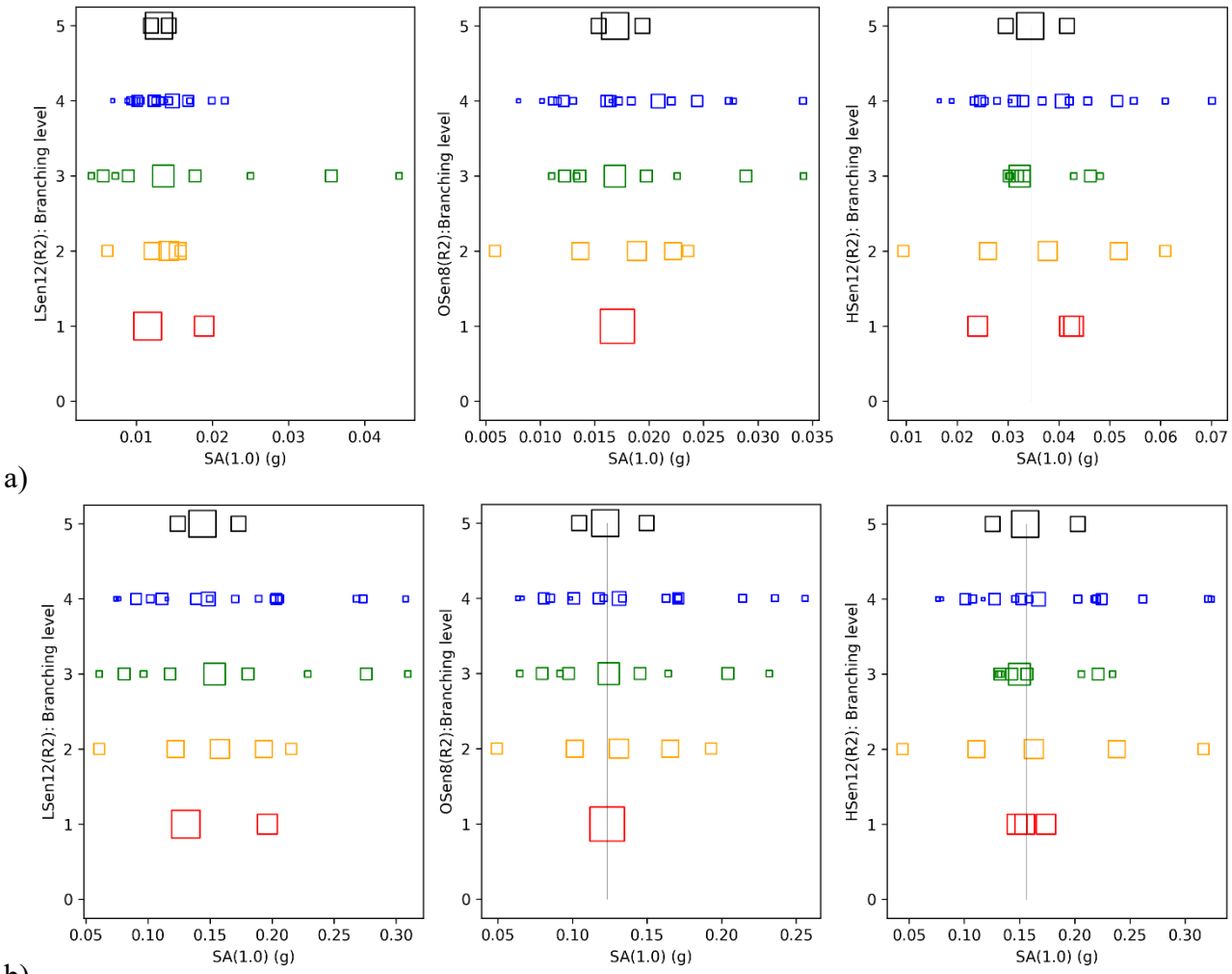

Figure 22. *Summaries of sensitivity of SA_{1Hz} hazard with input parameters at (a) AFE 10^{-5} and (b) AFE 10^{-7}. LSen12(R2) for Loviisa, OSen8(R2) for Olkiluoto, and HSen12(R2) for Hanhikivi. Level 1 (red) for SSA maps, Level 2 (orange) for M_{max}, Level 3 (green) for a and b parameters, Level 4 (blue) for GMPE mean prediction, and Level 5 (black) for GMPE σ. Grey line shows the overall weighted median hazard.*

10. On the distinction between median and mean hazard

This note is added here to document the topics discussed in the SENSEI project. Nuclear studies in Finland use the median hazard with an annual frequency of exceedance 10^{-5} as reference. It is sometimes claimed that the median hazard is more stable than the mean, and hence it is the preferred output of hazard analyses. The stability of the median hazard curve has been demonstrated in the synthetization process of the SENSEI project, when the original, complex logic-tree models were reduced to a few branches (e.g., 144 branches to 4), without affecting the median hazard curve for PGA (Tables L1, O1 and H1).

It is important to understand the reason for the stability of the median hazard curve, and take note of the disadvantages of using it. In its purest form, the median value of an IM (e.g., PGA), would be obtained by ordering the values corresponding to each logic-tree branch and taking the middle value. Not surprisingly, the middle value of hazard is obtained using the middle values of input parameters to the hazard model. In addition, the logic-tree branches corresponding to the middle value parameters are also weighted with higher weight, entrenching their influence on the median hazard. Hence, trimming of the outlier input parameters from the logic-tree does not change the median hazard output. Moreover, the median depends on the weight of the branches, which is often based on subjective judgement. This means that the epistemic uncertainty, incorporated within the logic-tree structure is largely ignored, when the output carried over to other analysis is the median.

An alternative to median would be the mean hazard, which was explored in the SENSEI project, e.g., with models LSen12(R2), OSen8(R2), and HSen12(R2) in Figures L5, O3, and H3 respectively. It can be noticed that the mean hazard is higher than the median. Like the median, in the context of weighted logic-tree branches, this mean is in fact a weighted mean. What is important is that the mean hazard is influenced by all logic-tree branches and their weights in the model, hence reflecting a broader view of the epistemic uncertainty perceived by the modeler. As a disadvantage, the mean hazard is more prone to changes, when the logic-tree is modified.

It also has to be mentioned that in risk calculations the convolution of mean hazard with mean fragility curves leads to clear output. However, it is questionable what is the outcome of convoluting the median hazard with the mean fragility. Based on the general discussion in the SENSEI project, it may be appropriate to plan a transition to mean hazard curves in the future.

Appendix 2

Internal working documents of the SENSEI project

Fülöp, L.A., 2019. Comparative plots of GMPEs.

Fülöp, L.A., Malm, M., 2019. Benchmark cases for EZ Frisk and OpenQuake.

Fülöp, L.A., Malm, M., Mäntyniemi, P., 2020. Minimum depth.

Fülöp, L.A., Mäntyniemi, P., 2020a. A prior distribution for SENSEI (Draft).

Fülöp, L.A., Mäntyniemi, P., 2020b. M_{max} using the Bayesian approach.

Fülöp, L.A., Mäntyniemi, P., Malm, M., 2019a. Variation of the activity parameters with M_{min} and M_{max}.

Fülöp, L.A., Mäntyniemi, P., Malm, M., Kaisko, O., 2019b. Arguments for a certain range of M_{min} in the PSHA sensitivity studies in Finland.

Mäntyniemi, P., Fülöp, L.A., 2020. On the completeness intervals of pre-instrumental seismicity records in Fennoscandia.

Mäntyniemi, P., Fülöp, L.A., Kaitila, O., Toro, G., 2020a. On the depth distribution of earthquakes in Finland.

Mäntyniemi, P., Malm, M., Rinne, L., Fülöp, L.A., 2020b. On seismic source areas in the Fennoscandian Shield, with focus on the Loviisa NPP.

Toro, G., 2019. Notes on Proposed Treatment of λ and β in Logic Tree.

References

Bender, B., Campbell, K.W., 1989. A note on the selection of minimum magnitude for use in seismic hazard analysis. Bull. Seism. Soc. Am. 79(1):199-204.

Fülöp, L., Jussila, V., Aapasuo, R., Vuorinen, T., Mäntyniemi, P., 2020. A ground-motion prediction equation for Fennoscandian nuclear installations. Bull. Seism. Soc. Am. 110(3):1211-1230, doi:10.1785/0120190230

Goulet, C., Bozorgnia, Y., Abrahamson, N., Kuehn, N., Al Atik, L., Youngs, R., Graves, R., Atkinson, G., 2018. Central and Eastern North America ground-motion characterization NGA-East final report, PEER Report No. 2018/08, Pacific Earthquake Engineering Research Center at the University of California.

Graizer, V., 2016. Ground-motion prediction equations for Central and Eastern North America, Bull. Seism. Soc. Am. 106:1600-1612, doi:10.1785/0120150374

Korja, A., Kihlman, S., Oinonen, K. (Eds.), 2016. Seismic source areas in Central Fennoscandia. Report S-64. Institute of Seismology, University of Helsinki, 314 pp.

Korja, A. & Kosonen, E. (Eds.), 2015. Seismotectonic framework and models in the northern part of the Fennoscandian Shield. Institute of Seismology, University of Helsinki, Report S-63, ISSN 0357-3060.

Leppänen, T., Varpasuo, P., 2017. Loviisa 1 ja 2, Olkiluoto – Loviisa NPP sites, ground motion prediction equation. Report LO1-T84252-00005, Fortum Oyj. 17.11.2017.

Malm, M., Kaisko, O., 2017a. Re-evaluation of seismic hazard spectra in Olkiluoto and Loviisa. Report DTVOSPF-5497, ÅF-Consult Ltd.

Malm, M., Kaisko, O., 2017b. Updated ground response spectrum for the Hanhikivi site. Report DFVUDBR-5638, ÅF-Consult Ltd.

Pezeshk, S., Zandieh, A. and Tavakoli, B., 2011. Hybrid empirical ground-motion prediction equations for Eastern North America using NGA Models and updated Seismological parameters. Bull. Seism. Soc. Am. 101:1859-2870.

Saari, J., Lund, B., Malm, M., Mäntyniemi, P., Oinonen, K., Tiira, T., Uski, M., Vuorinen, T., 2015. Evaluating Seismic Hazard for the Hanhikivi Nuclear Power Plant Site, Seismological Characteristics of the Seismic Source Areas, Attenuation of Seismic Signal, and Probabilistic Analysis of Seismic Hazard. Report NE-4459, ÅF-Consult Ltd.

Saari, J., Malm, M., 2016. Re-evaluation of seismic hazard in Olkiluoto and Loviisa. Report DTVOHAR-4652, ÅF-Consult Ltd.

Vuorinen, T., Tiira, T., Uski, M., Lund, B., 2018. Updated Fennoscandian GMPE. Report T-97, Institute of Seismology, University of Helsinki. ISBN 978-952-10-9591-7